# A Method for Transmission Network Expansion Planning

- A Monte-Carlo and Lagrangian Multiplier-based Optimisation Approach

Zongyu Liu

# A Method for Transmission Network Expansion Planning

## - A Monte-Carlo and Lagrangian Multiplier-based Optimisation Approach

**Proefschrift**

ter verkrijging van de graad van doctor
aan de Technische Universiteit Delft,
op gezag van de Rector Magnificus prof. ir. K.C.A.M. Luyben,
voorzitter van het College voor Promoties,
in het openbaar te verdedigen op woensdag 14 mei 2014 om 12:30 uur

door

Zongyu LIU
Electric Power Engineering, M.Sc., Chalmers University of Technology,
Gothenburg, Sweden

geboren te Harbin, China

Dit proefschrift is goedgekeurd door de promotor:
Prof. ir. L. van der Sluis

Copromotor:
Dr. ir. G. Papaefthymiou

Samenstelling promotiecommissie:

| | |
|---|---|
| Rector Magnificus | voorzitter |
| Prof. ir. L. van der Sluis | Technische Universiteit Delft, promotor |
| Dr. ir. G. Papaefthymiou | Technische Universiteit Delft, copromotor |
| Prof. ir. M.A.M.M. van der Meijden | Technische Universiteit Delft |
| Prof. dr. G. Strbac | Imperial College London |
| Prof. dr. N. Hatziargyriou | National Technical University of Athens |
| Prof. dr. ir. P.M. Herder | Technische Universiteit Delft |
| Prof. dr. ir. K.I. Aardal | Technische Universiteit Delft |

The research has been performed within the framework of 'Infrastructure Roadmap for Energy Networks in Europe, acronym 'IRENE-40', funded by European Commission Seventh Framework Programme.

ISBN: 978-94-6186-297-6



Printed by WŐHRMANN PRINT SERVICE B.V., Zutphen, the Netherlands

# Summary

Power systems conventionally have been designed and operated to facilitate electrical energy transportation from large centralized power plants to distant load centres. It is currently under development towards the purpose of being able to facilitate more distributed generation from renewable energy sources (RES), for instance wind and solar energy. Increasing the share of RES would allow us to replace carbon-intensive energy sources and achieve significant reduction of the greenhouse gas emissions, establish vast and inexhaustible energy supply, and offer more affordable electricity price amongst others.

On the other hand, the integration of RES to the existing power systems brings additional challenges to system planners and operators. Transmission system operators (TSOs) are already facing operational challenges of high power flows starting in the areas with large wind power installations in Germany to the remote load centres, observing substantial loop flows through Poland and the Czech Republic. As a consequence, the daily operation of Europe's electricity system is increasingly threatened by the risks of blackouts or component failures with wide-reaching impact. According to ENTSO-E the changing generation mix will contribute to upcoming congestion situations, resulting in a limitation in possible exports. The Commission's Priority Interconnection Plan also points out the danger arising from the operation of networks closer to their physical limits.

It is of utmost importance to develop a methodology that is able to identify transmission network bottlenecks, i.e. those components with a high potential to be the origin of a major blackout or cascading event, meanwhile incorporating the uncertainties caused by the RES integration as well as the diversified energy policies in terms of future generation mixes. The improvement of the transmission and distribution infrastructure begins with the identification of its current shortcomings.

Another aspect of power system assessment is to investigate transmission congestions, which is labelled as the 'symptom' of the insufficient transfer capacity when the existing capacity cannot facilitate the desired electricity demand. The reduction of congestions is an indicator of social and economic welfare assuming equitable distribution of benefits under the goal of the European Union to develop an integrated market as stated in the ENTSO-E

Ten Year Development Plan. A relative small number of additional capacity could lead to major economic benefits for many consumers, as advised by US Department of Energy.

For such demanding requests on the power system assessment, there is strong need to translate the explained challenges into an engineering problem, which requires a clear technical vision of the aforementioned challenges in the power system operation and planning, in addition to a clear understanding of power system modelling with substantial supporting material of mathematics.

To substantiate the knowledge of both engineering and mathematics, the thesis provides a structured way of elaborating the engineering background of power systems as well as the mathematical formulations that are essential for understanding the novelty of the proposed methods (Chapters 2, 3 and 4 of this thesis).

Chapter 5 provides a method for the transmission network assessment taking into account the wind stochasticity using a unified Monte-Carlo method and Copula approach. Two main reasons of using the Monte-Carlo method are a) the anti-aliasing property and b) the ability to quickly approximate the answer that otherwise would be very computation-intensive. The methodology is firstly elaborated and applied to a single scenario study, and further enhanced to a more general approach that allows taking into account multiple scenarios caused by uncertainties raised from energy policy perspectives. The solution set of the multiple scenario study captures the impact of uncertainties of all energy policy perspectives without increasing the size of stochastic infeed inputs.

A new method for the transmission expansion planning problem is presented in Chapter 6 and 7, which separate the topic into snapshot-based and multi-stage expansion planning methods. Actively optimizing Lagrangian multipliers as 'primal' variables in the optimization problem is used as a tool for the network expansion, providing the copper-plate topology from either a congested or an infeasible grid configuration. The method also emphasizes the over-investment issues by introducing a maximum allowable overloading factor, to prevent a large amount of inefficient investment on 'minor' congestions. The multi-stage expansion planning method further strengthens the snapshot-based method by proposing the optimal network topology at different time horizon chronologically, taking into account the possible scenarios of conventional generation mix, load and wind energy infeed at each stage. The modular approach of functionally partitioning the multi-stage planning methodology offers additional advantages including a) reducing computational effort, b) allowing easy modification of the existing modules, and c) allowing adaptation of other modules for enhancement, etc. The final optimal expansion plan at each stages guarantees the copper-plate network structure subject to various scenarios and wind generation infeeds at the lowest operational and investment costs.

# Samenvatting

Van origine worden elektriciteitsvoorzieningssystemen ontworpen en gebruikt voor het transport van elektrische energie van grote, gecentraliseerde, elektriciteitscentrales naar belastingcentra. Op dit moment is de ontwikkeling gaande om meer gedistribueerde opwekking van duurzame energiebronnen (RES) in dit systeem te faciliteren, denk hierbij aan wind- en zonne-energie. De toename van het aandeel RES maakt het onder andere mogelijk om koolstof-intensieve energiebronnen te vervangen en een aanzienlijke vermindering van de uitstoot van broeikasgassen te bereiken, een grote en onuitputtelijke voorraad energie te verkrijgen, tegen betaalbare elektriciteitsprijzen.

Aan de andere kant brengt de integratie van RES in de bestaande energiesystemen extra uitdagingen voor systeemontwerpers en exploitanten met zich mee. Transmissiesysteembeheerders (TSO's) worden al geconfronteerd met de operationele uitdagingen van grote vermogensstromen beginnend in de gebieden met grote windenergie-installaties in Duitsland naar de afgelegen belastingscentra, waarbij aanzienlijke stromen door Polen en de Tsjechische Republiek vloeien. Als gevolg daarvan wordt de dagelijkse werking van het Europese elektriciteitssysteem in toenemende mate bedreigd met het gevaar op black-outs of defecten van onderdelen, beide met verreikende gevolgen. Volgens ENTSO-E draagt de veranderende opwekkingsmix bij tot toekomstige congestiesituaties, resulterend in een beperking in mogelijke uitvoer. Het Priority Interconnection Plan van de Europese Commissie wijst ook op de gevaren die ontstaan als elektriciteitsnetwerken dichter op hun fysieke grenzen werken .

Het is van het grootste belang om een methode te ontwikkelen waarmee knelpunten in het transmissienet kan worden gedentificeerd, dat wil zeggen componenten die in potentie de oorzaak kunnen zijn van grote black-outs of cascade effecten, terwijl de onzekerheid die veroorzaakt wordt door de RES-integratie alsmede het ontwikkelen van een gevarieerd energiebeleid in termen van toekomstige generatie mixen, wordt meegenomen. De verbetering van de transmissie-en distributie-infrastructuur begint met de identificatie van de huidige tekortkomingen ervan.

Een ander aspect van assessment van elektriciteitsvoorzieningssystemen is om de congestiesituaties te onderzoeken, welke worden bestempeld als het 'symptoom' voor een ontoereikende transmissiecapaciteit wanneer de

bestaande capaciteit de gewenste vraag naar elektriciteit niet kan faciliteren. Volgens het ENTSO-E Ten Year Development Plan is, onder voorwaarde van een eerlijke verdeling van de voordelen (wat een doel is van de Europese Unie om een gentegreerde markt te ontwikkelen), de vermindering van congestie een indicator voor de sociale en economische welvaart. Zoals gesuggereerd door het Amerikaanse ministerie van Energie zou een relatief kleine hoeveelheid extra capaciteit kunnen leiden tot grote economische voordelen voor veel consumenten..

Voor dergelijke vergaande eisen aan de assessment van het elektriciteitsvoorzieningssysteem, is er een sterke behoefte om de hiervoor beschreven uitdagingen te vertalen ineen ontwerpprobleem. Dit vraagt naast een helder en degelijk inzicht in de wiskundige modellen, om een duidelijke technische visie op de genoemde uitdagingen in de planning en bedrijfsvoering van elektriciteitsvoorzieningssystemen.

Om de noviteit van de in dit proefschrift voorgestelde methoden te begrijpen, wordt in de eerste hoofdstukken de achterliggende wiskundige formuleringen en de achtergrondkennis van de techniek op een gestructureerde manier uitgelegd (hoofdstukken 2, 3 en 4 van dit proefschrift).

Hoofdstuk 5 geeft een methode voor assessment van het transmissienetwerk waarin, met behulp van een verenigde Monte-Carlo methode en Copula benadering, rekening wordt gehouden met de stochastiteit van de wind. De twee belangrijkste redenen voor het gebruik van de Monte Carlo-methode zijn a) de anti-aliasing eigenschap en b) het vermogen om snel het antwoord te benaderen, wat anders zeer berekeningsintensief zou zijn. De methode wordt eerst uitgewerkt en toegepast op enkele scenariostudies, en verder verbeterd tot een meer algemene aanpak die het mogelijk maakt rekening te houden met meerdere scenario's veroorzaakt door onzekerheden die worden veroorzaakt door het almaar veranderende energiebeleid. De oplossingsreeks van de meervoudige scenariostudie vangt de impact van onzekerheden in het energiebeleid af, zonder verhoging van de grootte van stochastische variabelen.

Een nieuwe methode voor het transmissie uitbreidingsplanningsprobleem wordt genoemd in hoofdstukken 6 en 7, welke het onderwerp verdeelt in een snapshot-gebaseerde en multi-stage uitbreidingsplanningsmethode. Het actief optimaliseren van de Lagrange multiplicators als 'oer' variabelen in het optimalisatieprobleem wordt gebruikt als een instrument voor de uitbreiding van het netwerk en levert de koperplaattopologie van ofwel een overbelaste of een onhaalbaar netconfiguratie. De methode benadrukt ook de overinvesteringsproblemen door invoering van een maximaal toelaatbare overbelastingsfactor, om een grote hoeveelheid van inefficinte investeringen op kleinere congesties te voorkomen. Verder versterkt de multi-stage uitbreidingsplanningsmethode de snapshot-gebaseerde methode door de optimale netwerktopologie op verschillende tijdstippen chronologisch voor te stellen, in elke fase rekening houdend met de mogelijke scenario's van conventionele opwekkingsmix, belasting en wind energie toevoer. De modulaire benadering van functioneel afscherming van de meerstaps planningsmethodologie biedt extra voordelen, waaronder a) vermindering rekentijd, b) het mogelijk maken van eenvoudige aanpassingen van bestaande modules, en c) het mogelijk maken van aanpassing van andere modules voor verbetering, enz. Het uiteindelijke optimale uitbreidingsplan bij elke fase garandeert dat de koperplaatnetwerkstructuur wordt onderworpen aan verschillende scenario's en invoeding van windenergievoor de laagste operationele en investeringskosten.

# Acknowledgement

First of all, I would love the express my sincere gratefulness to my promoter, Prof. ir. Lou van der Sluis, who offered me such a great opportunity to work in our group, Electric Power Systems group at Delft University of Technology. I cannot thank him enough for his valuable advice, not only about academic performance but also the view of life, in additional to his sense of humour while we travel together. My special thanks extends to my supervisor, Dr. George Papaefthymiou, who has been always supportive and caring. Without the valuable experience and support from Lou and George, managing the EU collaborative project cannot be this successful. Also, my appreciation deeply goes to Dr. Gabriel Olguin who was my master thesis supervisor, and Dr. Mohammad Reza, who together with Gabriel recommended me to TU Delft.

Secondly, my appreciation goes to all my colleagues in our group. The first name I would like to mention is Shahab Shariat Torbaghan, my office mate, who shared a lot of insightful ideas about both research and the Farsi language with me. I will keep the good memory of a lot of fun with you in the office. To other colleagues, Mart van der Meijden, Marjan Popov, Madeleine Gibescu, Freek Baalbergen, Gerben Hoogendorp, Arjen van der Meer, Jens Boemer, Alicja Lojowska, Ana Ciupuliga, Barry Rawn, Bart Tuinema, Laura Ramirez Elizondo, Romain Thomas, Andreas Theocharis, Mario Ndreko and those who are not working with us anymore, Nima Farkhondeh Jahromi, Ralph Hendriks, Bob Paap, and Ioanna Xyngi, I am proud of working with all of you. Thank you so much for making an international student feel like home. To my long lost friend, Nima, I hope you are enjoying your life. Needless to say, our secretaries, Deborah Dongor, Iris de Jel, Laura Bruns, Ellen Schwenke-Karlas and Veby Agus who showed their smiles every time I needed help in administrative tasks. Thank you all for such great assistance.

Special thanks goes to Jacqueline Gerritsen and Freek Baalbergen who helped me in translating the summary of this thesis work from English to Dutch.

My thankfulness extends to all the students I have supervised, Betty Tessema, Rutger Kerkkamp and Ruoshi Wang. During your master or bachelor thesis period, we worked together and strived together to achieve what we aimed at. It is my pleasure to work with each and every one of you.

Special thanks to Rutger, who generously helped me in designing a more elegant thesis in Latex.

Then, it is all about IRENE-40 partners. During the period of the IRENE-40 project, I am the most thankful of working with all of you. I have learned a lot from you during these four years. The experience of involving in an EU-wide research programme was genial and pleasant. To all colleagues and friends from ETH Zurich, RWTH Aachen, Imperial College London, NTUA, ECN, Siemens, Alstom and ABB, I believe that we together made some great achievements there. Special thanks to Nils Meijer, who is always kind to arrange the financial tasks.

Also, the committee members of my PhD thesis are greatly acknowledged. I thank you for devoting your precious time to read and comment my thesis. Your valuable yet insightful comments not only strengthen my thesis work by increasing its credibility, but also generously share your broad knowledge with me who is a relative new-comer of the research world.

To all my other friends, you made my PhD period more colourful and lively. I cannot list your names, as the list will be too long. For the ups and downs during the period, I can always count on your constructive support. Sometimes, a few meaning words are more than enough to bring me back from the lousy mood.

Last but not least, my whole heart belongs to my family, my strict father Liu Zhilin, my caring mother Zhao Qinghua and my lovely wife Sun Rui. With your unconditional love and support, the PhD journey had been truly amazing. Especially to my father, your encouragement brought me on the right track of pursuing a PhD degree. I respect your insightful suggestion and now it is the rewarding moment of the choice we made together. To all my other family members, especially grandparents, uncles, aunts and cousins, your support makes me strong and fearless of any challenges. I left the country for receiving higher education abroad 14 years ago. During all these years, you have generously done so much that should be have been done by the only son of the family. I admire your caring support, which significantly helped me to focus more on the study and work abroad. I believe this is the right moment to thank all of you. I love you all.

Zongyu Liu
Arnhem, April 22, 2014

# Contents

# List of Figures

# List of Tables

# Chapter 1

# Introduction

The electrical power system is an indispensable carrier that facilitates the power transfer from the primary energy sources to the consumers. It is under development towards the purpose of being able to facilitate more distributed generation and enabling bulk power transfer at high voltages. In the context of the European continent, the ambitious so-called '20-20-20' targets (standing for 20% de-carbonization of the EU greenhouse gas emissions from 1990 levels, 20% share of renewable energy sources (RES) and 20% improvement in energy efficiency by 2020) imply that the share of RES in the generation mix is now rapidly growing favoured by the current legislative climate, and brings additional challenges for the grid to catch up. Such intentions voiced by the EU necessitate more research effort on the pressing issues related to the RES integration in the power system in both operation and planning phases.

Wind power is gaining wide recognition as a valuable and economical option for future power generation. With a total of more than 238 GW installed capacity world wide at the end of 2011 [Cou12], almost half of the energy production from wind is located in European countries of 96.6 GW, mainly in Germany and Spain and the north sea region. The wind power infeeds are managed by the continental European transmission system operators (TSOs) in their day-to-day operation of the European interconnected system.

The integration of wind energy into the power system requires a thorough assessment of the existing power system infrastructure in Europe, both on the generation side due to additional requirements for balancing power, and on the grid side to enable transferring the bulk power from wind farms. Not only the integration of wind energy affects the individual national grids, but also the cross-border interconnectors. It can also be foreseen that the wind forecast-related balancing power may affect the energy trading in the electricity market. That is, TSOs may introduce additional measures to reduce the import/export transfer capacities available to the market to allow for sufficient security margin for balancing requirements, such as utilizing additional power plants outside their own jurisdiction. This will further require a solid legal framework to prevent disputes between the market players at the national and European regulatory level [EE09].

## 1.1 Problem Statement

### 1.1.1 Power System with Uncertainties

The share of stochastic generation in the power system energy mix has significantly increased in recent years. Stochastic generation refers to electrical power production by the use of an uncontrolled primary energy mover, corresponding mainly to renewable energy sources. Traditionally, the main system variability comes from the power consumption. The uncertainty of the load varies with different seasons, weeks, days and hours. The incorporation of stochastic generation in power systems further increases the variability of the system power flows, resulting in potential congestions in the transmission and distribution networks. The combined estimation of the variability from wind power and system loads is important for the planning of the necessary system reinforcements, including first the identification of transmission bottlenecks and the development of strategies for system expansion. For the assessment of this variability, the uncertainty in the system inputs should be modelled. Another important aspect related to uncertainty analysis originates from diversified energy policies. Energy policy directive is one of the driving forces that encourages the generation fleet to operate in a certain direction, which in turn changes the power flow pattern in the power system. A comprehensive methodology of evaluating the steady-state power system behaviour is thus of importance, taking into account the possible future energy directives into assessment in addition to other uncertainties aforementioned.

### 1.1.2 Congestions

Transmission network congestion appears when the transfer capacity is not sufficient to facilitate the power delivery from the generating units to the load. Why do we care about the congestion? A few reasons may answer. Economically speaking, generators with higher cost have to generate in order to compensate the 'shut-down' of low-cost generators, resulting in higher system generation cost. Moreover, in the liberalized market structure, congestion increases the chances of abusing market power, meaning that the higher cost generator theoretically can offer higher price than its marginal production cost due to less competition from other cheaper generators constrained by the insufficient transfer capacity. Technically, the stressed network is less reliable and further reduces network manoeuvrability. To relieve congestions in the network meanwhile maintaining the investment cost at the most economical level is essential for the network planner. The congestion-free network structure with its associated cost may be further used for the policy-makers as the benchmark system structure to compare with other network structures which allow congestion in the system, i.e. the most economical congestion-free expansion plan versus other expansion plans that allows congestion.

### 1.1.3 Research Objectives and Scope

The goal of this thesis work is to define the optimal solutions for upgrading transmission networks under demand and stochastic generation uncertainty. Optimal solutions are considered ones that lead to minimization of operation and investment costs meanwhile keeping the required levels of system security. To be more specific, this thesis tackles the following objectives in terms of different related tasks,

- To provide methodology for identifying weak network points
- To provide methodology for power system expansion

for future networks with high penetrations of stochastic renewable energy sources with main focus on wind. Both objectives are achieved taking into account the system variability caused by stochastic generation. The methodology for identifying weak network points should be able to reflect the impact from the stochastic nature of wind, by providing the probability spectrum of system output variables (i.e. power flow, node power injection, price, etc.). Similarly, the system expansion planning includes the probability of new potential generation capacity in the future and potential transfer capacity for the optimal solution of congestion alleviation. The expansion strategy from the methodology should be able to point out one single expansion solution under the scenario including various stochastic generation, and possible new generation capacity. Dynamic behaviour of the system is beyond the scope of the thesis work.

The optimization software tool AIMMS and technical computing software MATLAB have been used in this research. AIMMS is used for solving optimal solution of OPF problems. Meanwhile, MATLAB is used for stochastic modelling and post data processing.

### 1.1.4 General Approach

In this work, Optimal Power Flow (OPF), combined with a unified Monte-Carlo simulation (MCS) methodology is presented that identifies the network congestions taking into account the correlated stochastic generation. MCS consists of the combination of a deterministic model, in this case OPF, with a stochastic perturbation of the inputs. OPF is a deterministic method to analyse the power flow with respect to the objective function and constraints. MCS, on the other front, is suitable for coping with significant uncertainty in inputs. This thesis adopts OPF, combined with MCS, to calculate the spectrum of the loading of transmission corridors, power outputs from each generating unit as well as the price levels of each node. The novelty of the methodology is the combination of the Copula modelling of wind infeed with the OPF studies. The advantage of such MCS modelling is a) Wind MCS sample space is fixed for possible generation scenarios. That is to say, power generation from conventional power plants and wind power infeed are completely decoupled. Assuming 10000 wind power infeed samples are being investigated, the sample space of 10000 wind infeed can be used for different possible generation mix in the future. This may significantly improve the computation speed when more generation scenarios are foreseen. b) The wind variability can be modelled, providing spectrum of variables (i.e. power flow) rather than a deterministic result of a snapshot of the system state.

Furthermore, network expansion strategies for congestion alleviation are proposed using similar optimization techniques taking into account the uncertainty of stochastic inputs. The Lagrangian multipliers (dual variables) have been explicitly controlled in the optimization problem to achieve the expansion target. The novelty is to explicitly link the locational marginal price (LMP) to the network expansion decision variables. By controlling the LMPs, the expansion target can thus be achieved. Mathematically speaking, in the optimization problem, Lagrangian dual variables are explicitly calculated and controlled in order to indirectly control the primal variables in the primal problem. The advantages of the proposed expansion method include a) alleviation of all congestions in the system at the minimum cost, b) selection of the optimal expansion solution that is technically and economically feasible, c) expansion to congestion-free network from either congested or infeasible network topology.

## 1.2 Research Framework

The research presented in this work has been conducted under the project named 'Infrastructure Roadmap for Energy Networks in Europe', (Acronym: IRENE-40). IRENE-40 is a collaborative project under EU Research Framework Programme 7. The mission statement of the project is to identify the strategies for investors and regulators enabling a more secure, ecologically sustainable and competitive European electricity system [IRE12]. The partners involved in the project comprise with universities, a research institute and industrial manufacturers. IRENE-40 consists of six work packages, Fig. 2.1 shows the project overview.

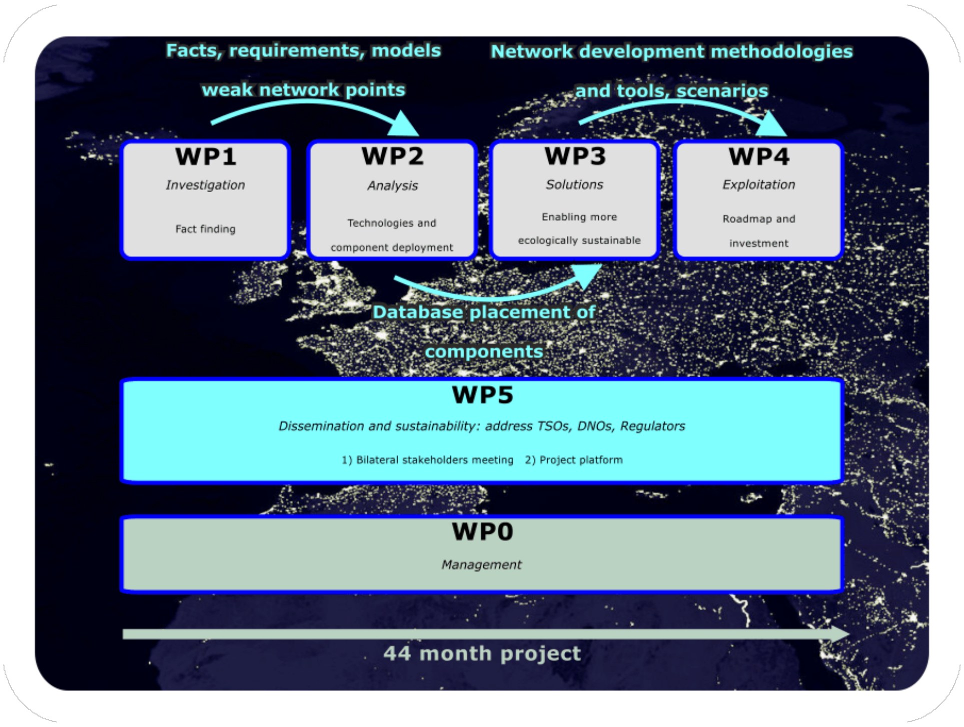


Figure 1.2.1: Project overview of IRENE-40

Work package 0: Top level management concerns coordination of the interactions between the EC and the project and ensuring overall legal, contractual; ethical, financial and administrative management of the consortium. This task involves monitoring of progress and ensuring any corrective actions necessary for maintaining the schedule and achieving the technical targets are properly determined and implemented. This includes operation of the Steering and Technical Committees and the Consortium Knowledge Panel and implementation of the deliverables and reporting plan.

Work package 1: The overall objective of WP1 is to investigate the current situation in European energy networks in terms of technology, communication, control methods, markets, and weak network points as well as to set the boundaries of the roadmap. The first objective for this work package is that an overview of existing generation/consumption models (focussed on electrical energy) is established. Existing energy markets are evaluated and new criteria for the development of markets are identified. The second objective for the work package is that a methodology to identify weak network points and elements (i.e. those components with a high potential to be the origin of a major blackout or cascading failure) is developed. The technical, regulatory and economic barriers impeding the establishment of the pan-European grid and the technological scope of the measures to be studied in the project are identified.

Work package 2: This work package identifies the technologies that will be available over the coming 40 years. These technologies have been characterised in order to quantify the impact of their use within system development scenarios, paying special attention to the enabling technologies identified by the SmartGrids platform. The second step is the development of methodologies for the selection of new technologies and their placement at the weak network points (after having identified associated operational risks). Finally, scenarios describing the boundary conditions for the deployment and economic assessment of components and new network schemes is derived. Furthermore, the work package implements a component database including present and emerging technologies (for conversion, transmission and storage of electrical energy), and establish methods to identify and quantify the expected evolution of component characteristics over the next 40 years. The last objective is to develop technological communication requirements for interlinking of demand, energy supply and networks. A particular focus is laid on the potential contribution of responsive demand in system development.

Work package 3: This work package develops strategies for the development of electric power systems by the addition of new components (transmission, conversion or storage) to increase environmental sustainability, security and competitiveness. Methods for the quantification of the potential impact of these measures in technical and economic terms are developed as well. Furthermore measures for a better coordination of neighbouring systems are investigated. Moreover, based on the quantitative analysis of different scenarios and options, a preferred scenario for Europe's electricity infrastructure development towards a pan-European electricity network is established.

Work package 4: A roadmap document is produced indicating the best possible steps to be undertaken by the network participants and the regulators (in terms of incentives) during the coming 40 years. The roadmap will seek to realise an electrical energy system with higher environmental sustainability, higher security and more competitiveness and to encourage the completion of a pan-European electricity network. At the end, electrical network infrastructure as well as Research and Development investment strategies for the stakeholders (policy makers, owners, operators and manufacturers) are elaborated.

Work package 5: Establish and exploit mechanisms for efficient communication, transfer of knowledge and provision of training to the user and decision making community. Ensure sustainability of knowledge and tools following completion of the project.

## 1.3 Outline

The thesis is organized as follows,

- In Chapter 2, the fundamental principles of the power system operation are presented. This chapter includes the structural evolution of power systems from vertical to horizontal. The emphasis goes to classification of generation technology, ranging from conventional generation of nuclear, coal, hydroelectric to non-conventional generation of wind and solar power.

- In Chapter 3, the mathematical formulation of modelling the power system are addressed. The chapter consists of mathematical background of optimal power flow (OPF), organized in terms of objective function definition and various constraints including energy balance, network and generator constraints.

- In Chapter 4, introduction to mathematical background has been reviewed. This chapter includes both theoretical and mathematical background of stochastic modelling of wind energy. The second section introduces optimization essentials for the network expansion studies.

- In Chapter 5, the methodology of the identification of weak network points has been presented, combining OPF and stochastic modelling of wind power infeed. A case study of a reduced version of the UCTE (stands for Union for the Coordination of the Transmission of Electricity) network has been investigated using the methodology. Uncertainties caused by diversified energy policies, in addition to intermittent energy integration are also modelled and investigated.

- In Chapter 6, the methodology of network expansion has been discussed, providing the most economical solution for the system operators to build the copper-plate grid topology.

- In Chapter 7, a comprehensive multi-stage network expansion methodology is presented, taking into account the variability of wind power infeed and possible generation mixes by further utilizing the snapshot-based expansion method presented in Chapter 6 as the core assessment within a single stage, accompanied by clustering technique and decision making risk assessment.

- Conclusions and recommendations are provided in Chapter 8.

# Chapter 2

# Power System Structure and Operation

## 2.1 Introduction

This chapter explains the fundamental principles of the power system operation in terms of the evolution of the power system structure from vertical to horizontal. Because generation and load changes are the main driving forces of the transmission and distribution networks reinforcement, they are discussed extensively in this chapter. At the end of this chapter, a collection of the TSOs' operational experiences and challenges is presented, covering the current situation and foreseen future challenges with large renewable integration to the system.

## 2.2 Vertical Power System

Power systems have been designed and operated to supply the power from generation to load. Traditionally they are built based on the vertical structure. Vertical refers to the power flow direction, specifically from the generating units to the load centres via meshed transmission and radial distribution grids. The electrical power is generated from a small number of large power plants, (see Fig. 5.1), which are usually sited near the energy source or its supply routes, and sometimes remote from the load centres. After its generation, the power is transported through transmission and distribution grids to the load. One of the fundamental differences between the transmission and distribution grids is the voltage level. In general, 380 kV and above belong to the transmission voltage level, while the voltage level from 220 kV and below belong to the distribution grid. Fig. 5.1 shows the visual illustration of the top-down design of the vertical power system. To increase the availability and reliability of the power supply, the transmission grid is further designed to be meshed, which provides alternative path for power flow in case of a fault. The distribution grid are designed mostly in a radial way, which enables the protection scheme to operate only at the certain location when a fault occurs, without interrupting other loads.

## 2.3 Horizontal Power System

The large scale incorporation of non-conventional power plants (wind farms, Photovoltaics plants) leads to a new power system structure, shown in Fig. 6.1. From the system structure point of view, the change happens on the load side. Originally, the load side only consumes power without any power generating capability, In other words, no generating units are installed on the load side. The transition observed in the power system evolution is that more non-conventional generators (i.e. wind farms, solar panels, etc) are installed on the distribution systems which provide the generation capacity to support the distribution and transmission grids locally. From the power flow viewpoint, the power flow direction is not uni-directional (i.e. from the large conventional generators to the load centres), but bi-directional (i.e. from non-conventional generators to the load centres within the distribution grid, or from non-conventional generators back to the distribution or transmission grids to support the power system). Recall that in the vertical power system structure, the load side does not actively participate in the system operation. Given a certain load profile, conventional generators are responsible for producing sufficient power to support all loads required. With the large scale implementation of non-conventional generators, the non-conventional units installed on the load side actively participate in the system operation by supporting the load locally within the distribution grid or sending the power back to the distribution or transmission grids.

### Smart Grid

Smart grid is a widely used term that refers to the idea of incorporating information and communications technology (ICT) to the distribution system. The distribution system is thus transferred from radial and dumb to meshed and intelligent. The desired functionalities include [Bro08]

- Self healing
- High reliability and power quality
- Resistance to cyber attack
- Accommodation of a wide variety of distributed generation and storage options
- Optimized asset utilization

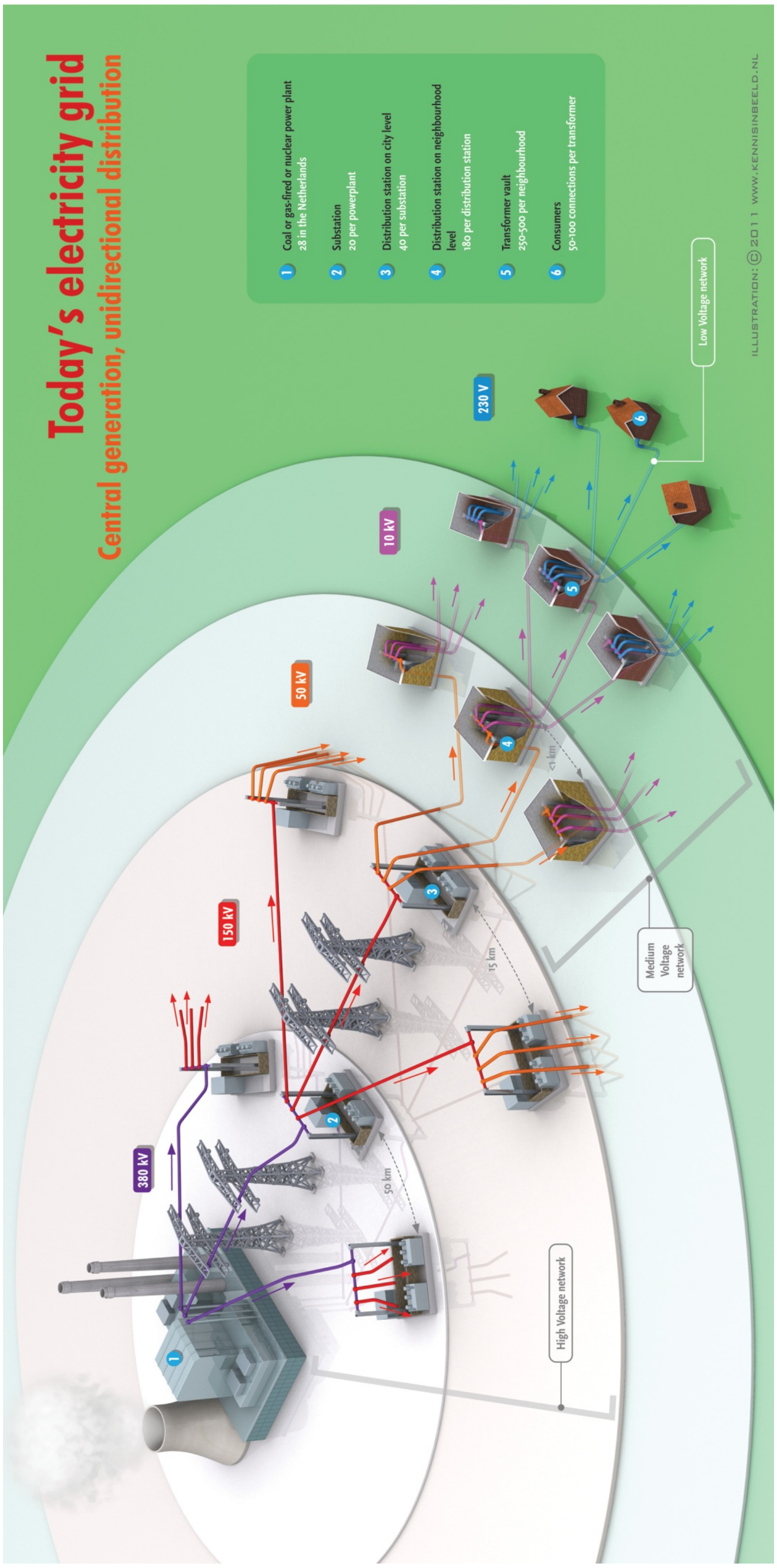


Figure 2.2.1: Vertical power system (Courtesy of Eric Verdult)

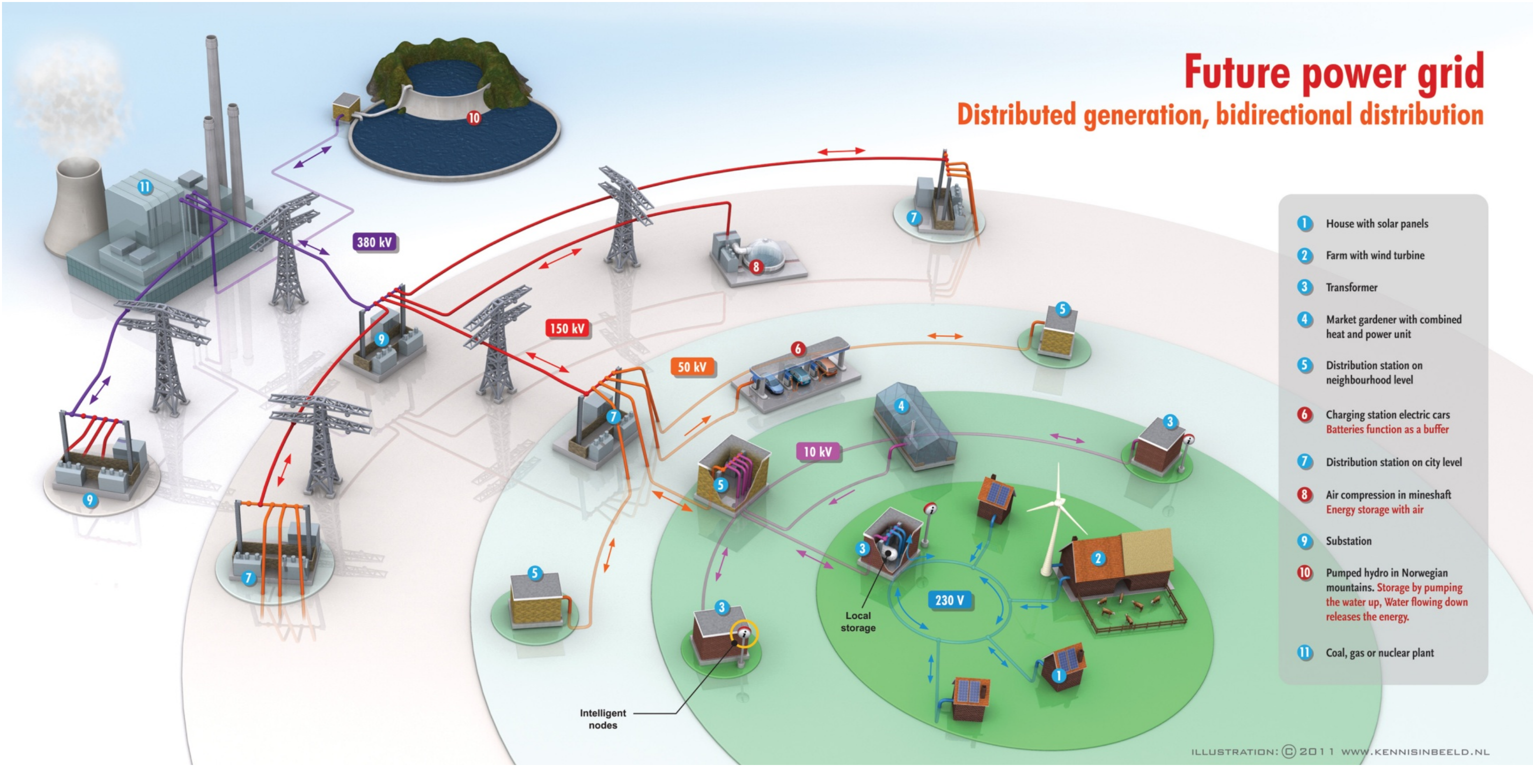


Figure 2.3.1: Future power system (Courtesy of Eric Verdult)

- Minimized operation and maintenance costs

Traditionally, distribution systems and consumers played a minimal role in power system in terms of operation and control. Although many distribution utilities have used demand side management schemes, the controllability of such schemes is rather limited. The lack of such involvement can be at least partially explained as the consequence of absence of enabling communication and control infrastructure. Smart grid technology promises cost-effective solutions that overcome these limitations, allowing consumers to react to power system conditions in real-time and thus actively participate in the system operation.

One of the practical challenges related to smart grid, especially in the demand side participation, is the data acquisition and the control strategies.

It is anticipated that the smart grid technology market increases 20% annual increase, reaching about \$ 171 billion by 2014, according to market reports by Specialist in Business Information (SBI). Mckinsey estimated China's smart grid market could total \$20 billion annually by 2015, the markets for smart meters and wind power connectivity could reach \$ 2 billion and \$ 800 million respectively on an annual basis by 2015 [McK10]. The European Electricity Grid Initiative (EEGI) is one of many EU projects focused on smart grid research and implementation. The total budget for this program is about €2 billion.

## 2.4 Evolution of Power Systems

The evolution of the power system is shown in Fig. 7.1. Phase *a* refers to the vertical power system discussed above, where only centralized generation supplies the load via the transmission grid. In phase *b*, distributed generators appear on the load side and partially support the load. At this stage, since the penetration of distributed generators is relatively low, the conventional generators still play an important role in terms of the number of being committed in the system. In other words, the distributed generators do not have much influence to the number of committed centralized generators. Phase *c* represents the large penetration of distributed generators that strongly influence the committed centralized generators, since most of the load is served by local distributed generators. In phase *d*, we anticipate the scenario that enough distributed generators are installed to supply all loads. The system structure might finally reach the stage where no centralized generators are necessary in the power system. Currently, we are in the transition period between phase *b* and *c*. The concept of smart grid, as discussed in the above section, substantiates the transition by facilitating the deployment and utilization of the distributed generation to a larger scale.

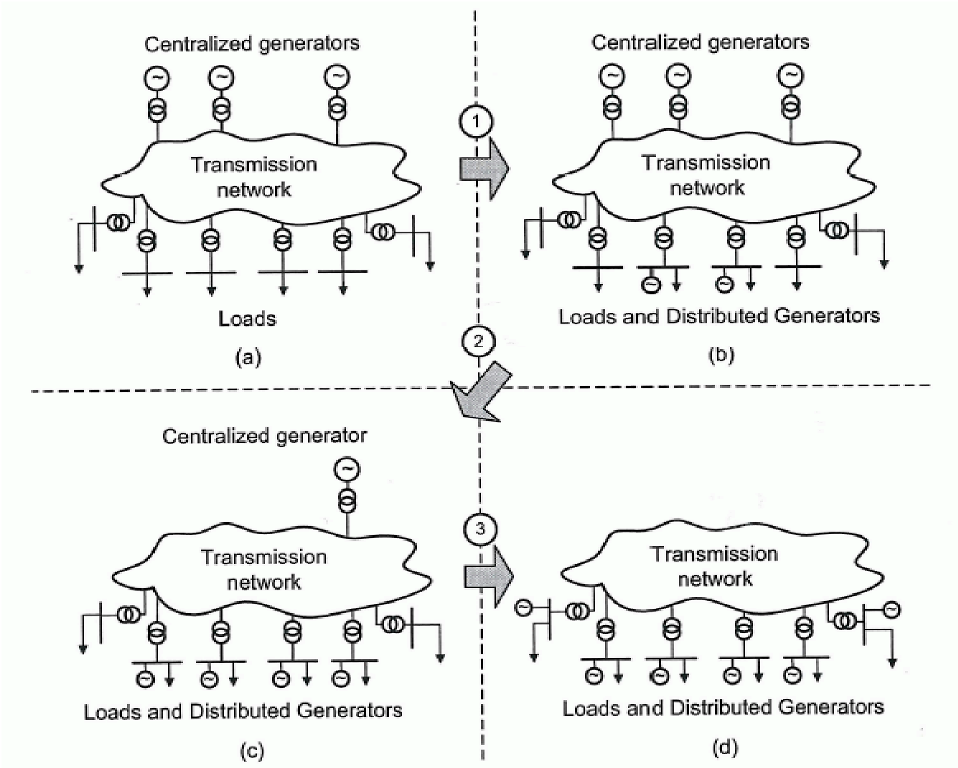


Figure 2.4.1: Vertical to horizontal transformation of power systems [Rez06]

## 2.5 Conventional Generation

### 2.5.1 Conventional Thermal Plants

Conventional thermal plants convert the primary energy from nuclear, coal, gas into electrical energy. The first step of the conversion process is to transform the chemical energy of fossil fuels into thermal energy, either by fission (nuclear) or by combustion (coal and gas). Thermal energy produces steam to rotate the turbine. The mechanical energy is then converted to electrical energy by electrical induction [SvdS08]. The problems caused by the conventional generation are mainly the safe deposit of nuclear waste, the depletion of fossil fuels, greenhouse gases emission, etc.

#### Nuclear

Nuclear power plants supply baseload demand, because of the low production cost relative to other production facilities and the ability to continuously produce energy at a constant rate. Building a nuclear plant is mostly politically and environmentally constrained. One of the advantages of using nuclear energy is that it does not create air pollution, reduces $CO_2$ emission and increase energy security by decreasing dependence on other fossil fuels. Newly built nuclear power plants can reach an average capacity factor [1] of 90% [Wikb]. On the other front, critics believe that nuclear energy is a potential dangerous energy source, with the radioactive waste that cannot be stored safely for a long period of time. Also, the criticism goes to the operational safety of nuclear power plants, as the Chernobyl disaster happened in 1986. In 2011, after Fukushima Daiichi nuclear disaster, Germany has permanently shut down eight of its reactors and pledged to close the rest by 2022.

Traditionally, many claim that nuclear power plants have been viewed and operated as the most inflexible facilities within the conventional power plant fleet. Because nuclear plants are hardly adjustable, frequent starts and shut-downs should be avoided for safety reasons, if possible [BfU09b]. Others further concur that power plants that are supposed to balance the fluctuation of energy production based on wind and sunlight need to be flexible above all. Nuclear power plants are exactly the opposite - inflexible and limited adjustable. They are designed to operate preferably at 100% load, constantly producing the same amount of energy, no matter if it is needed or not [BfU09a]. Nowadays, utilities such as RWE, EON [FT11] and other technical reports [BEF10] conclude that the nuclear power plants are able to adjust their power output over a wide range within a short period of time. This means technically nuclear plants can be operated safely both in base-load and in load-following modes. The main concern is the contribution of nuclear plants to grid regulation impairs their economic profits due to possible higher operation and maintenance costs.

Generally speaking, nuclear power plants are base load power plants that operate at the maximum output because of their lowest fuel cost. The shut down or reduce the power output level only for maintenance or repair purposes. In terms of the nuclear power plants modelling, they are generally treated as the must-run units, mainly because these units are online continuously due to the nature and cost concerns of the plants. Some TSOs (APG[2], TTB[3]) do not use nuclear power plants for redispatching activities. To this extent, as far as the unit commitment in the operation modelling is concerned, the nuclear plants can be treated as always on, reducing the search space of binary variables and allowing faster computational speed in the optimization process.

[1] The net capacity factor of a power plant is the ratio of the actual output of a power plant over a period of time and its potential output if it had operated at full nameplate capacity the entire time.

[2] Austrian Power Grid

[3] TenneT B.V. the Netherlands

### Coal

Certain advantages of using coal as primary energy source include abundant reserve, reliable energy source, and well understood conversion process. Coal-fired power plants are designed to produce electricity in large scale for continuous operation. Similar to nuclear plants, coal-fired plants serve baseload demand in many counties. However, coal combustion in the thermal power plants results in greater amount of $CO_2$ emission per unit of electricity generated,than other fossil fuel combustion, typically 2249 lbs/MWh (1020 kg/MWh) depending on the plant efficiency [Age09a].

Generally speaking, coal power plants are base load power plants as well due to the low fuel cost. However, the dispatch of a coal power plant can be achieved within a few hours range, depending on the generator type and the system operator. Thus, unlike nuclear power plants, the coal power plants are usually considered in the unit commitment optimization process. That is, the dispatchability of coal power plants falls into the electricity market framework (i.e. day-ahead market). The unit commitment and economic dispatch need to be considered when performing the network studies, especially cost-related optimization framework.

*Lignite*: Often referred as 'brown coal', and considered as the lowest rank coal. Lignite is used almost exclusively for steam-electric power generation, contributing up to 50% of Greece's and 11% of Germany's electricity. The heat content of lignite ranges from 10 to 20 MJ/kg on a moist, mineral-matter-free basis. The RWE Power Lignite-Fired plant, located in Neurath, Germany, consists of 2 blocks of 1100 MW, increases efficiency from traditionally 35% to the new level of 43% [Pow11]. One of the pressing issues related to the lignite plants is the higher $CO_2$ emission, comparing with the hard coal plants in general.

*Hard coal*: Literally referred to 'anthracite', is a hard, compact variety of mineral coal that has the highest carbon count and contains the fewest impurities of all coals. It is primarily used for residential and commercial space heating. According to European Environmental Agency, the $CO_2$ emission factor of hard coal power plants in European Union is 94.6 kg/GJ, less than 101 kg/GJ of lignite plants. Evaluating other gases by-products of burn coals such as $SO_x$, $NO_x$, the comparison shows once again that hard coal is the preferred fuel source over lignite [Age08].

*Clean coal technology*: To reduce the high greenhouse gas emission, clean coal technology are being developed to mitigate the environmental impact from coal power plants, or broadly speaking, fossil fuel plants. Many techniques have been developed to fulfil such task, including chemically washing minerals and impurities from the coal, integrated gasification combined cycle

(IGCC), which aim at removing $CO_2$ and other pollutants before combustion. Another technique to reduce the $CO_2$ emission from fossil fuel plants is to employ carbon capture and storage (CCS), which refers to technology capturing $CO_2$ from fossil fuel use in power generation, and pumping it into underground geologic formations. North America and Europe contain most of the large scale integrated projects for gas plants as of 2011. Specifically, the United States and Europe account for 25 and 21 projects respectively [Ins11].

**Gas turbines**

A gas turbine is a rotary engine that extracts energy from a flow of combustion gas. Compared to nuclear or coal-fired power plants, the advantages of gas turbines is the ability to be turned on or off within minutes, much faster than nuclear and coal plants. This is particular helpful to supply electricity during peak load period. The $CO_2$ emission per unit of electricity generated is 1135 lbs/MWh (515 kg/MWh) [Age09b].

Gas power plants are known for its high flexibility of its output power level, but are also among the most expensive to operation due to the higher fuel cost. Therefore, they are generally used as the peak power plants when maximum demand is being supplied.

*Open-Cycle Gas Turbine (OCGT)*: A gas turbine prime mover in which air is compressed in the compressor element, fuel is injected and burned in the combustor, and the hot products are expanded in the turbine element and exhausted to the atmosphere. Heat engines are only able to use a portion of the energy their fuel generates. The remaining heat (e.g. hot exhaust fumes) from combustion is generally wasted. The typical efficiency of an OCGT ranges from 30% to 35% [Pou03].

*Combined-Cycle Gas Turbine (CCGT)*: A gas turbine generator generates electricity and the waste heat is used to make steam to generate additional electricity via another steam turbine. This last step enhances the efficiency of electricity generation. Most new gas power plants in North America and Europe are of this type. The efficiency of combined-cycle power plants can exceed 55% [Pou03].

Gas turbines have a relatively high availability factor ranging from 80% to 99% [Wika]. The high availability offers high degree of generation flexibility, which has direct impact on the penetration level of intermittent energy into the power system. A more flexible system of more hydro- and gas-powered electricity can achieve a certain level of wind energy integration with less effort and cost than in a less flexible system. For instance, In Portugal, a high level of generation flexibility containing a large amount of fast responding hydroelectric power plants in the system enables a high penetration level without significant additional costs [vHG09].

### 2.5.2 Hydroelectric

Hydroelectric power plants are considered as conventional plants as well. Similar to the coal power plants that use steam to turn the turbine blades for the electricity production, hydroelectric power plants use falling water to turn the turbines. In terms of energy conversion, the hydraulic turbine converts of flowing water into mechanical energy, and the hydroelectric generator converts this mechanical energy into electricity.

Hydroelectric power plants play a very important role in the power system. Brown et al. [BMD11] claims that hydroelectric power is the most mature, reliable and cost-effective renewable power generation technology available. Because of its significant flexibility in their operation and hydro plants can be designed to meet base-load demands with relatively high capacity factors, or have higher installed capacities and a lower capacity factor, but meet a much larger share of peak demand. Plants that have large amount of water on a continuous base can run as the base load plants; others that have limited water resources may be operated as the peak plants.

Hydroelectric power makes substantial amount of electricity generation in Europe and worldwide. It produced 63% of the total electricity produced from renewable energy in the Europe in 2008, or 10% of the total electricity production in the EU-27. Currently, it produces nearly 20% of world's electricity [Sys12]. Norway, one of 25 countries depending on the hydroelectric power for more than 90% of their electricity supply, currently relies on 99.3% of its total electricity supply [Age12b].

The main classification of hydroelectric power plants distinguishes reservoir, pumped storage hydro plants, and run-of-river.

*Reservoir hydro*: Hydroelectric power plants mostly site on water source such as rivers or canals that do not have steady water inflow. To ensure the reliable water supply, dams are needed to form reservoirs that can store water for later use of producing electricity. The reservoir behaves as long-term energy storage. It can store over long period of time, and release stored water to generate steady power on demand, relatively independent from variations in short-term inflow.

*Pumped-storage hydro*: It stores energy in form of water, which can be pumped from a lower elevation reservoir to a higher elevation. During the low-cost period, pumped-storage hydro plants (PHPs) operate in a so-called pumping mode, which is to pump water to the higher elevation reservoir consuming electricity. During the peak demand, PHPs, operating in the 'generating mode' similar to conventional hydro plants, sells electricity to increase revenue. In general, PHPs pump water during night time and weekends when the electricity demand is low, and start electricity generation during peak periods, normally during daytime. According to Muller [LWH08], a modern PHP plant can reach the efficiency level between 70 to 80%.

*Run-of-River*: Run-of-river power plants are built on rivers with a consistent and steady water inflow. The power output from run-of-river plants mainly depends on the water inflow. Due to the lack of energy storage, run-of-river cannot co-ordinate the output power to match the demand, in contrast to hydro power plants with reservoirs.

Note that PHPs cannot be modelled as conventional thermal plants, mainly due to its ability to store and release large amount of energy. When a PHP plant is operating in the pumping mode, it consumes the cheaper energy to store the the water, and release the water to produce the electricity when the electricity price is higher. The operational scheme of PHPs provides the most commercially viable means of large-scale energy storage, facilitating higher penetration of intermittent RES integration into the power system. These PHP plants are very important in the system stability because of the ability to react within seconds to smooth out the fluctuations in the system loads. More detailed modelling information can be found in the ELMOD project [LWH08].

## 2.6 Non-Conventional Generation

Non-conventional generation, also re-phrased as stochastic generation in this thesis work, refers to electricity produced by intermittent renewable sources such as wind and solar energy. It is not evident that baseload are being served by solely using wind and solar energy. However, in combination with storage facilities and advanced control schemes on turbines, there is potential for wind and solar power stepping into the baseload territory. Looking at the non-conventional generation as independent energy sources, due to the use of a non-controllable prime energy mover, the power production from such units presents three main characteristics:

- *Low dispatchability*: Since the power output follows the fluctuations of the primary energy mover, the main control option is the reduction of the power output by reducing the energy yield of the converters (curtailment of production). The combination of stochastic generation with energy storage is considered for enhancing the dispatchability of stochastic generation offering a time-shift in the power production to better fit the system load. However, the consideration of energy storage depends on the options offered by the specific prime energy movers and the respective conversion technologies (e.g. wind turbines and photovoltaic generation convert the prime energy mover to electricity without offering energy storage options in the conversion process, while solar thermal conversion (i.e. CSP) offers the option of thermal storage as an intermediate step in the conversion process).

- *Low predictability*: Due to the use of a non-controlled primary energy source, the power output from such energy sources presents low predictability. This low predictability has a direct impact on the operation, reliability and efficiency of power systems with high penetration levels of stochastic energy sources, necessitating the need of increased operational reserves. As for wind prediction, level of accuracy improves when combining predictions for larger areas. Also, the level of accuracy decreases when the forecast horizon increases. For a single wind power plant the mean error for day-ahead forecasts is between 10% to 20%. For a single control area this error is below 10% [HMO+07].

- *High variability*: This characteristic corresponds to the fluctuating nature of the stochastic primary energy source. Again the conversion technology plays an important role on this aspect, e.g. the output from photovoltaic is highly volatile while solar thermal offers a more constant output due to the thermal inertia of conversion process. In terms of variability of wind energy, general findings are summarized in [HMO+07]:

    1. Very fast variations of distributed wind power are low
    2. The largest hourly step changes recorded from regional distributed wind power ranges from ±10% to ±35% depending on region size and how dispersed the wind power plants are.
    3. Wind power production can vary a lot in longer time scales, around 4-12 hours.

### 2.6.1 Wind

Unlike conventional thermal plants producing electricity from steam turbines, wind power extracts kinetic energy from wind. Wind turbines are generally sited where there is a favourable wind source, either onshore or offshore. Significant development of European wind energy is expected offshore, where the wind blows stronger and smoother and larger turbines can be installed. Another credible concern is that in densely populated Europe there is limited space on land and relatively large offshore areas with shallow water, e.g. in North Sea region.

Wind energy has certain impact on the efficiency and reliability of power systems due to the stochastic behaviour of wind. In [HMO+07], the following focus areas according to different time scales are presented.

- *Regulation and load following*: The time scale of regulation and load following ranges from seconds to half an hour. The variability and uncertainty of wind power affect the allocation and use of reserves in the system. General conclusions on the increase in balancing requirements depend on region size relevant to balancing, initial load variations and geographic dispersion of wind power plants, as well as the type of terrain and local wind structure and typical behaviour.

- *Efficiency and unit commitment*: The time scale ranges from hours to days. The investigation focuses on how the conventional capacity is run and how the variations and prediction errors of wind power change the unit commitment: both the time of operation and the way the units are operated, taking into account generation unit constraints. The technical impact of wind power and cost on the power system is assessed by simulation. In electricity markets, prediction errors of wind energy can cause high imbalance costs.

- *Adequacy of power generation*: the time scale is several years. Adequacy refers to the total supply available during peak load situations. The proper assessment of wind power's aggregated capacity credit in the relevant peak load situations is of importance, taking into account the effect of geographical dispersion and interconnection.

- *Transmission adequacy and efficiency*: The time scale falls from hours to years. The impact of wind power on transmission depends on the location of wind power plants relative to the load, and the correlation between wind power production and load consumption. Wind power integration affects the power flow in the power network, resulting in changing the power flow direction, reducing or increasing power losses and congestions. Measures can be taken by using FACTS, online measurements of temperature and loads, and wind power plants output control to increase the usage transmission lines. In terms of grid reinforcement, both steady-state power flow and dynamic system stability are needed.

- *System stability*: The time scale ranges from seconds to minutes. This aspect is very much related to voltage and power control and to fault ride through capability. Different wind turbine types have different control characteristics and consequently also different possibilities to support the system in normal and system fault situations. The location of wind power plants relative to load centres will have some influence on this issue as well.

### 2.6.2 Solar

Solar radiation can be converted to electric power directly from photovoltaic (PV), or indirectly from concentrating solar power (CSP) mostly. A PV cell is a device that converts the sun radiation directly to direct current using photoelectric effect. Stand-alone PV cells serve well in providing electricity to cover summer noon peak load in areas where cool demand is high. PV has mainly been used to small- or medium-sized application, typically off-grid homes powered by PV arrays.

CSPs concentrates the solar radiation using mirrors to create heat, which can be used to drive steam turbines to provide electrical energy. Heat storage vessels, e.g. molten salt tanks or concrete blocks, can be used to store heat during the day, and drive steam turbines during the night or during the peak demand. The main reason of focusing more on CSP over PV is its ability of supplying power on demand 24 hours a day. Similar to conventional power plants, CSPs can deliver base load or balancing power, directly from the sunshine radiation. Heat storage vessels guarantee power availability during the night or periods without sunshine with the help of backup heat source such as fossil fuel or biomass. CSP plants have the availability that is close to 100% like conventional plants but with significant less fuel consumption [Fou10]. The wasted heat from the CSP power generation process may be used locally to desalinate seawater or for cooling. The annual solar efficiency varies from 8% to 25% depending on the technology [EBD09].

In Europe, the potential of using CSP can be realized around the Mediterranean, where the amount of solar radiation is abundant. The Direct Normal Irradiation (DNI) is above 2000 $kWh/m^2a$. The European Solar Industry Initiative (ESII) aims at a cumulative installed CSP capacity of 30 GW in Europe out of which 19 GW would be in Spain by 2020 being able to supply about 85 TWh or 2% of final electricity consumption. Desertec project proposes an energy solution to meet the future electricity demand by transferring huge amount of solar energy from North Africa areas to the continental Europe, meeting 15% of the total EU electricity demand [Fou10].

## 2.7 Load

The consumers are supplied with the requested amount of active and reactive power at constant frequency and with a constant voltage. The load connected to the power network, however, is not constant and affected by many factors [SYL02].

- *Economic factors*: An economic situation of an area could affect its load pattern, from type of customers, industrial activities, and population.
- *Time factors*: Load pattern varies seasonal, weekly, and daily. For

instance, industrial load on weekdays will be higher than that of weekends.

- *Weather factors*: Temperature has strong influence in load pattern. Heating demand in winter and air conditioning in summer are typical examples.

- *Random disturbances*: Large industrial customers, such as steel mills may cause sudden load changes. Certain event, such as the shutdown of an industrial operation may also affect load patterns.

- *Price factors*: In electricity market, electricity price is volatile and sends price signal to customers to influence their willingness of purchasing electricity.

Electricity can not be stored in large quantity, so that the generation and load need to be in balance in a real-time base. The power system is operated to generate and transmit bulk power to fulfil the load demand. The load forecast is then essential due to the above mentioned factors, and will affect [SYL02]

- *Generation scheduling*: Load forecast is used for unit commitment, taking into account the generating unit constraints and network constraints.

- *Power system security*: The effect of scheduled power system operation can be predicted using load forecast. Preventive and corrective actions can be taken to mitigate the impact of generation scheduling before violation of any generating unit or network constraints.

- *Generation reserve of the system*: Reserves balance the system when there is a sudden load change. The appropriate amount of reserves can be determined based on load forecast.

- *Market operation*: With deregulated electricity market structure, load forecast becomes more important to all market participants, so that adequate energy transactions can be scheduled and appropriate operational plans and bidding strategies can be established [IEE01].

### Demand Side Management

Demand side management (DSM) is a broad concept about re-shaping the consumer demand for energy through various methods. System-level benefits of utilising DSM include improved long-term system security, more efficient system balancing and ancillary services, and improved utilisation of generation and network capacity. The benefits have been found to be the greatest in systems with scarce operational flexibility, such as those based on high contribution of intermittent renewable electricity and less flexible low-carbon technologies (nuclear and carbon capture and storage). Such flexibility can be obtained from programs of direct load control and/or market incentives to encourage demand side participation. Various means nowadays are used in the DSM, including electric vehicles, residential heat pumps, heating, ventilating and air conditioning, and other smart appliance. Intensive discussion about DSM can be found in [pro11].

## 2.8 TSOs Challenges

Challenges reported by TSOs concerning system operation with a significant contribution from RES relate to [ea12a, ea12b]

- Coordinating the operation of flow controlling devices across Europe.
- Coordinating system arrangements to adjust power flows in the event of faults and other events.
- Developing and using dynamic equipment ratings reflecting ambient conditions, loading, and conductor temperatures.
- Shared intelligence on developing generation and load conditions (including wind forecasts).
- Suitable monitoring and control facilities.
- Procedures for using enhanced operational measures so that maximum benefit is achieved across each region.

In terms of the operational risk, almost all major TSOs in continental Europe are already experiencing huge difficulties to operate the network with large wind power installations and increasing solar power installations. TSOs are already facing operational challenges due to loop flows and analysis of the 2015 snapshots identified high power flows starting in the areas with large wind power installations in Germany and directed to the remote load centres, substantial loop flows through Poland and the Czech Republic, and increasing flows significantly above those that are currently expected to result from market transactions. Also high loop flows through Benelux countries with similarly increasing flows have been found. There is hence a substantial risk of cascading failures and disruption should a fault event occur. E.g. on the German-Czech Republic border, flows could exceed line capacities even with all circuits in service, risking network failure without an initiating fault event. On the German - Poland border, flows reach line limits with all circuits in service, risking network disruption in the event of a fault.

As the share of RES increases in the generation mix every year, TSOs expect the future challenges such as

- Increasing uncertainties due to the growing share of electricity generation from intermittent renewable energy sources as well as increasing market-based cross border flows
- Enhancement of grid capability and grid flexibility
- New planned interconnections including new technologies, devices for power flow control, and FACTS for system services will offer new possibilities in network operation
- Better system coordination and cooperation by using common tools.

## 2.9 Summary

This chapter provides the fundamental information about the power system operation in general. The topics follows the power system structure evolution, from solely centralized conventional generation structure (vertical power system) to increasing installation of de-centralized non-conventional generation structure on the demand side (horizontal power system, smart grid). Moreover, the general overview has been given to conventional generation ranging from nuclear, coal, to hydroelectric and non-conventional generation of wind and solar power. The essential knowledge of the physical structure of the power system lays the foundation for the next chapter of mathematical modelling of each component and the system operation in general. Beyond the introduction of physical power system infrastructure, this chapter touches upon the operational challenges with large scale RES integration to the system from the viewpoint of the Central European TSOs. The time frame includes the current situation and anticipated challenges in the future.

# Chapter 3

# Optimal Power Flow

## 3.1 Introduction

The idea of optimal power flow (OPF) was introduced in the early 1960s as an extension of economic dispatch to determine the optimal settings of control variables with respect to various constraints [MH99, Mom08, GH91]. This chapter provides an overview of OPF and its application to power systems. Optimal power flow theory in this chapter is discussed in terms of objective functions and various constraints. Moreover, AC- and DC-OPF formulation are elaborated as two sets of constraints.

## 3.2 OPF Theory

The OPF problem attempts to optimize steady-state power system performance with respect to an objective $F$, subject to various constraints. Mathematically, The OPF problem may be defined as follows,

$$min \quad F(\mathbf{x}, \mathbf{u}) \tag{3.2.1}$$

subject to

$$g(\mathbf{x}, \mathbf{u}) = 0 \tag{3.2.2}$$

$$h(\mathbf{x}, \mathbf{u}) \leq 0 \tag{3.2.3}$$

where $F\mathbf{(x,u)}$ is the objective function to be optimized, $g(\mathbf{x}, \mathbf{u})$ represents non-linear equality constraints from nodal power equations, and $h(\mathbf{x}, \mathbf{u})$ is non-linear inequality constraints on dependent and independent variables. Vector $\mathbf{x}$ includes dependent variables such as load (PQ) node voltages, generator reactive power, whereas $\mathbf{u}$ is the vector of control variables including bus voltage magnitudes, active power output, etc. [Lai01]. Some control variables come with a cost, such as active power production of conventional generating units. Others do not have a cost, such as magnitude of voltage, phase angles, etc.

The lists presented below shows a selection of objectives and constraints commonly found in OPF formulation. It is known that objectives must be mathematically constructed with possible solutions, and the constraints also have to be designed to satisfy upper and lower bounds in order to obtain feasible solutions. To find the optimal dispatch of units or social welfare, the OPF is largely based on static optimization method for optimizing a scalar objective function (e.g. cost) [Mom08].

**Common Objectives**

- Active Power Objectives
  - Economic dispatch (minimum fuel cost, MW generation or transmission losses)
  - Environmental dispatch
  - Maximum power transfer
- Reactive Power Objectives (MW and MVar Loss Minimization)
- General Goals
  - Minimum deviation from a target schedule
  - Minimum control shifts to alleviate violations
  - Least absolute shift approximation of control shift

**Common Constraints**

- Limits on Control Variables
  - Generator output in MW
  - Transformer-tap limits
  - Shunt capacitor range
- Operating Limits on
  - Line and transformer flows
  - Active and reactive power interchanges
  - Active and reactive power reserve margins
  - Voltage, angle magnitudes and differences
- Control parameters

The solution from OPF calculation may not be the most desired due to certain other factors such as additional constraints. The following assumptions are made in the modelling the objectives and constraints:

- Fuel cost curves are smooth and quadratic in nature if they are approximated in quadratic forms

- Only active power generations are controlled for cost minimization. Generation voltages, shunt capacitors and other devices are held at their nominal set values throughout the optimization

- Current flows are controlled approximately using voltage and phase angle restriction across the lines

- Contingency constraints are neglected

## 3.3 Objective Function

As they are listed in the previous section, objective functions can be defined in various ways, depending on the problem of interest. Specifically, the objective function in the thesis adopts power system fuel cost minimization, which is shown as follows [Mom08],

$$min \quad \sum_{i=1}^{N_g} C_i(P_{gi}) \tag{3.3.1}$$

where
$N_g$ is the number of generating units
$C_i$ is the hourly quadratic cost function of generating unit $i$,
$C_i(P_{gi}) = a(i)P_{gi}^2 + b(i)P_{gi} + c(i)$ $[e/h]$
a,b,c are the cost coefficients
$P_{gi}$ is the active power output of generating unit $i$

Note that the cost minimization requires the fuel cost information of each generating unit in the system. Such fuel cost information can be approximated in several ways, including piecewise linear, quadratic, cubic and piecewise quadratic, etc. A piecewise linear form of fuel cost function is commonly used in many linear programming (LP) applications. A quadratic cost curve is used in most non-linear programming (NLP) applications. The system fuel cost minimization usually refers to economic dispatch, which aims at obtaining the active power generation of the units committing for operation with the least system fuel cost, meanwhile fulfils the technical and operational constraints.

## 3.4 Constraints

In mathematical formulation of the optimization problem, a constraint is a condition that a solution to an optimization problem must satisfy. Two types of constraints can be defined, namely equality constraints and inequality constraints. The following constraints are characterized in terms of the operational property to power systems, each of which is formulated as equality or inequality constraint.

- Power balance constraints
- Transmission network constraints
- Generating unit constraints

These are usual constraints for a regular OPF formulation. The list can be expanded to include more customized constraints with respect to the problem of interest. The listed constraints are elaborated in details in the following sections.

### 3.4.1 Power Balance Constraints

**Active power balance constraint**: The net active power injection at each node is the difference between the active power generation and the active power demand at that node.

$$P_i = P_{g,i} - P_{d,i} \tag{3.4.1}$$

where
$P_i$ is the net active power injection at node $i$
$P_{g,i}$ is the active power generated at node $i$
$P_{d,i}$ is the active load at node $i$

**Reactive power balance constraint**: The net reactive power injection at each node is the difference between the reactive power generation and the reactive power demand at that node.

$$Q_i = Q_{g,i} - Q_{d,i} \tag{3.4.2}$$

where
$Q_i$ is the net reactive power injection at node $i$
$Q_{g,i}$ is the reactive power generated at node $i$
$Q_{d,i}$ is the reactive load at node $i$

Note that $P_i$ can be calculated in either AC optimal power flow (AC-OPF) formulation or DC optimal power flow (DC-OPF) formulation. Both AC- and DC-OPF are briefly presented in the following section.

### 3.4.2 Transmission Network Constraints: AC Optimal Power Flow

During the solution of the OPF, it is necessary to solve the load flow problem numerous times. Let us start off with the derivation of the AC power flow equations [GJ94] with the $Y$ admittance matrix. How to build the $Y$ matrix can be found in [SvdS08, GJ94]

$$Y_{ij} = |Y_{ij}|\angle\theta_{ij} = |Y_{ij}|cos\theta_{ij} + j|Y_{ij}|sin\theta_{ij} = G_{ij} + jB_{ij} \tag{3.4.3}$$

$$V_i = |V_i|\angle\delta_i = |V_i|(cos\delta_i + jsin\delta_i) \tag{3.4.4}$$

$$I_i = Y_{i1}V_1 + Y_{i2}V_2 + ... + Y_{iN_b}V_{Nb} = \sum_{j=1}^{N_b} Y_{ij}V_j \tag{3.4.5}$$

$$P_i - jQ_i = V_i^* \sum_{j=1}^{N_b} Y_{ij}V_j \tag{3.4.6}$$

$$P_i = \sum_{j=1}^{N_b} |Y_{ij}V_iV_j|cos(\theta_{ij} + \delta_j - \delta_i) \tag{3.4.7}$$

$$Q_i = -\sum_{j=1}^{N_b} |Y_{ij}V_iV_j|sin(\theta_{ij} + \delta_j - \delta_i) \tag{3.4.8}$$

where

| | |
|---|---|
| $G_{ij}$ | is the real part of $Y$ admittance matrix at the $i$th row and $j$th column |
| $B_{ij}$ | is the the imaginary part of $Y$ admittance matrix at the $i$th row and $j$th column |
| $V_i, V_j$ | are the voltage at node $i, j$ |
| $I_i$ | is the current injection at node $i$ |
| $N_b$ | is the number of buses (nodes) |
| $Y_{ij}$ | is complex admittance matrix element at the $i$th row and $j$th column |
| $\delta_i, \delta_j$ | are the phase angles at bus $i, j$ |
| $\theta_{ij}$ | is the phase angle of the complex admittance matrix element at position $i, j$ |

**Apparent power flow constraint**: This inequality constraint limits the upper bound on the power flowing through every branch in the system.

$$|S_{ij}| \leq \overline{S_{ij}} \tag{3.4.9}$$

where

| | |
|---|---|
| $S_{ij}$ | is the apparent power flow from bus $i$ to bus $j$ $\quad (S = \sqrt{P^2 + Q^2})$ |
| $\overline{S_{ij}}$ | is the rating of the transmission line |

**Voltage constraint**: This inequality constraint limits the upper and lower bounds on the voltage level at every node in the system.

$$\underline{|V_i|} \leq |V_i| \leq \overline{|V_i|} \tag{3.4.10}$$

where $\underline{|V_i|}$ and $\overline{|V_i|}$ are the lower and upper bound of the voltage magnitude at bus $i$.

### 3.4.3 Transmission Network Constraints: DC Optimal Power Flow

DC formulation uses the same parameters, with the exception of the following assumptions:

- Branch resistance $R$ is and charging capacitance $B$ are negligible (i.e. lossless lines)
- All buses voltage magnitudes are close to 1 p.u.
- Voltage angle differences are small enough that $sin\delta_{ij} = \delta_{ij}$, and $cos\delta_{ij} = 1$
- Only active power is considered. Reactive power is ignored.

In AC formulation,

$$\begin{aligned} y = \frac{1}{Z} = \frac{1}{R + jX} = G + jB \\ \Rightarrow \quad G = \frac{R}{R^2 + X^2}, \quad B = -\frac{X}{R^2 + X^2} \end{aligned} \tag{3.4.11}$$

Since $R \ll X, G \ll B$, the above equation is approximated to the following as,

$$G = 0, \quad B = -\frac{1}{X} \Rightarrow G = 0 \tag{3.4.12}$$

Rewrite the power flow equations in terms of $G$ and $B$,

$$P_i = \sum_{j=1}^{N_b} |V_i||V_j| \left( G_{ij} cos(\delta_i - \delta_j) + B_{ij} sin(\delta_i - \delta_j) \right) \tag{3.4.13}$$

Applying the Eq. (16.11) to (16.12), we simply $P_i$ to

$$P_i = \sum_{j=1}^{N_b} |V_i||V_j| \left( B_{ij} sin(\delta_i - \delta_j) \right) \tag{3.4.14}$$

Further because $\delta_i - \delta_j$ is rather small, $sin(\delta_i - \delta_j) = \delta_i - \delta_j$, the above equation can be further simplified to,

$$P_i = \sum_{j=1}^{N_b} |V_i||V_j| \left(B_{ij}(\delta_i - \delta_j)\right) \tag{3.4.15}$$

Rewrite the $P_i$ a little by taking out the $i = j$ term, we obtain

$$P_i = \sum_{j=1}^{N_b} |V_i||V_j| \left(B_{ij}(\delta_i - \delta_j)\right) = |V_i|^2(B_{ii}(\delta_i - \delta_i)) + \sum_{j=1, j\neq i}^{N_b} |V_i||V_j| \left(B_{ij}(\delta_i - \delta_j)\right) \tag{3.4.16}$$

We immediately see that the first term is zero, because $\theta_i - \theta_i = 0$, so that

$$P_i = \sum_{j=1, j\neq i}^{N_b} |V_i||V_j| \left(B_{ij}(\delta_i - \delta_j)\right) \tag{3.4.17}$$

Lastly, the voltage profile at each bus is assumed to be 1 p.u. The active power can finally be formulated as,

$$P_i = \sum_{j=1, j\neq i}^{N_b} \left(B_{ij}(\delta_i - \delta_j)\right) \tag{3.4.18}$$

$$|P_{ij}| \leq \overline{P_{ij}} \tag{3.4.19}$$

Note that Eq. (16.19) is derived from Eq. (16.9) by neglecting the reactive power $Q$.

General remark on AC & DC formulations: Due to the non-linear property of AC formulation, iteration is necessary to solve the AC power flow problem. On the contrary, DC formulation linearises the relationship between power and phase angles. Iteration is then not necessary to solve linear problems, which in turn speeds up the computation process. However, in the context of optimal power flow, both AC- and DC-OPF require iterations to find the optimal solution.

### 3.4.4 Generator Constraints

The generator constraints define the power generators working range. The lower boundary defines the minimum required generation (active and reactive power) to meet technical generation conditions and the upper boundary limits the generator output cannot exceed the maximum.

$$\underline{P_{gi}} \leq P_{gi} \leq \overline{P_{gi}} \tag{3.4.20}$$

where
$\underline{P_{gi}}$ is the minimum active power output
$\overline{P_{gi}}$ is the maximum active power output.

$$\underline{Q_{gi}} \leq Q_{gi} \leq \overline{Q_{gi}} \tag{3.4.21}$$

where
$\underline{Q_{gi}}$ is the minimum reactive power output of unit $i$
$\overline{Q_{gi}}$ is the maximum reactive power output of unit $i$

## 3.5 Additional Outputs from OPF

Apart from the control variables optimized from the in the OPF, more information regarding the network condition and buses can be obtained, such as line loading and marginal fuel cost at each bus.

### 3.5.1 Line Loading

From the equation above, power flow through any line in the network can be calculated at the optimal dispatch point. From this, we are able to evaluate the loading of lines in the network. In the DC formulation, the loading of each line is defined as

$$\zeta_{ij} = \frac{|P_{f,ij}|}{\overline{P_{f,ij}}} \tag{3.5.1}$$

where
$\zeta_{ij}$ is the loading factor of line $ij$
$P_{f,ij}$ is the active power flow through line $ij$
$\overline{P_{f,ij}}$ is the thermal rating of line $ij$

Note that in the AC formulation the line loading is defined as

$$\zeta_{ij} = \frac{|S_{f,ij}|}{\overline{S_{f,ij}}} \tag{3.5.2}$$

where
$S_{f,ij}$ is the apparent power flow through line $ij$
$\overline{|S_{f,ij}|}$ is the thermal rating of line $ij$

### 3.5.2 Locational Marginal Price

*Locational marginal price* is defined as a change in production cost to optimally deliver an increment of load at the location, subject to all constraints [Lit09]. One of the most salient by-products of OPF calculation is the knowledge concerning the economics of the power system. Locational marginal price (LMP), derived from the optimization, can be interpreted as the incremental cost to the system for meeting an additional

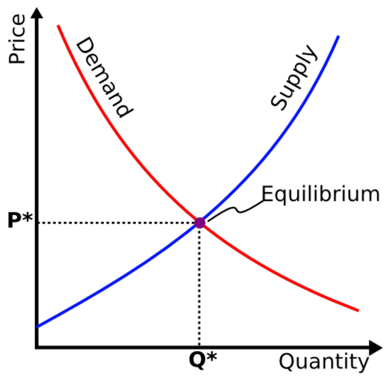


Figure 3.5.1: Market clearing price at market equilibrium [SDM07]

demand of 1 MW, subject to the generator and transmission lines constraints [SYL02, Lai01]. LMP or the nodal pricing mechanism, has been used in some electricity markets in the world, including PJM interconnection, New England in the US and New Zealand, among others.

Using LMP, power producers and consumers agree on the actual price of the energy at their locations in the transmission system. If there is no power flow constraint violation on the transmission lines, LMPs are the same for all buses in the system. This is not only the marginal cost of the most expensive dispatched generation units, but also is the market clearing price (MCP) that is agreed by both producers and consumers. In this case, no congestion rent will be charged. On the contrary, if any line is congested, LMPs vary throughout the system, which may incur additional charge on congestion rent.

MCP refers to the intersection of the supply curve and the demand curve in the electricity market, see Fig. 17.1, where $P^*$ and $Q^*$ are the agreed price and quantity between generation and load in the market. Note that in the competitive market environment, $P^*$ is the highest marginal cost of the bus that defines the MCP.

## 3.6 Summary

This chapter presents the transmission network modelling, emphasizing on the optimal power flow formulation. Both AC and DC formulations have been derived and discussed in order to present a clear picture of the classical deterministic model of the power system. Such deterministic models will form the computational core in the Monte-Carlo simulation with stochastic system infeeds. In terms of OPF, a set of an objective function and constraints are firstly presented, and then the meaning and the economic implication of LMP from the engineering viewpoint are intensively discussed.

The LMP concept will be later used not only as an economic indicator but also as the controllable variable in the expansion studies in chapter 6 and 7.

# Chapter 4

# Stochastic Modelling and Optimization

## 4.1 Introduction

This chapter presents the necessary mathematical background for the readers to continue reading the following chapters. The first section provides an overview of the Monte-Carlo simulation in general and the Copula approach applying to the wind and load modelling. This section is essential for the understanding of the following chapter related to weak network points identification taking into account the wind/load variability in Chapter 5. The second section provides the general knowledge of optimization, focusing on the primal and dual problems and variables. This section facilitates the understanding of the modelling of transmission network expansion in Chapter 6 and 7.

### 4.1.1 Monte-Carlo Method

Monte-Carlo simulation (MCS) [Liu01,BG09] is a sampling method that the inputs are randomly generated from probability distribution to simulate the process of sampling from the actual dataset. It has been intensively used in dealing with sensitivity, reliability analysis with uncertainties [SB95,HA06], and is able to capture the stochastic dependency structure of wind speed, as well as load [PK09]. In general, MCS runs iteratively a large series of system simulations, given a set of inputs derived from random samples from the input's probability distributions. The set of the outputs forms a probability distribution of the considered variables. Thus, an MCS provides information of the possible system outputs and the corresponding probability of any choice of action. Two main reasons of using the Monte-Carlo method are [Pen02, Rub81, SLK06]

- the anti-aliasing property

- the ability to quickly approximate the answer that otherwise would be very computation-intensive to obtain an exact answer from other deterministic answers

Such properties greatly facilitate the power system analysis when taking into account the correlated wind energy integration and its variability.

### Anti-aliasing

Intuitively speaking, wind speeds at different locations are very much correlated when the locations are not far away from each other with similar geographical conditions. When dealing with modelling wind energy integration to the power system, it is of importance to take into account this correlation, emphasizing the analysis of the impact of wind energy variability upon the power system operation. The alias thus corresponds to the objective of the analysis, i.e. power system analysis with intermittent wind energy infeed. Monte-Carlo method by default is able to anti-alias the wind correlation modelling from the deterministic power system analysis. In other words, the anti-aliasing property of the MCS comes in handy by taking the 'pre-simulated' wind infeed data as one of the inputs to the power system analysis. This means that the complex analysis of stochastic generations has then been investigated before the main power system analysis, and thus reduces the complexity of the problem formulation.

### Fast computation under multiple scenarios

The other salient feature of MCS is its ability of providing one set of solutions using the same MCS forecasts under different foreseen generation/load scenarios. Wind is an intermittent energy source, i.e. a random variable that constantly varies with time. Conventionally, due to the nature of intermittent energy sources, the analysis of power system operational behaviour (e.g. power flows, congestions, voltages) taking into the variability of intermittent energy source subject to different generation/load scenarios can be a time-consuming task, because each scenario in general is an independent task with a set of wind power infeed. Thus, $n$ scenarios require $n$ set of wind power infeed respectively. MCS circumvents the problem by first sampling the random variable of wind speed, (i.e. providing MCS samples) and second using this set of MCS samples for the assessment of all generation/load scenarios. In the first step, the set of MCS samples is simulated based on the characteristics and dependence structure of original datasets, thus it can be further used to analyse the system behaviour subject to all scenarios. In this sense, the intermittent energy infeed is independent from the number of scenarios, thus further reduces the computational speed.

MCS was previously considered as a computational demanding method and usually used as a verification method, rather than a direct power system modelling tool [LLZ08, ZL04, MCC90, MR07]. However, with the boost of computer technology and faster algorithm development, it is possible for a modern computer to perform millions of simulations much more efficiently and quickly than before. This in general implies that more accurate results can be obtained by running more simulations [Pen02].

### Single variable transformation

The first step of understanding the modelling technique is to understand the single variable transformation. By definition, for a r.v. $X$ with an *invertible* Cumulative Density Function (CDF) $F_X(x) = P(X \leq x)$, the r.v. $F_X(X)$ follows a uniform distribution on the interval $[0, 1]$[1]. This relationship forms the basis for the sampling of any r.v. in MCS studies. For the sampling of a r.v. $X$ with invertible CDF $F_X$, first a random realization $u$ from a uniform r.v. $U$ in $[0, 1]$ is generated and then the transformation $x = F_X^{-1}(u)$ is applied. In this case, the samples $x$ follow the distribution $F_X$. The above mentioned procedure is presented in Fig. 19.1. The reason of doing the transformation from the marginal domain to the CDF in [0,1] domain is to remove the marginal effect of the marginal distribution. The transformation separates the pure dependence structure from the blended structure of dependence and marginal effect [Pap07].

### Multivariate random variable modelling using Copula

A multivariate random variable is a list of mathematical variables each of whose value is unknown, either because the value has not yet occurred or because there is imperfect knowledge of its value. The individual variables in a random vector are grouped together because there may be correlations among them [Wikc]. *Copulas* are functions that join or 'couple' multivariate distribution functions to their one-dimensional marginals. Alternatively, copulas are multivariate distribution functions whose one-dimensional marginals are uniform on the interval [0,1] [Pap07, Nel06].

*Copula (Sklar's Theorem [Skl])* states that the random variables $X$ and $Y$ with CDF $F_X$ and $F_Y$ are joint by copula $C$ if their joint distribution can be written:

$$F_{XY}(X, Y) = C(F_X(X), F_Y(Y)) \tag{4.1.1}$$

If $F_X$ and $F_Y$ are continuous, then $C$ is unique; otherwise, $C$ is uniquely determined on $[Ran(F_X) \times Ran(F_Y)]$. Conversely, if C is a copula and $F_X$ and $F_Y$ are distribution functions, then the function $F_{XY}$ is the joint distribution function with marginal functions $F_X$ and $F_Y$.

[1] The proof of this statement is as follows: *For* $r \in [0, 1] : P(F_X(X) \leq r) = P(X \leq F_X^{-1}(r)) = F_X[F_X^{-1}(r)] = r$. Thus, if $U$ is the uniform distribution, $F_X(X) = U \Leftrightarrow X = F_X^{-1}(U)$. Therefore, $F_X^{-1}(U)$ follows the distribution of $X$.

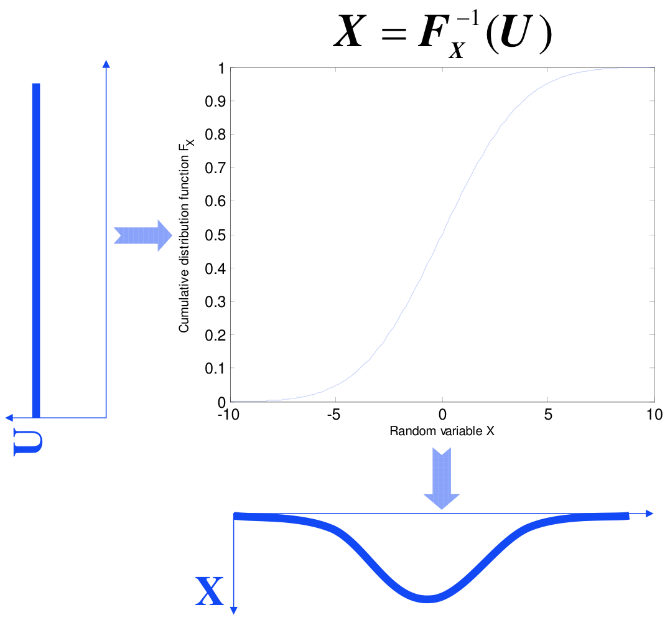


Figure 4.1.1: Sampling of a r.v. in MCS.

Using copula to join the r.v. distributions, the dependence structure among all r.v. distributions is thus captured in one dimension. Iteratively running the copula function to produce the MCS samples (e.g. 10000 times), such data reproduction is particularly applicable and beneficial when

- the adequate data is not available
- the data are poorly collected

The first problem can be dealt by using copula joint function, which does not require large amount of data to capture the dependence structure. The second problem mostly related to high uncertainty, where it is not possible to define all mutual correlations between system stochastic inputs. The treatment for this type of problem is to capture the most important dependence relations and leave the rest unspecified. For more detail about the Copula modelling, one can refer to [Pap07].

*Application to wind speed modelling*
Fig. 19.2 shows an overview of the wind speed modelling using Copula. Suppose $W1$ and $W2$ are the historical wind speed time series data at location 1 and 2. First, we can obtain the empirical cumulative distribution functions (empirical CDF) [GW86] of $W1$ and $W2$, represented by $U_{W1}$ and $U_{W2}$ ranging from 0 to 1 [2]. The uniform distribution $U_{W1}$ and $U_{W2}$

[2] One may also use other standard distributions to represent the wind speed statistical behaviour, i.e. Weibull distribution

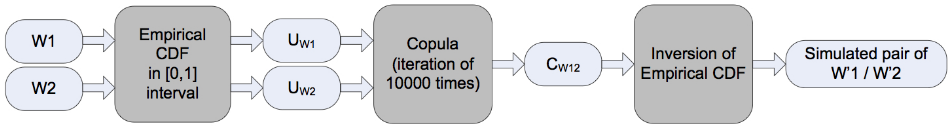


Figure 4.1.2: Overview of modelling wind speed using Copula

can then be joined by the Copula function to obtain the multivariate distribution that captures the dependence structure between $U_{W1}$ and $U_{W2}$, represented by $C_{W12}$, which has the same dependence structure as between $W1$ and $W2$. Finally, we are able to inverse the copula function $C_{W12}$ to the wind speed domain $W'$, which is the simulated wind speed that contains the dependence structural information of original series $W1$ and $W2$. Suppose that we generation 10000 samples of $W'$, they serve as the random samples of MCS inputs. The procedure is shown in Fig. 19.2.

### Illustrative Example

In order to depict the mutual dependence structure between the input r.v.'s, in Fig. 19.3, three scatter diagrams are presented, corresponding to the consecutive steps for the generation of dependent wind power distributions of the simulation algorithm. In particular, in Fig. 19.3a, the scatter diagram for two uniforms correlated with rank correlation $\rho_r = 0.7$ is presented, as it is obtained by the first step of the algorithm. In Fig. 19.3b, we can see how the scatter diagram for the correlated uniforms is transformed into the given Weibull marginals. Finally, in Fig. 19.3c, the obtained wind power scatter diagrams are presented[3]. In these plots we may clearly see the impact of the marginal transformations to the scatter diagrams.

### Application: Stochastic Dependence applied to Power System Analysis

#### Case $A$: Copula approach on historical time-series data

In order to proceed to the MCS analysis of power systems, the system uncertain inputs are sampled based on the theory presented above[4]. For specific study case of UCTE countries where the time-series of wind speed dataset is available, the dependence structure of wind speed can be obtained directly using the empirical distribution from the time-series data.

[3] In the power system analysis, wind speed needs to be converted to wind power and fed into the system at different buses. Converting the wind speed to wind power, one may refer to [PK09, pro08b]. Since it is not in the scope of the thesis, the conversion process will not further discussed here.

[4] Case $A$ is applied in Chapter 5

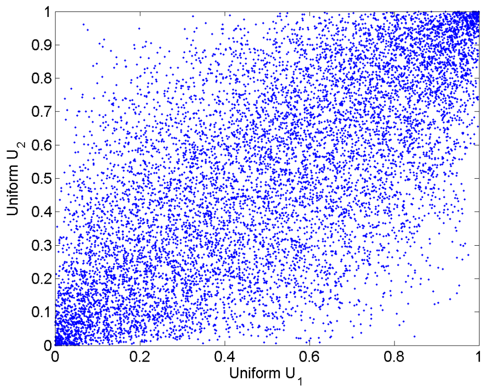


(a) Correlated Uniform distributions

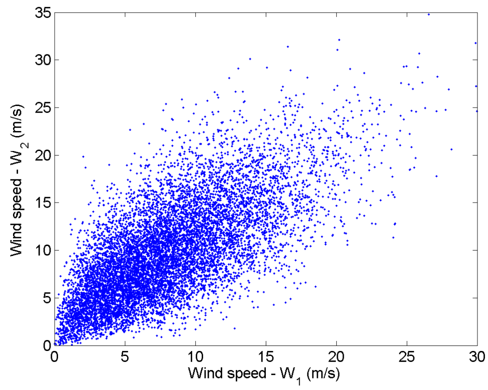


(b) Correlated Weibull distributions

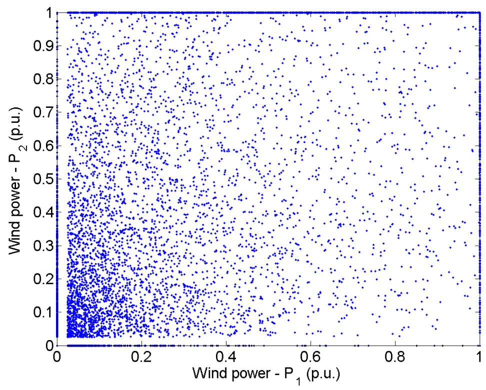


(c) Correlated wind power distributions

Figure 4.1.3: Scatter diagrams for the generation of correlated wind power distributions, according to rank correlation $\rho_r = 0.7$ (10000-sample MCS).

Wind speed dependency structure in Fig. 19.4 is scatter-plotted using the 6-hour measuring data at two adjacent measuring points in the Netherlands obtained from the Tradewind project [pro08b], originated from [ea02]. In the original dataset, the distributions of measured wind speed at two measuring points in the Netherlands are shown in Fig. 19.4a and 19.4b. Fig. 19.4c shows the scatter plot of these two time-series wind speed datasets. We observe the positive correlation of the wind speed datasets, showing that the wind speed at measuring point 2 increases as the wind speed increases at point 1. This is expected as the strength of the dependency is correlated to geographic relations such as the distance and the height between two measuring points. Fig. 19.5a and 19.5b show 10000 MCS samples after performing the Copula modelling technique. We further observe that simulated dataset is very close to the original dataset with respect to the dependence structure. Moreover, the original wind speed dataset consists of 1460 time stamps within one year due the 6-hour measurement interval, whereas the MCS simulation is able to enhance the dataset with more data entries fol-

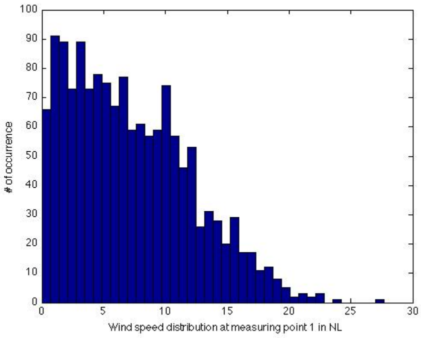


(a) Wind speed distribution at measurement point 1 in the Netherlands

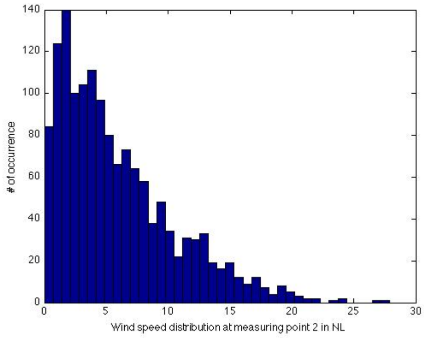


(b) Wind speed distribution at measurement point 2 in the Netherlands

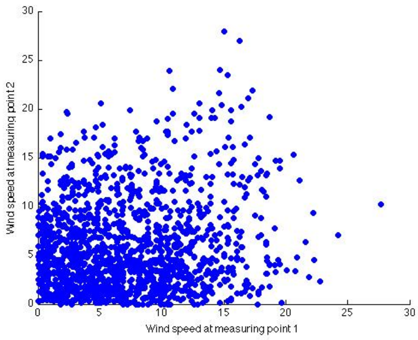


(c) Correlation of wind speed distribution at measurement point 1& 2 in the Netherlands

Figure 4.1.4: Dependence structure of wind speed inputs in Case $A$

lowing the same dependence structure of the original dataset. Fig. 19.5d shows the MCS samples of wind power after converting the wind speed to wind power via the speed-power curve in the Tradewind project [pro08b]. In terms of system loads, the correlation between the countries can be explained as, when the power demand in one country is low in the evening, it is expected that the power demand at the same time in the neighbouring country also stays in a rather low level. Applying the same modelling technique, in Fig. 19.6a, the system load behaviour of Germany is shown, and the MCS samples of the load profile is also presented in Fig. 19.6b.

### Case $B$: Copula approach on expert judgement

Generally speaking, in real applications measured data (historical time-series data) should be used to assess the stochasticity of the system inputs[5]. In case such datasets, for instance in IEEE 39-bus test system, are not avail-

[5] Case $B$ is applied to the 39-bus New England test system in Chapter 5, where 10 wind farms are assumed in different locations in the test system.

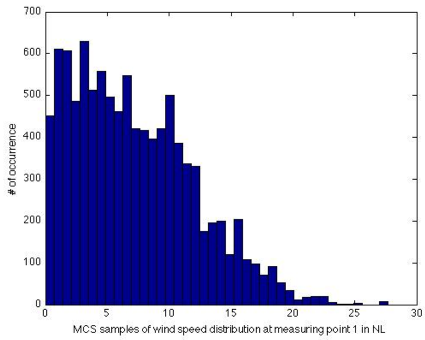


(a) MCS samples of wind speed distribution at measurement point 1 in the Netherlands

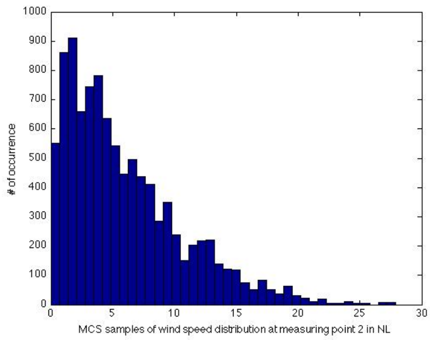


(b) MCS samples of wind speed distribution at measurement point 2 in the Netherlands

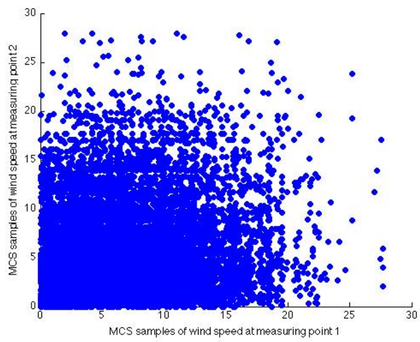


(c) Correlation of MCS samples of wind speed distribution at measurement point 1& 2 in the Netherlands

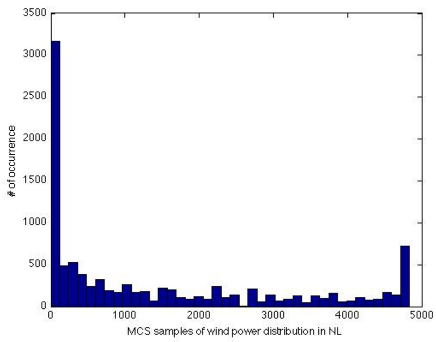


(d) MCS samples of wind power distribution in the Netherlands

Figure 4.1.5: Wind speed/power characteristics of the Netherlands in Case $A$

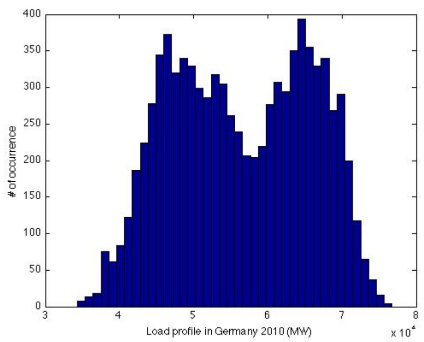


(a) Load distribution in Germany

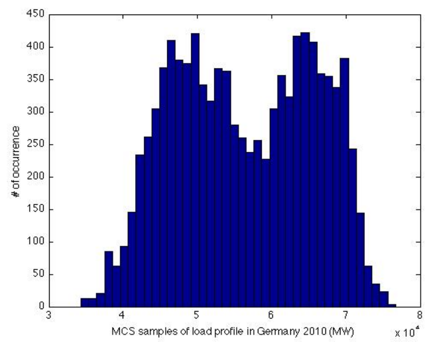


(b) MCS samples of load distribution in Germany

Figure 4.1.6: Original and MCS samples of load distribution in Germany in Case $A$

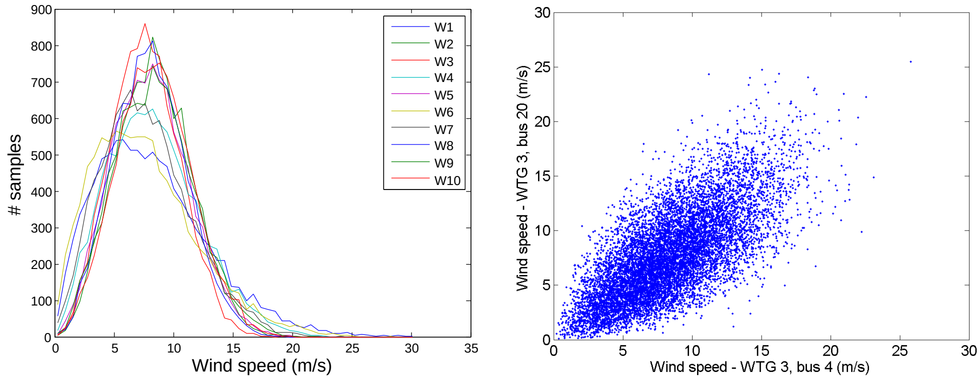


(a) Wind speed distributions of all 10 wind farms

(b) Scatter plot between wind farm at bus 4 and 20

Figure 4.1.7: MCS samples of stochastic inputs in Case $B$: Wind

able, expert opinion could be used to assess the the marginal distributions and dependence structure. For the specific case it is assumed that expert judgement is used to assess the correlations between the wind infeeds; for the sake of simplicity the mutual correlation between the wind speed random variables is defined as 0.8. As discussed in [PK09], any feasible correlation matrices could be used as well as ones derived directly from data. The Weibull parameters $\beta$ and $\eta$ for the wind speed distributions at hub height for each generation site are generated as random numbers drawn in the interval: $\beta \in [1.6, 3]$ and $\eta \in [8.5, 9.5]$. Fig. 19.7 shows the dependence structure of wind speed MCS samples.

Stochasticity of load can also be modelled using Copula, which has been intensively presented in [Pap07]. Due to lack of the historical load values of the New England system on one hand, and available UCTE hourly load dataset of 2008 on the other hand, we assume that New England system has the same dependence structure as countries of the UCTE load datasets. Thus, the MCS samples corresponding to the EU countries are adopted to capture stochasticity in the New England test system using Copula.

#### Case $C$: Copula approach on wind data

Case $C$, applied in Chapter 7, follows the same modelling idea as Case $B$ with different settings which are to be applied to the New England test system in Chapter 7. Ten wind farms are assumed to locate in various locations other than Case $B$ in the test system.

Wind is modelled similarly to Case $B$ using Copula. The characteristics are shown in Fig. 19.3 in the example in Section 19.1.4. Load modelling has been treated the same as in Case $B$. The nominal load for each bus is multiplied by 1.2, i.e. a factor that provides a general indication of a high

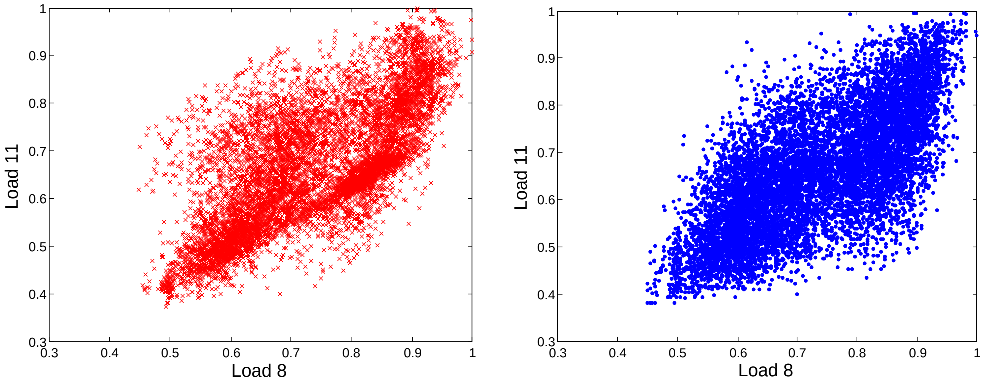


(a) Scatter plot between Load 8 and Load 11, original data

(b) Scatter plot between Load 8 and Load 11, MCS samples

Figure 4.1.8: MCS samples of stochastic inputs in Case $B$: Load

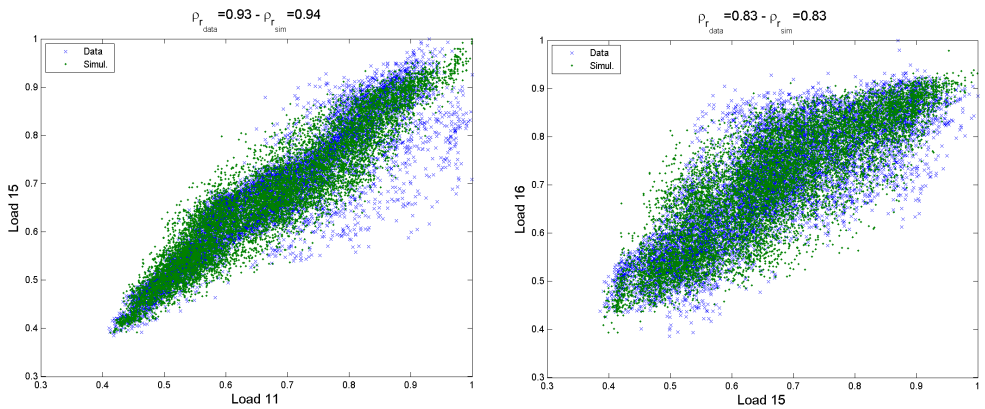


(a) Scatter plot between Load 11 and Load 15

(b) Scatter plot between Load 15 and Load 16

Figure 4.1.9: MCS samples of stochastic inputs in Case $C$: Load

loading scenario. The characteristics of the stochastic inputs are shown in Fig. 19.9.

### 4.1.2 Optimization Background: Lagrangian Multiplier and Duality in Linear Programming

As discussed in the previous chapter, the shadow price interpretation is very useful in the power system modelling, which gives us directly the marginal cost of an additional unit of the resources. Duality in linear programming is a unifying theory that develops the relationships between a given linear program (the primal problem) and another related linear program (the dual problem) stated in terms of variables with this shadow price interpretation.

Understanding the duality problem not only brings additional benefits in understanding the implication of a particular linear-programming model, but also may solve the dual problem with the shadow prices as the variables in place of, or in conjunction with, the primal problem, resulting in possible improvement of computational efficiencies [BHM77].

The main purpose of this section is to present the relationships between primal and dual variables. In linear programming, the objective function solutions from the primal and dual problems are the same. By introducing the Lagrangian function, we have a very nice way of calculating the dual variables, in this case the Lagrangian multipliers or so-called shadow prices. In the later chapter where a methodology of transmission network expansion planning is presented, we will use the Lagrangian function to explicitly calculate the dual variables and further control them inside the primal problem, in order to achieve the expansion target. In this section, the basic mathematical background related to duality and Lagrangian multipliers is presented.

### Duality

In the constrained optimization, it is often possible to convert the primal problem (i.e. the original form of the optimization problem) to a dual form, which is termed a dual problem. Usually dual problem refers to the Lagrangian dual problem. The Lagrangian dual problem is obtained by forming the Lagrangian, using nonnegative Lagrange multipliers to add the constraints to the objective function, and then solving for some primal variable values that minimize the Lagrangian [PS98, BHM77].

The general form of the duality principle in the optimization can be formulated as

**Primal**

$$Maximize \quad z = \sum_{j=1}^{n} c_j x_j \tag{4.1.2}$$

subject to:

$$\sum_{j=1}^{n} a_{ij} x_j \leq b_i (i = 1, 2, ..., m), \qquad x_j \leq 0 \quad (j = 1, 2, ..., n). \tag{4.1.3}$$

Associated with the primal problem there is a corresponding dual problem given by:

**Dual**

$$Minimize \quad v = \sum_{i=1}^{m} b_i y_i, \tag{4.1.4}$$

subject to:

$$\sum_{i=1}^{m} a_{ij} y_i \leq c_j (j = 1, 2, ..., n), \qquad y_i \leq 0 (i = 1, 2, ..., m).$$

The relationship between primal and dual problems is shown in Table 19.1.

Table 4.1.1: Relationship between primal and dual problems

| Primal var / Dual var | $x_1 \geqq 0$ | $x_2 \geqq 0$ | $x_3 \geqq 0$ | $\cdots$ | $x_n \geqq 0$ | | Min $v$ |
|---|---|---|---|---|---|---|---|
| $y_1 \geqq 0$ | $a_{11}$ | $a_{12}$ | $a_{13}$ | $\cdots$ | $a_{1n}$ | $\leqq$ | $b_1$ |
| $y_2 \geqq 0$ | $a_{21}$ | $a_{22}$ | $a_{23}$ | $\cdots$ | $a_{2n}$ | $\leqq$ | $b_2$ |
| $\vdots$ | $\vdots$ | $\vdots$ | $\vdots$ | | $\vdots$ | $\vdots$ | $\vdots$ |
| $y_m \geqq 0$ | $a_{m1}$ | $a_{m2}$ | $a_{m3}$ | $\cdots$ | $a_{mn}$ | $\leqq$ | $b_m$ |
| | $\geqq$ | $\geqq$ | $\geqq$ | | $\geqq$ | n/a | n/a |
| Max z | $c_1$ | $c_2$ | $c_3$ | $\cdots$ | $c_n$ | n/a | n/a |

We can also view the constrained optimization problem as a game between players: one player controls the primal variables and tries to minimize the Lagrangian, whereas the other player controls the multipliers and tries to maximize the Lagrangian [Gor].

A small example is provided to demonstrate the relationship between primal and dual problems and their associated variables.

**Example:** Consider a *primal problem* of

$$Maximize \quad 0.043x_A + 0.027x_B + 0.025x_C + 0.022x_D + 0.045x_E$$

subject to

$$\begin{aligned} x_A + x_B + x_C + x_D + x_E &\leq 10 \\ -x_B - x_C - x_D &\leq -4 \\ 0.6x_A + 0.6x_B - 0.4x_C - 0.4x_D + 3.6x_E &\leq 0 \\ 4x_A + 10x_B - x_C - 2x_D - 3x_E &\leq 0 \\ x_A \geq 0, \quad x_B \geq 0, \quad x_C \geq 0, \quad x_D \geq 0, \quad x_E &\geq 0 \end{aligned}$$

According to equation (19.4) the corresponding *dual problem* is:

$$Minimize \quad v = 10y_1 - 4y_2$$

subject to

$$\begin{aligned} y_1 + 0.6y_3 + y_4 &\geq 0.043 \\ y_1 - y_2 + 0.6y_3 + 10y_4 &\geq 0.027 \\ y_1 - y_2 - 0.4y_3 - y_4 &\geq 0.025 \\ y_1 - y_2 - 0.4y_3 - 2y_4 &\geq 0.022 \\ y_1 + 3.6y_3 - 3y_4 &\geq 0.045 \\ y_1 \geq 0, \quad y_2 \geq 0, \quad y_3 \geq 0, \quad y_4 &\geq 0 \end{aligned}$$

The optimal solution to both primal and dual problems can be found:

*Primal*: $x_A = 3.36, \quad x_B = 0, \quad x_C = 0, \quad x_D = 6.48, \quad x_E = 0.16$, and $z = 0.294$;

*Dual*: $y_1 = 0.0294, \quad y_2 = 0, \quad y_3 = 0.00636, \quad y_4 = 0.00244$, and $v = 0.0294$.

As shown above, the optimal values of the objective functions of the primal and dual solutions are equal. To be more specific, the solution to the dual problem finds the best lower bound of the optimal solution to the primal problem. When strong duality holds, the solution to the dual problem is equal to that to the primal problem.

**Lagrangian multipliers**

Lagrangian multipliers is a way to solve constrained optimization problems. Consider

$$Maximize \quad f(x, y) = x^2 + y^2 \tag{4.1.5}$$

subject to the constraint

$$g(x, y) = x + y - 2 = 0 \tag{4.1.6}$$

The simplest version Lagrangian theorem states that this will always be the case for equality constraints: at the constrained optimum, if it exists, $\triangledown f$ will be a multiple of $\triangledown g$. Translating into numerical formulation

$$g(x, y) = 0 \tag{4.1.7}$$

$$\nabla f(x, y) = \lambda g(x, y) \tag{4.1.8}$$

The first equation states that the variables must satisfies the original constraint. The second equation complements the aforementioned Lagrangian theorem, and the multiplier $\lambda$ is called Lagrangian multiplier.

**Inequality constraints**

A more general formulation of Lagrangian function can be defined when inequality constraints are considered in the optimization problem. Consider again the following non-linear problem in Eq. (19.2), to simplify the notation, only variable $x$ is shown here.

$$Minimize \quad f(x) \tag{4.1.9}$$

subject to

$$g_i(\mathbf{x}) = 0 \tag{4.1.10}$$

$$h_j(\mathbf{x}) \leq 0 \tag{4.1.11}$$

where $g_i(i = 1, ..., m)$ and $h_j(j = 1, ..., l)$. The number of equality and inequality constraints are represented by $m$ and $l$. Suppose that the objective function $f$, constraints $g$ and $h$ are continuously differentiable at a point $x^*$. The Lagrangian function is then defined as

$$L = \nabla f(x) + \sum_{i=1}^{m} \lambda_i \nabla g_i(x) + \sum_{j=1}^{l} \mu_j \nabla h_j(x) \tag{4.1.12}$$

If $x^*$ is a local minimum, then there exists constants $\lambda_i(i = 1, ..., m)$ and $\mu_j(j = 1, ..., l)$ called Lagrangian multipliers, such that

$$\nabla f(x^*) + \sum_{i=1}^{m} \lambda_i \nabla g_i(x^*) + \sum_{j=1}^{l} \mu_j \nabla h_j(x^*) = 0 \tag{4.1.13}$$

$$g_i(x^*) = 0, \quad \text{for all} \quad i = 1, ...m \tag{4.1.14}$$

$$h_j(x^*) \leq 0, \quad \text{for all} \quad j = 1, ...l \tag{4.1.15}$$

$$\mu_j \geq 0, \quad \text{for all} \quad j = 1, ...l \tag{4.1.16}$$

$$\mu_j \nabla h_j(x^*) = 0, \quad \text{for all} \quad j = 1, ...l \tag{4.1.17}$$

When $l = 0$, i.e. no inequality constraints, the KKT condition becomes Lagrangian conditions.

The above section presented the duality of the optimization problem, focusing on the relationship of primal and dual problem and dual variables derivation. The complete picture of the dual problem and dual variables enables us to further utilize the Lagrangian multipliers in the optimization process in the power system network expansion studies. The dual variables can be obtained in both the primal problem and the dual problem. In the power system modelling, primal variables such as generator outputs are crucial for the system analysis. Dual variables, as an important economic indicator, are the by-products of the optimization problem which cannot be controlled in the conventional optimization process. The ideal case would be having the full controllability of both primal and dual variables in the optimization process. In this regard, the better option to utilize the dual variables is to calculate them within the primal problem, which as the result, gives the full controllability of primal variables and dual variables. That is to say, when controlling the dual variables in the optimization, the primal variables will change accordingly. To this extent, it is of importance to understand and derive the relationship between the primal variable and dual variable. Remark: In the optimization of the power system problem, the dual variables $\lambda$ and $\mu$ represent the locational marginal price and multipliers related to the power flow constraints, respectively.

## 4.2 Summary

This chapter contains mathematical background that readers should possess in order to proceed to the transmission network assessment and the expansion studies in the following chapters. The first part of this chapter presents the concept of Monte-Carlo method which takes random samples as inputs and iteratively runs the deterministic method to investigate the full spectrum of the possible outcome. The randomness and dependence structure of the wind energy and system load are modelled by Copula function, which provides the possible combination of wind power and load of the system as the input of the Monte-Carlo simulation. Three cases of wind speed modelling applied to reduced UCTE network (Case $A$) and IEEE-39 bus test system (Case $B$ and $C$) are presented.

The second part of this chapter focuses on the mathematical overview of optimization formulation, where the primal and dual variables are of interest. The introduction establishes the mathematical background of the relationship between primal and dual variables, serving as the base of the expansion studies, i.e. controlling dual variables in the primal problem in order to affect the primal variables thus reaching the optimization target.

# Chapter 5

# Weak Network Points Identification

## 5.1 Introduction

This chapter presents a methodology for the identification of the weak network points (WNPs) using stochastic optimal power flow (S-OPF) method. The S-OPF analysis combines a Monte-Carlo simulation setup with a deterministic OPF calculation. The MCS process is used to sample the stochastic inputs such as wind power injection and load patterns at each bus of the system. The inputs are fed into the optimization process, which iteratively determines the power system operation. The outcome of the S-OPF analysis of a scenario[1] provides the probability spectrum of all relevant technical and economic parameters such as loading of transmission lines and nodal price ranges under different MCS samples. The methodology is extended to incorporate more scenarios, i.e. caused by policy uncertainties in order to provide the overall assessment of weak network point identification subject to all foreseen future generation mixes. Because the MCS simulation is processed prior to the deterministic OPF method, the de-coupled method offers great flexibility for the improvement of both MCS and OPF methods separately. To this extent, energy export due to excessive wind and time independent unit commitment (UC) are modelled in the OPF formulation to further enhance the applicability of the methodology.

Fig. 21.1 shows the schematic layout of this chapter. First, the methodology is elaborated by the introduction of the modelling framework focusing on the analysis of one scenario under different MCS samples. Then, the modelling framework is extended to incorporate more scenarios. Second, the modelling frameworks of unit commitment and energy export are presented to focus on the situation when strong wind energy integrated throughout the system. Case studies are presented at the end of each section for the

[1] A scenario refers to a possible future of a certain generation mix.

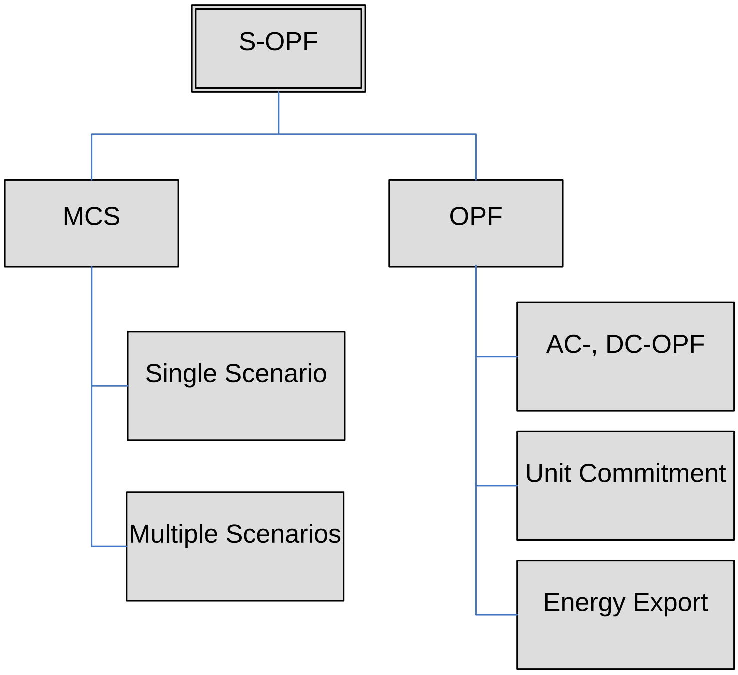


Figure 5.1.1: Schematic layout of Chapter 5

demonstration of its validity and usefulness.

## 5.2 Background

The share of stochastic generation in the power system energy mix has been significantly increased in recent years. As stochastic generation we refer to electrical power production using an uncontrolled primary energy mover, corresponding mainly to renewable energy sources such as wind energy [Pap07]. This ubiquitous power generation leads to an increase in the variability of the system power flows, allowing reverse power flows from the distribution systems towards the transmission system, when the local generation exceeds the consumption.

The power system operation may be regarded as the transition between consecutive steady-state 'snapshots'; each of these snapshots consists of a different set of wind power infeed and system load. Instead of evaluating the power system operation under a single-snapshot condition, a methodology that enables the assessment of the variability of the inputs should be employed for the evaluation of the system behaviour, i.e. weak network points. To evaluate the system variability, one should therefore estimate the system steady state for all the different operational snapshots. For this,

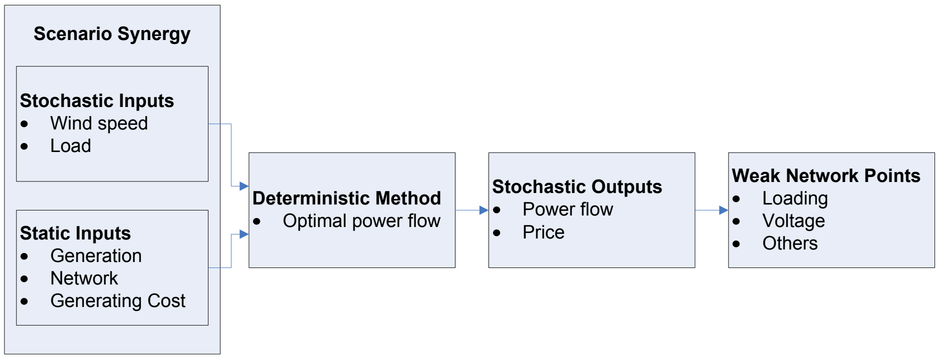


Figure 5.3.1: Overview of modelling methodology

the stochasticity in the system uncertain inputs (i.e. wind infeed) should be appropriately modelled.

The methodology proposed in this chapter combines MCS and OPF to enable the power system analysis, taking into account the aforementioned system inputs variabilities.

## 5.3 WNPs Identification - Single Scenario analysis

The essence of the proposed methodology is to combine the deterministic method (i.e. OPF) with the stochastic inputs. Fig. 23.1 below presents the overview of the modelling methodology.

The wind speed dataset is firstly obtained in time series, and later represented to MCS samples. The wind speeds in MCS are then converted to wind power with respect to wind-power curves [pro08b, Ack05]. The 'static' data are generation data, network data and cost data, which remain the same throughout the whole simulation process, corresponding to the so-called 'Single-Scenario' analysis. The OPF simulation evaluates the network performance of each scenario sequentially and provides the power flows of all transmission corridors and prices at all buses. The weak network points are identified based on the results from all scenarios evaluation.

The weak network points in the contribution are defined as the overloading of transmission corridors. Recall Eq. 3.5.1 in chapter 3, the loading factor of a line is defined as,

$$\zeta_{ij} = \frac{|P_{f,ij}|}{\overline{P_{f,ij}}} \tag{5.3.1}$$

The loading percentage $\zeta_{ij}$, ranging from 0 to 1, directly shows the severity of the line loading. The $\zeta_{ij}$ of all overloading scenarios is 1, because one of the constraints in the OPF assures the power flow of the line must be equal or less than the maximum transfer capacity. This means that the loading percentage of a line will be 1 if there is congestion occurring between two connected buses. Incorporating MCS samples into the OPF analysis, we may further draw conclusions on the overall performance of the network subject to possible wind and load combination, and most importantly the weak network points. The ranking of loading percentage from high to low provides the severity and the frequency of such weak network points in the system.

### 5.3.1 Case Study: Single Scenario

#### Static inputs

The power system under the investigation consists of 26 nodes in which each node represents one EU country (also former UCTE member states), and 46 branches in which each branch represents the aggregated cross-border lines between two countries. The network model has been generated from a snapshot case study of the UCTE 2008 winter case model [UCT08]. Conventional dispatchable generation types of total 103 generators are included in the model, whereas renewable non-dispatchable generation type such as wind and solar power injections are to be modelled exogenously per country [pro10]. Generator costs adopt linear cost curves to form the merit order, assuming the same cost for the same fuel type [pro07]. Fig. 23.2 shows the geographical overview of the reduced network model. Each member country is represented by a red dot. The cross border interconnectors are represented by black lines in the figure for better visual illustration. The total active and reactive power demands of the model are 205.23 GW and 55.855 GVar respectively, and are aggregated per country and connect to each country node accordingly. The reduce network model has certain features listed as follows [pro10],

- It covers large geographic scope of former UCTE member countries, and is expandable to a larger geographic area.
- It enables the analysis of interconnection strategies to create a single pan-European grid and development of new markets for cross-border trade.
- It is capable of integrating different generation/load scenarios [rep11].
- It requires less computational effort, suitable for hourly or Monte-Carlo simulation, and offers reasonable accuracy of the results.
- It adapts external solvers from both open source and licensed optimization packages.

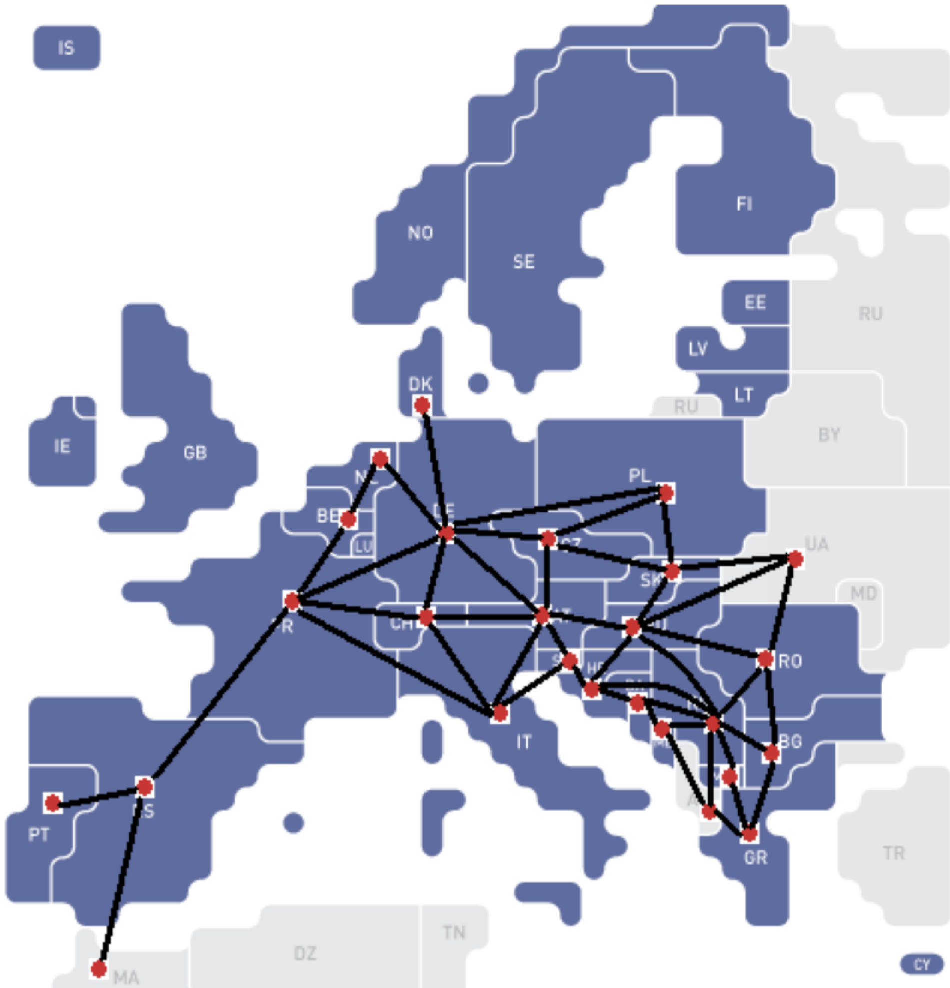


Figure 5.3.2: Schematic view of reduced UCTE network

**Stochastic inputs: wind power injection and load**

The stochastic inputs consisting of wind speed and system loads have been taken from various data sources of Tradewind project and ENTSO-E. The detailed stochastic modelling can be found in Chapter 4, Section 4.1.1, where Case $A$ have been intensively discussed.

### 5.3.2 Simulation Setup and Tool

DC-OPF method has been used to evaluate the network performance, mostly because of the scope and the network that we are investigating. Due to the large scale of the pan-European network with insufficient data, the cross-border lines between countries are the main focus for the investigation and the EU electricity network has been reduced to country-based node, which in turn do not contain the voltage information for a particular country. In the DC-OPF simulation, the dispatch of the generators in the system are optimized in the OPF calculation for each system state, defined by factors such as the sampling of the system loads and wind infeeds, generation and network constraints. The MCS wind and load data are written to an excel file which is read by an optimization tool 'AIMMS' [AIM99c, AIM99a, AIM99b] in which the optimization problem is implemented. The built-in non-linear solvers in AIMMS are able to handle the optimal power flow problem as well as the iterative process for different MCS samples. The numerical results from AIMMS are loaded to MATLAB [MAT10] for further data processing.

### 5.3.3 Results

The distributions in box-plots of the loading factor on each line in the system are presented in Fig. 23.3. In the constraints of OPF the loading factor is set to equal or less than 1. In case that the loading factor is 1, it means that the power flow has reached the maximum allowable transfer capacity. In the box plot[2], the median is denoted in red line within the each box (bound by upper and lower quartiles). We can clearly identify the potential weak network points by inspecting the median of the distribution of each line. Fig. 23.3 provides the direct visual illustration of the line loading percentage. In order to further specific the weak network points in a more precise manner, a ranking of severity has been plotted in Fig. 23.4.

After simulating 10000 scenarios of possible combination of wind power infeed and load, the frequency of the overloading are listed in Fig. 23.4. We observe that line 40, 44, 27, 28, 3, 16 and 20 experience overloading more than 60% of the scenarios. Translating back to the time domain, these lines are most likely to experience the overloading more than 60% of the time under the normal operation. To this extent, these lines are the weakest links in the network that deserve most attention. Less severe lines are 31, 13, 24, 19, 37, 26, 2, and 9 that experience the overloading between 6.02 to 38.98%. The relative safe lines classified as the overloading probability ranging from 0.01 to 2.12%, which consists of line 7, 1, 12, 18, 30 and 32. The rest of the lines never encounter overloading throughout the entire scenario simulation, and thus are classified as safe in the analysis. From ranking of the overloading frequency under 10000 different scenarios taking into account the stochastic wind and load, we thus identify the weak network points of the system. The outliers are denoted in red lines outside the box. Their occasional existence underlines the fact as follows. In case

[2]In a box-plot, the box has lines at the lower quartile, median, and upper quartile values. Lines extending from each end of the box to show the extent of the rest of the data (whiskers). Outliers are data with values beyond the ends of the whiskers. Each of these data is represented by the marker $'+'$ and corresponds to the tails of the distributions.

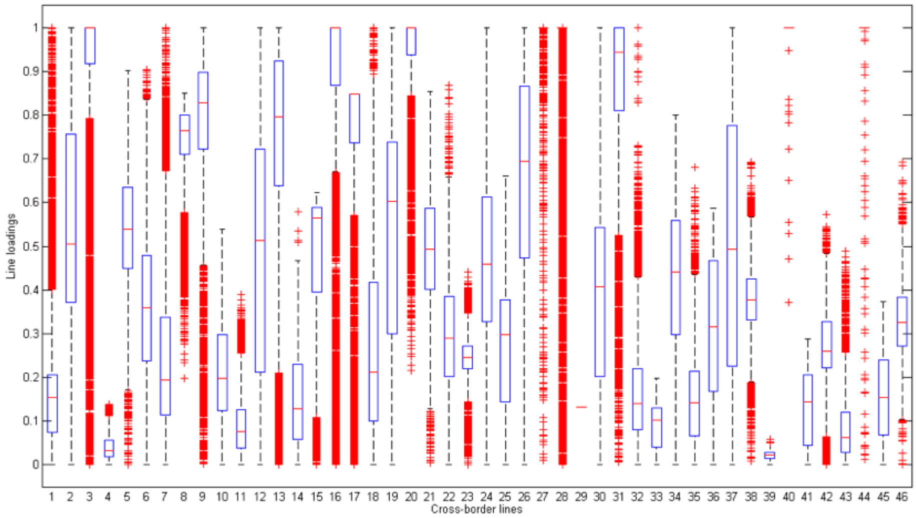


Figure 5.3.3: Line loading distribution

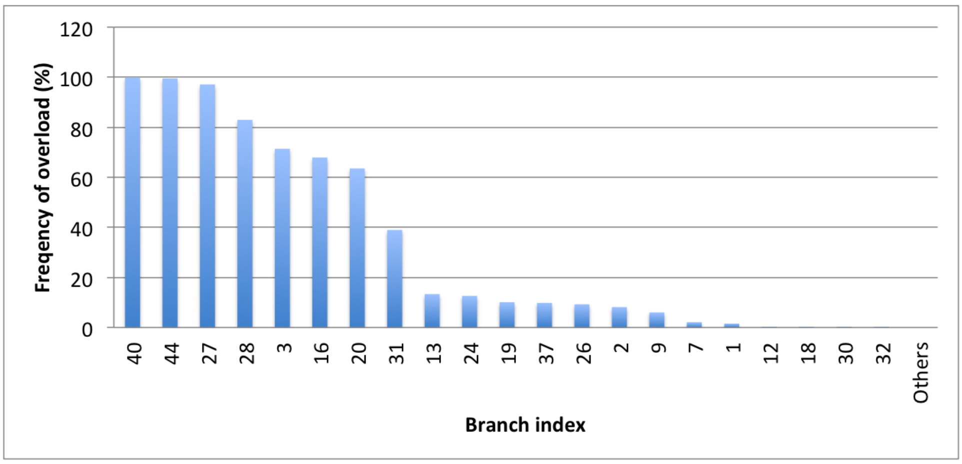


Figure 5.3.4: Frequency of overload

of no congestion between adjacent nodes and the same merit orders at all buses, there may be more than one optimal solution with the same total operation cost. This can be explained, that if the load needs to be served by two generators with the same cost, the optimal solution then are not unique. Without any constraint violations, any combination of output levels of the two generators is the optimal solution. The power flows are strongly related to the power outputs of generators, and thus some of the power flows are then not close to the upper and lower quartiles in the box plot, forming the outliers. Also, it is worth noting that some distributions of the wind speed dataset have long tails, which in turn create outliers.

## 5.4 Policy Uncertainties - Multiple Scenario Analysis

Energy policy directive is one of the driving forces that encourages the generation fleet to operate in a certain direction, which in turn changes the power flow pattern in the power system. In 2011, Germany officially launched plans to abandon its nuclear energy from 17.7% or nothing, meanwhile encouraged efficient renewable integration to the power system. The stress on steady-state system operation may be drastically escalated with more weak network points occurring in the system. Taking into account the possible future energy directives is thus very important in the power system analysis, especially in evaluating the transmission network behaviour subject to all uncertainties aforementioned.

The methodology presented in the previous section can be further expanded to incorporate the uncertain policies into the weak network point analysis. The overview of the extended methodology is shown in Fig. 24.1.

An energy policy scenario represents the possible future generation mix, including the generation information such as capacity, location and fuel type, etc. Each policy scenario has an estimated percentage of occurrence in the future, 100% in total. Based on these probabilities, a supervising sampling process can be added which enables the random choice between the different scenarios. In Fig. 24.2, this supervising sampling process is presented schematically. Based on this approach, a 10000 sample MCS for two scenarios $S_1$ and $S_2$ with respective probabilities $P_{S_1} = 0.4$ and $P_{S_2} = 0.6$ results in the random mixing of 4000 samples for $S_1$ and 6000 samples for $S_2$. Based on the theory of Monte-Carlo techniques, such random sampling from multiple scenarios allows the estimation of the joint statistics of the system outputs, which in the current context translates into the estimation of the system impacts from both possible future developments, weighted by their probability of occurrence.

At this point, we can perform two approaches to perform the system assessment. The underlying assumption is we consider the wind and load

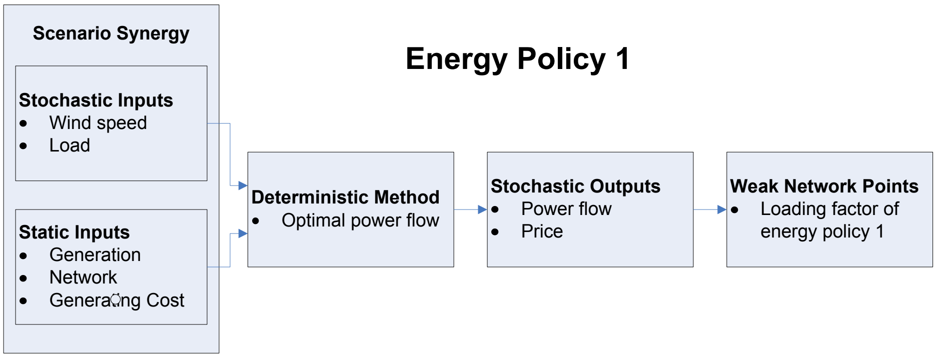


(a) Stochastic modelling of policy scenario 1

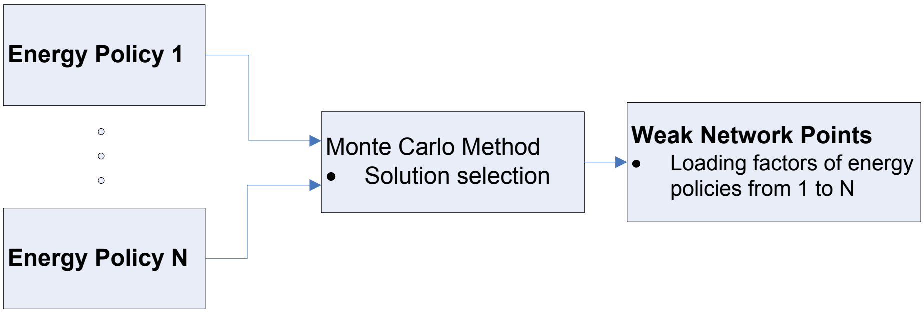


(b) Stochastic modelling of multiple scenarios for weak network points identification

Figure 5.4.1: Overview of stochastic modelling of multiple scenarios for weak network points identification

variations are independent of the energy policy uncertainties.

- Approach 1: As described above, the 10000 MCS samples will feed in from policy 1 to $n$. Taking energy directive 1 as an example, after feeding 10000 MCS into policy directive 1, the total number of this intermediate result is 10000. In order to refine the weak network points from the intermediate results, random selection from the intermediate results are chosen, using the same pre-defined percentage of policy possible occurrence as the selection percentage for the final results. Denote $P_1$ as the probability of energy policy 1, and the final refined selection out of policy 1 is $P_1 * 10000$. The energy policy iterates to $n$, and the total number of the final refined results is 10000 taking into account all possible energy policies.

- Approach 2: Since we know the $P_1$ ahead of the system analysis, we can randomly select the $P_1 * 10000$ samples from the MCS dataset, as the possible wind/load future that policy 1 may subject to. Similar treatment toward $P_n$, and the analysis should yield the same results

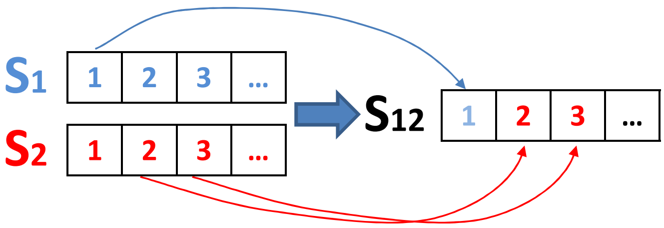


Figure 5.4.2: Process for sampling from multiple scenarios

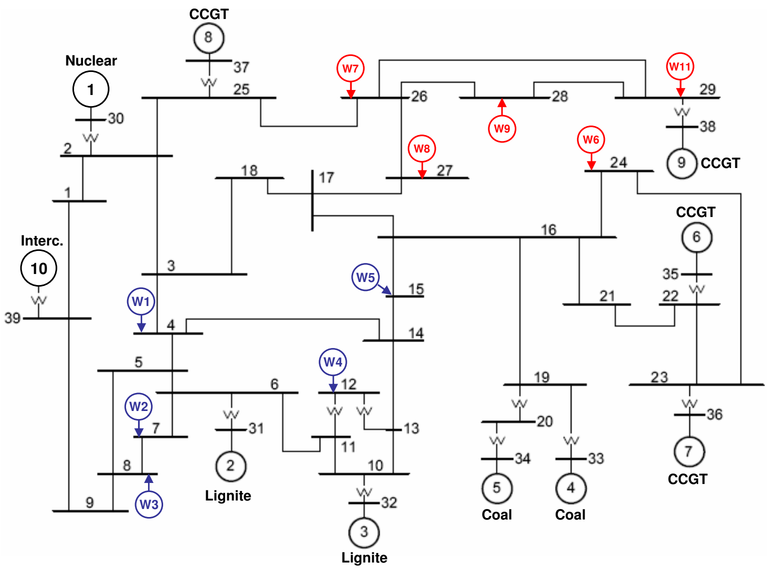


Figure 5.4.3: Single line diagram of the modified 39-bus New England test system [Pai89]

as in approach 1.

The salient feature of the methodology is to provide one single solution that incorporates all uncertainties induced by stochastic generation and various energy policy directives. The same MCS dataset can be used repeatedly in all possible energy directives, resulting in great reduction of computational time. Moreover, in approach 2, the computational effort is even less since the random selection process starts even before the simulation assessment.

## 5.5 Case Study: Diversified Scenarios

### 5.5.1 System and Wind Deployment Scenarios Data

A study case is presented concerning the assessment of the impact of wind power deployment under two locationally diversified scenarios. A modified version of the IEEE 39-bus New England test system is used as system model [Pai89]. The network parameters, generation and load data are taken from case39.m in [ZST11]. The single-line diagram for the system is given in Fig. 24.3. The system comprises 39 buses, 10 generators and 46 transmission lines (100 kV) with total installed capacity 7367 MW and total load 6254 MW/1387 MVar. The following modifications were applied for the specific study case:

- *Generator types*: Four types of generators are assumed in the system according to the fuel used as indicated in Fig. 24.3, namely Nuclear (Gen. 1-1040 MW), Lignite (Gen. 2-646MW, 3-725 MW), Coal (Gen. 4-652 MW, 5-508 MW) and CCGT (Gen. 6-687 MW, 7-580MW, 8-564 MW, 9-865 MW).

- *Cost Curves*: Linear cost curves are assumed for the generators with typical values per fuel at 3€/MWh (Nuclear), 18€/MWh (Lignite), 35€/MWh (Coal) and 80€/MWh (CCGT).

- *Operational limits*: Nuclear and Lignite units are considered as must-run units. The minimum operational levels are set to: 70% for Nuclear units, 50% for Lignite units, 40% for Coal units and 30% for CCGT units.

- *Interconnection*: Generator 10 represents the interconnection to the rest of the system with total capacity 1100 MW. The cost of importing/exporting is set at the same level as the CCGT units, therefore 80 €/MWh.

The deployment of 2000 MW of wind power is investigated under the following diversified scenarios:

- *Wind at South-East*: 2000 MW of wind are uniformly distributed in 5 locations in the system buses 4, 7, 8, 12, 15 (indicated by blue color in Fig. 24.3). The probability of this scenario is assumed as 0.4.
- *Wind at North-West*: 2000 MW of wind are uniformly distributed in 5 locations in the system buses 24, 26, 27, 28, 29 (indicated by red color in Fig. 24.3) The probability of this scenario is assumed as 0.6.

In both scenarios a 10% increase in the total system load is assumed, assigned pro-rata to all system loads.

### 5.5.2 Stochastic Modelling of Inputs Data

For this study case, both types of data (Case $A$ and $B$ presented in Chapter 4, Section 4.1.1) were used in order to show the applicability of the methodology. Due to lacking time-series wind speed, Case $B$ is an effective approach to model the MCS behaviour of stochastic wind infeeds. When the time-series datasets are not available, expert opinion could be used to assess the the marginal distributions and dependence structure. The settings of the stochastic modelling of wind infeed can be found in Section 4.1.1, as shown in Case $B$ in Section 4.1.1. In terms of system load modelling, the country load data from ENTSO-E were used to assess the stochasticity of the system loads [EE, PLvdS11]. The data for the year 2008 were used to assess the load variability in each system bus and the stochastic dependence between system loads at different locations are shown in Fig. 19.8.

### 5.5.3 OPF Formulation: Estimated Unit Commitment (UC)

To incorporate the main operational constraints of the conventional generators, a unit commitment decision is incorporated in the algorithm based on a double-loop solution of the OPF problem. In the first loop an OPF is estimated with the minimum power output for all generators set to zero; the generators that are dispatched below their operational limits are identified; these generators should be de-committed. In a second model run the OPF solution for the system is estimated by including only the committed units as they are derived from the previous model run. This formulation allows replacing the integer unit commitment problem by solving two times the OPF problem. This allows decreasing the computational time significantly, which can be crucial when solving large problems.

## 5.6 Results

A stochastic AC-OPF was solved for a 10000-sample MCS. The Monte-Carlo simulation was performed in Matlab. For solving the stochastic AC-OPF, a modified version of the Matpower solver was used [ZST11]. For

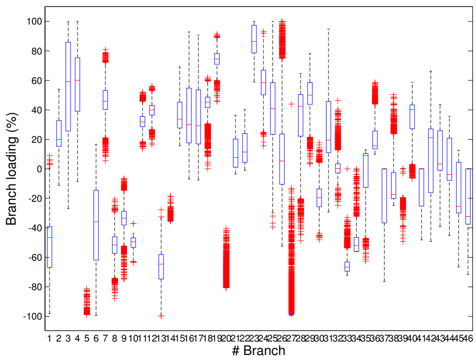


(a) Scenario 1

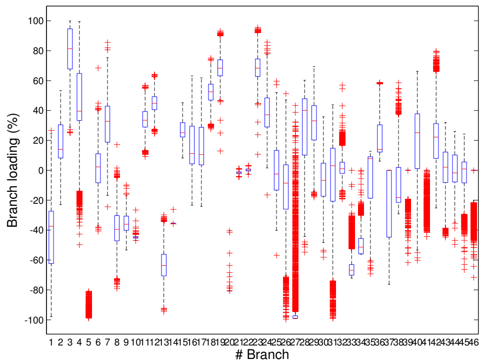


(b) Scenario 2

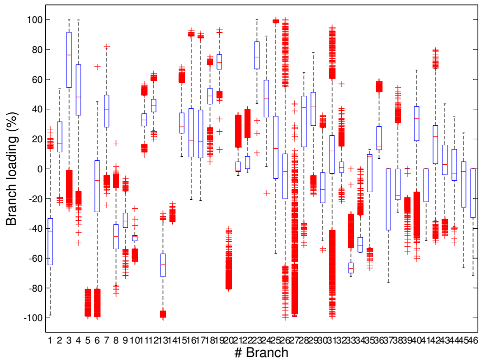


(c) Scenario 12

Figure 5.5.1: Box plots indicating the loading of the system branches (10000-sample MCS)

each sample, a double solution of the AC-OPF problem was performed in order to obtain the unit commitment. To investigate the differences, all three scenarios were estimated: wind deployment in South-East (Scenario 1), wind deployment in North-West (Scenario 2) and the joint scenario based on the above-mentioned scenario probabilities (Scenario 12).

In Fig. 25.1 the results from the 10000-MCS AC-OPF simulation are presented in box-plots for the power flow distributions in the system lines. Such plots provide a concise overview of the total network operation by giving the statistics of all the line power flows. We can see that the wind power integration leads to a high variability of the system power flows; in most system lines power flows in both directions are observed (the power flow distributions extend to both positive and negative axes).

As can be seen in Fig. 25.1a and 25.1b, the power flow patterns change between the scenarios due to the different location of the wind parks. By applying the methodology of Section 24 on sampling both scenarios, the scenario 12 is obtained. The branch power flow results are summarized in Fig. 25.1c. Using these results, the prominent congested corridors under

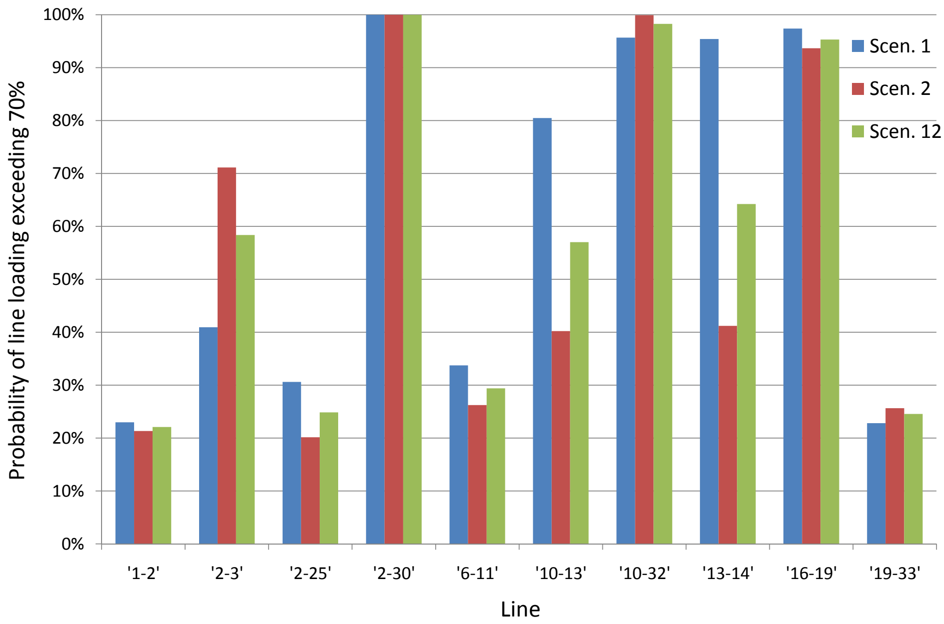


Figure 5.5.2: Line overloading probability for joint scenarios

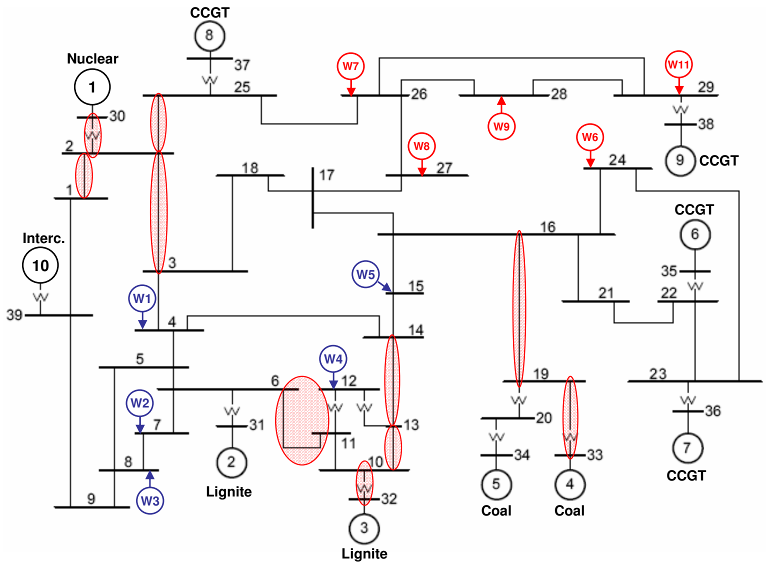


Figure 5.5.3: Identified weak network points for the 39-bus New England test system

both scenarios can be identified based on the specific scenario probabilities. These points should be prioritized for the future network development, since they form the prominent network weaknesses under all possible future developments.

In Fig. 25.2 these prominent weak network points are indicated based on the results of all scenario model runs. The indicator chosen for the identification of weak network points is the probability of line loading exceeding a pre-defined level, at this case chosen at 70% of maximum branch capacity. This probability can be interpreted as the percentage of time that the line loading exceeds the threshold of 70%.

The location of these points is presented in Fig. 25.3. As can be seen, the main congested corridors are identified in the connection of the Nuclear power plant (Gen. 1), at the area of the Lignite plant 2 (Gen. 3) and at the connection of the coal plants. As indicated in Fig. 25.2, the joint scenario captures the characteristics from both locational deployments. Therefore, a single model run can provide the required insight for network planning than the analysis of multiple possible future scenarios.

## 5.7 Excessive Wind Treatment

In a low-load-high-wind situation, either wind power must be cut off or baseload generation must be de-committed when the net load is below the minimum load capability of the conventional generators. De-committing baseload generation may have adverse impacts on the optimal generation mix for the following day due to the technical constraints of the conventional units. The ability to perform the wind curtailment on one hand keeps the system balance. On the other hand the curtailment challenges the renewable energy initiation of exploring the full potential of free energy and its environmental friendly advantages. As will be discussed later, the minimum load 'problem' may be a real opportunity for the appropriate type for exporting the excessive wind power.

Although the wind energy profile varies from minutes to hours, to months, it is possible to predict minimum load problems on power systems with high wind penetration with reasonable accuracy years in advance. The assessment of power system analysis taking into account the surplus energy forecast would allow the power system operators to plan the operation with sufficient security margins.

### 5.7.1 Power Export Modelling

One possible way to tackle the minimum-load 'problem' is to export the excessive surplus energy to other areas via interconnectors. This does not imply that free wind energy should be exported directly to other areas, but to utilize the wind energy as much as possible locally within the control area, and to export the rest of energy generated from other 'must-run' units. It is economically beneficial when the free energy is fully utilized locally because the energy price and the total fuel cost of the system will be reduced. As long as the neighbouring area offers a better marginal price that is higher than the current system locational marginal price, the local generating units continue to produce to meet the new economical equilibrium point. The exporting feature can be modelled as dispatchable load [ZS11], which can be further modelled as negative power injection to the system.

Taking 39-bus New England test system for instance, generator 10 is the interconnector that connects to rest of US/Canada. In the conventional interconnector modelling, it is modelled as a nuclear power plant that is only capable of injecting power to the local system. However, to deal with the minimum-load problem as the wind infeed is excessive to the load, the system should be able to export the excessive wind to neighbouring areas where the generation cost of other areas is higher. Such price difference generates incentives for the original generating units (the price cheaper area) to export more power to the higher price area.

To enable the export and import features in the system modelling, an additional generating unit has been connected to the system. However, the additional units are modelled with the following features

- The additional unit (export unit) with the same generating output capacity should be connected to the same bus with the interconnector, resulting in two generating units connecting to the same bus
- The exporting unit is mutually exclusive to the importing unit, assuming the interconnector is either being operated to export or import power. Moreover, it is also theoretically possible not to import or export at all if no economic incentive (i.e. price differences) is provided.

### 5.7.2 Time-Independent UC

In the process of identifying the weak network points, UC becomes of importance in terms of considering the limitation of generating units over a certain period of time. Constraints that affect each unit individually are categorized as follows,

- Maximum and minimum generation boundaries
- Flexibility
- Minimum up and down time
- Ramp rate

Conventional UC modelling consists of various time-dependent operational limitations of generating units, such as ramp rate, minimum up and down time, etc. Considering the methodology of stochastic modelling of wind power infeed, such time-dependent constraints has minor impact on the network analysis. In other words, Monte-Carlo simulation is a time-independent method that emphasizes the impact assessment of wind variability on the system operation. The time-dependence of UC is not applicable to be incorporated in the methodology. Thus, time-independent features of unit commitment modelling are of interests to be taken into account when the generating units limitations are of concern.

Flexible plants such as coal-fired, oil-fired, OCGTs, CCGTs and hydro plants with storage are of interest in their operational status and output. The common characteristic of such plants is the flexibility of their on-off status and the adjustment of the power outputs. On the contrary, the inflexible plants of nuclear, run-of-river hydro, renewables of solar and wind, and combined-heat and power plants (CHPs) are treated differently. The nuclear plants are modelled with 0 and 1 with a high minimum power output up to 70% of the maximum capacity. Wind energy are incorporated as given negative load due to its inflexible dispatch.

To emphasize the time-independent UC, the corresponding optimal power flow equations in Chapter 3 can then be rewritten as

**Objective function**

$$Minimize \quad \sum_{i=1}^{N_g} C_i(P_{gi}) * n_g \tag{5.7.1}$$

where $n_g$ is a binary number indicating the UC status, 1 represents unit ON, and 0 otherwise.

**Constraints**

*Power balance constraint:*

$$P_i = P_{g,i} * n_g - P_{d,i} \tag{5.7.2}$$

$$Q_i = Q_{g,i} * n_g - Q_{d,i} \tag{5.7.3}$$

*Generator unit constraint:*

$$\underline{P_{gi}} * n_g \leq \quad P_{gi} * n_g \quad \leq \overline{P_{gi}} * n_g \tag{5.7.4}$$

$$\underline{Q_{gi}} * n_g \leq \quad Q_{gi} * n_g \quad \leq \overline{Q_{gi}} * n_g \tag{5.7.5}$$

It should be noted that $n_g$ denotes binary vector that controls 'on-off' states of all generating units. In the generator constraints, in stead of $\underline{P_{gi}} \leq P_{gi} \leq \overline{P_{gi}}$ for all committed units, all generator related terms i.e. $P_{gi}$ and $Q_{gi}$ need to multiply $n_g$ to cover the de-committed generators [SYL02]. It is also worth mentioning that the objective function and constraints related to generators are indexed separately from the power balance constraint, which applies to all buses. When indexing, non-generator buses are not taking into account in the objective function and generator unit constraints, whereas all buses are necessary to fulfil the power balance constraint.

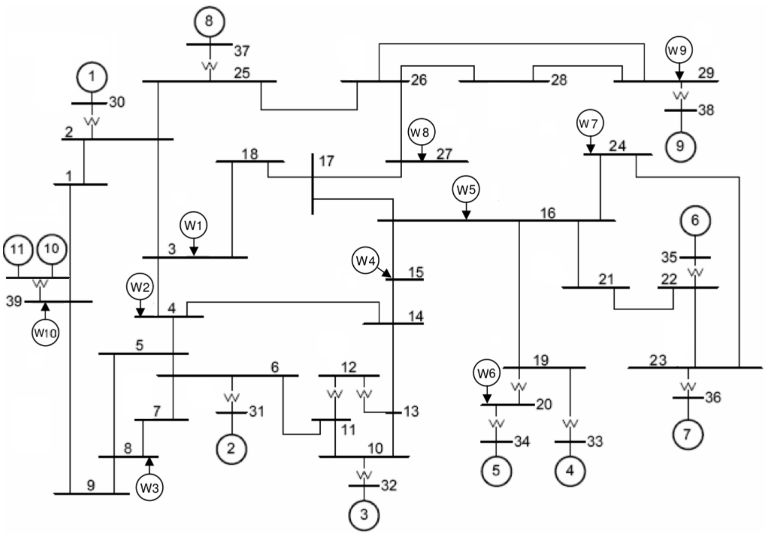


Figure 5.7.1: Modified New England test system with 3000 MW wind penetration

### 5.7.3 Case Study

To test the method with UC and exporting capability, we apply it to another modified IEEE 39-bus New England test system. Basic assumptions have been set to be the same as the previous, except the locations and installed capacity of wind power plants, as well as the introduction of exporting capacity of unit 11. The marginal cost of the export unit is set to 80€/MWh, the same as the import cost of unit 10. The non-discriminative cost setting ensures that the generator dispatch is not affected by the price incentive between importing and exporting activities, but the system balance and other technical constraints. The deployment of 3000 MW of wind power is investigated: 3000 MW of wind are uniformly distributed in 10 locations in the system. A modified New England 39 bus system has been shown in the following Fig. 27.1.

The system load is considered as independent from the wind activity in the system. AC-OPF formulation has been adopted in the case study for the accurate analysis of the system behaviour.

### 5.7.4 Results

The results have been presented in the following figures. In Fig. 27.2a, the box plot of line loadings shows the distribution of power flows through all branches in the system. We can clearly identify the possible weak network points by visualizing the upper bound of the box plot. Line number 1, 9, 12, 20, 21 and 41 experience the overloading issues subject to the MCS scenarios, shown in Fig. 27.3. Besides the weak network points assessment, we may further look at the distribution of the operational cost in Fig. 27.2b. Generally, the operational cost is a positive value, indicating the total cost of fuel burned in the conventional power plants. However, we do observe that the operational costs of 1.56% of the investigated MCS scenarios are negative, meaning that the fuel burned in the conventional power plants can be compensated by selling the excessive energy to the neighbouring area, yielding some extra income from the exporting activity. Since the marginal export price is 80 €/MWh, which is higher than the rest of conventional and wind power plants, the UC and ED will keep the system in balance with minimum outputs possible from the conventional units in additional to the free wind energy to feed the load. Anything additional will be exported due to incentive caused by the marginal price difference. The export price appears in the system as the negative cost. With large amount export and sufficient local wind power infeed, the system operational cost could become negative in a broad sense. Fig. 27.2c presents the percentage of committed units under the MCS spectrum. We can see that the first five units are always ON, including nuclear, lignite and coal power plants serving the base load. The rest gas turbines ranging from unit 6 to 9 vary the ON-OFF status depending on the wind and load conditions. Unit 10 and 11 are the interconnectors that are mutually exclusive. We can thus conclude the impact of the large amount wind power infeed on the conventional generators. With the export capability, the base load units are not affected due to their technical constraints such as minimum generate output. They are mainly kept ON, and producing for the based load. The affected ones are mainly the flexible units, due to their flexibility and price, they responds to the export price and sensitive to the wind and load conditions. In Fig. 27.4b and 27.2c, the importance of export is strongly emphasized when large amount wind energy is introduced to the system.

Fig. 27.4a and 27.4b show the system behaviour under a selected scenario of a low-load-high-wind situation. The total net active load in this scenario is 1.54 GW, much less than the original system load of 6.3 GW. In Fig. 27.4a, the generator outputs are presented. The first five units are ON, together with the wind power infeed, supporting the system power demand. Four out of five units are operated at their minimum output levels, respectively. However, due to the strong wind infeed, even almost all committed units are running at their minimum, there are still more power than the power demand. The excessive power are then to be exported. Unit 10 is OFF due to the excessive power from the ON units and wind power plants, in additional to the necessity of export. All excessive power, generated from conventional units and wind power plants, will be exported to the neighbouring area via unit 11. The capacity level of all units is shown in 27.4b. The committed conventional units of 1, 3, 4, 5 are operated at 70%, 50%, and 30%'s of their maximum values, in accordance with their minimum output levels. Unit 2,

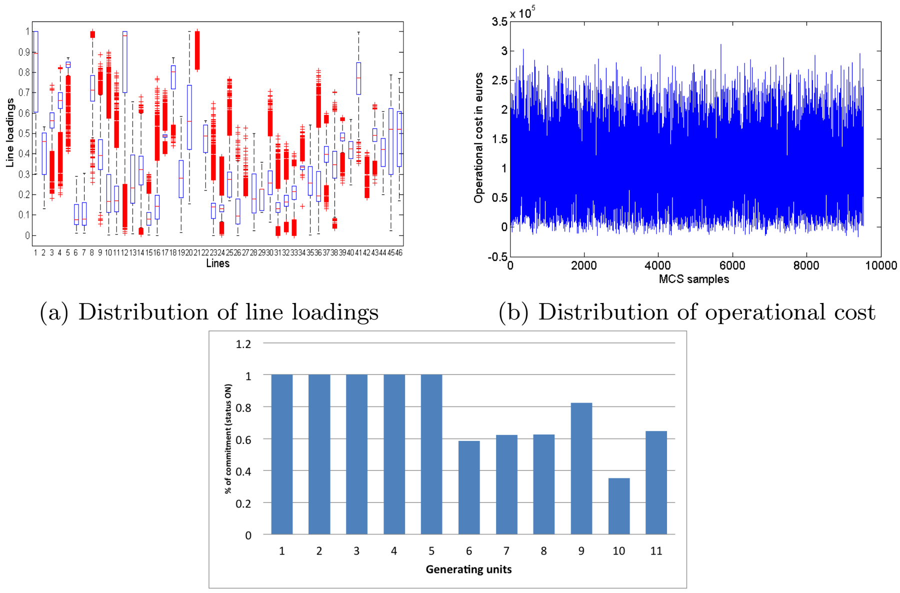

(a) Distribution of line loadings (b) Distribution of operational cost

(c) Percentage of committed generators

Figure 5.7.2: Distributions of network parameters

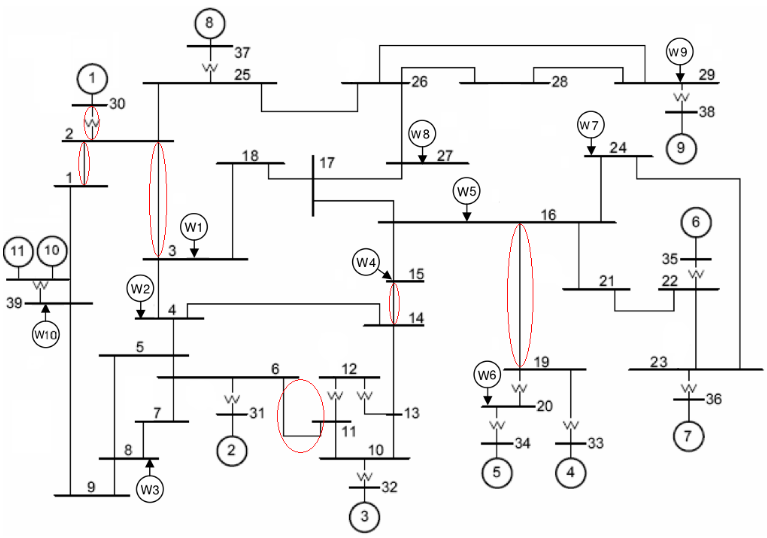

Figure 5.7.3: Identified weak network points

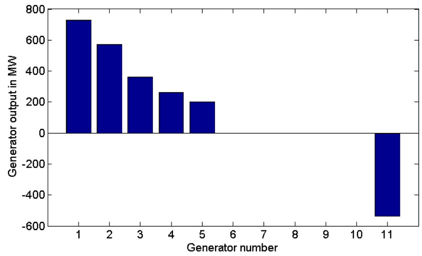


(a) Generator UC and dispatch of a low-load-high-wind condition

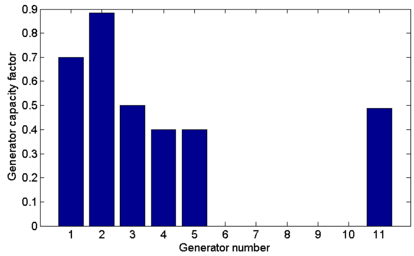


(b) Generator capacity factor of a low-load-high-wind condition

Figure 5.7.4: Generator UC and dispatch under a low-load-high-wind condition

the coal plant is operating around 90% of its maximum, which still remains within its technical boundaries.

## 5.8 Summary

This chapter proposes a methodology for the transmission network assessment taking into account the wind variability and dependence structure using a unified Monte-Carlo method and Copula approach. The methodology is firstly elaborated and applied to a single scenario study, and further enhanced to a more general approach by taking into account multiple scenarios caused by uncertainties raised from energy policy perspectives. With pre-defined probability of different energy directives of generation mix, the methodology is able to assess the steady-state behaviour using the same set of MCS samples, assuming the independent relationship between the generation mixes and the wind/load scenarios. Later in this chapter, the modelling of export capability and unit commitment have been incorporated to tackle the high-wind-low-load situation, providing a more comprehensive overview of the power system (i.e. weak network points) for system operators.

## 5.9 Conclusion and Comments

In this chapter, we first found out the stochastic optimal power flow (S-OPF) is suitable for the steady-state assessment of the power system operation when the variability of system input parameters is taken into account. The essential input for the Monte-Carlo simulation is to feed the deterministic method with the random samples that are able to mimic the original dataset. Previous studies have proven that the Copula approach is an effective sampling method in modelling the variability and the dependence structure of wind data. Combining Copula approach and OPF calculation, the distribution of the investigated variables (i.e. generator outputs, power flows) genetically contains the impact from variability of stochastic generators.

One important aspect of the S-OPF methodology is to incorporate the probability of the system parameters, i.e. future generation mix. We found that after properly assign the probability of the possible future policy directives, the S-OPF simulation is able to assess all possible future scenarios first, and concludes the final system behaviour in a distribution spectrum according to the probability assignment. Since MCS samples are independent from the future generation mix, the S-OPF greatly improves the computational speed by repeatedly using the same MCS samples for all different possible future generation scenarios. The final spectrum of the system behaviour incorporates all possible system generation mix subject to different wind conditions.

In the previous two main findings, the effort goes to the improvement of $S$ part of the S-OPF methodology. In the last section of the this chapter, we tried to improve the OPF functionality by introducing the export capability and unit commitment. We found that the export capability of the grid is essential in order to fully utilize the wind power potential. 'Excessive' is a relative terminology. If the system only tries to consume the wind energy with its own power demand, there is a higher chance when the wind power infeed becomes 'excessive' due to the power imbalance of the grid. On the contrary, as long as export is permitted with correct price signal, local wind energy has an additional option to be utilized rather than being curtailed. The meaning of the term 'excessive' becomes 'adaptable'.

Additional comments on the MCS simulation applicability: Previously Monte-Carlo method has been viewed as computational-intensive method, although it has been mainly used for more computational-demanding studies, such as in the Manhattan project. It has been widely recognized as an effective method only for offline assessment, according to the feedback from TSOs. However, besides the computer technology grows rapidly in the past ten twenty years, the algorithm of power flow calculation also improves dramatically. A new method of using Newton-Krylov solver to solve very large scale network of million buses power flow achieved very promising results of 120 times faster than a direct solver [ILVvdS12]. We may further conclude that MCS in the near future will be applicable to the online assessment of power system.

# Chapter 6

# Snapshot-based Expansion Planning

The main focus of the transmission expansion planning is to find the optimal structure and least cost transmission investment plan given the anticipated load and generation configuration. This chapter proposes a transmission expansion methodology, which aims at alleviating congestions in the transmission network meanwhile minimizing the combined operational and investment cost. The proposed methodology originates from the conventional DC-OPF formulation. Beyond that, its novelty contributes to the active control of dual variables, i.e. Lagrangian multipliers (LMs) in the network expansion studies in order to achieve the optimal network topology. That being said, the methodology is able to provide the ultimate congestion-free grid topology at the least expense, departing from the original congested or infeasible grid topology.

## 6.1 Introduction

Congestion alleviation is one of the driving forces for solving transmission network expansion problems. Congestion, in general, implies that more power transactions are desired than can be facilitated by the available transmission capacity [SF04]. Practices related to internal and cross-border congestion management have been investigated in [PSR05]. Countries like Belgium seldom experience internal congestion, and thus can model their own control area as a 'virtual copper-plate'. In case that congestions due to increasing demand or incorporation of renewable energy or distributed generation in the system, there are three ways to mitigate congestion from the planning viewpoint,

- reduce electricity demand in the congested area through energy efficiency measures and demand side management

- build more generation capacity near the load-intensive area
- build additional transmission capacity to facilitate the power transfer to the load

This chapter addresses the common option of transmission expansion towards a copper-plate network structure. From the transmission system operational viewpoint, remedial actions such as corrective switching can also alter the power flow, which consequently could remove the congestion from the operational level [HOO11,SV05,RM99]. However, such remedial actions, as the name implies, do not prevent congestion problems from occurring. Thus, it is necessary to allocate new capacity in the system in order to alleviate the anticipated congestions in the planning stage.

In general, energy markets become more robust and efficient when transmission investments are made for congestion removal, as has been the case in Nordic countries. Sufficient transmission capacity contributes to reducing the risk of abusing market power and can be assured by transmission network congestion alleviation [pro08a]. The reduction of congestions is an indicator of social and economic welfare assuming equitable distribution of benefits under the goal of the European Union to develop an integrated market [EE12]. A relative small number of selective additions to transfer capacity could lead to major economic benefits for many consumers, evidenced by US Department of Energy [oE06].

Transmission network expansion studies are typically based on some extreme loading snapshots (e.g. winter peak). Such design indicates the network is able to cope with normal system operation most of the time [pro08a]. From the system security point of view, the power system should always fulfil the N-1 criteria in operation, which imposes tighter constraints on the transfer capacity in the system. If the grid experiences congestions in the normal operation, it is likely that the grid cannot withstand the stress when one component is out of service in the system due to failure or maintenance.

When planning in the power system, conventional OPF calculation generally provides two types of solutions:

- There is an optimal solution, where the load can be supplied by the generation, but congestion occurs in the system.
- The solution is infeasible because the local power demand cannot be supplied by the generation due to limited transmission capacity.

Both issues translate into an inefficient network infrastructure and can be solved in the context of transmission expansion planning. The methodology proposed in this chapter is able to expand the network from an insufficient network topology, i.e. either infeasible or congested existing grid, to a copper-plate structure meanwhile minimizing the total operational and investment costs.

The proposed methodology in addition to answering how o deal with transmission congestions, also answers the question on where to install transmission in order to deal with generation/load scenario projections. When to install is tackled directly related to the generation/load scenario by considering a stepwise network development. In other words, if the generation/load scenario of 2020 is under investigation, the network should be expanded and operated before 2020 to meet the challenging scenario.

Section 39 presents the methodology for the expansion studies, including the mathematical formulation of the modified OPF with the special emphasis on the formulation of LMs in the context of OPF and additional congestion alleviation constraints. Section 33 presents a test case to demonstrate the applicability of the methodology. Based on the generic modelling property, further enhancement emphasizes on implementation infeasibility of expansion options adopted with a similar test case as in Section 33.

## 6.2 Methodology

### 6.2.1 Overview

Congestions can be identified by an optimal power flow calculation, attempting to optimize the steady-state power system performance with respect to an objective function, subject to various constraints. One of the most salient features of OPF calculation is the results concerning the economics of the power system. It has been shown that Locational Marginal Price (LMP) can be interpreted as the summation of marginal costs of energy, congestion and losses [Lit09, SYL02].

In the DC-OPF calculation, where losses are neglected, LMPs are represented by LMs associated with constraints on the output of generating units and on transmission capacity. LMs indicate the increment in optimal cost with respect to small changes in the parameters of the network [SW03]. If congestion occurs in the system, the LMP at each bus will be different from each other due to violations of the transmission capacity. The conventional OPF formulation does not directly optimize LMs, which is treated as by-products of the optimization.

The contribution is to use LMs not only as the congestion indicator, but also as control variables in the optimization formulation. As introduced in Chapter 4, the LMs are the dual variables of the optimization formulation, which are determined by the values of the primal variables. Some of the multipliers are associated with the power flow constraints, and their values are strongly influenced if congestion occurs in the system. The expansion methodology consists of three major steps:

- derive the LMs
- introduce congestion alleviation constraints related to LMs

- perform expansion from the expansion candidates inventory if congestion occurs

In order to manipulate LMs in the optimization formulation in the expansion studies, first it is necessary to explicitly derive LMs (i.e. dual variables) that establishes the link between the primal variable (i.e. generator power output $P_g$ and power flow $P_f$) and the multipliers. Thus, controlling the multipliers indirectly controls the primal variables. Also, Karush-Kuhn-Tucker conditions [BV04], also known as KKT conditions, introduce extra constraints linking primal and dual variables.

To alleviate the congestions in the network, derived LMs related to the power flow constraints are forced to be zeros by adding extra constraints in the optimization problem (i.e. primal problem), targeting no congestion in the system. To fulfil the congestion-free requirement, the best expansion option from the expansion inventory is automatically selected and integrated into the existing grid to facilitate the future generation and load conditions.

In DC-OPF, the $B$ matrices refer to the backbone of the network representation, which relates to the admittance matrix $Y$. Conventionally, $B$ matrices contain only the existing network structure. In the proposed methodology, $B$ matrices contain two parts, namely the existing network structure and all possible expansion candidates, defined as the multiplication of the possible expansion candidates (i.e. location, type) and the required number of these candidates. The contribution in this paper assumes that the potential candidates are installed in parallel with existing lines, mainly due to the raising concerns on the right-of-way authorization and other practical implementation limitations. However, further modelling enhancement to include new transmission corridors, can be easily implemented based on the proposed modelling framework, in particular based on the modification of the $B$ matrices.

All possible expansion candidates are further specified in both location and type, offering a wide range of possible locations and types for the selection of the best expansion candidate. The contribution in this chapter focuses more on the expansion location and type as shown in Fig. 31.1a where the potential candidates are installed in parallel with existing lines, mainly due to the raising concerns on the right-of-way authorization and other practical implementation limitations. However, further enhancement to include new transmission corridors, as shown in Fig. 31.1b, can be easily implemented based on the proposed modelling framework, in particular based on the modification of the $B$ matrix.

- *Location*: All possible expansion candidates include
  - Existing transmission corridors: candidates are placed in parallel to the existing lines, shown in Fig. 31.1a

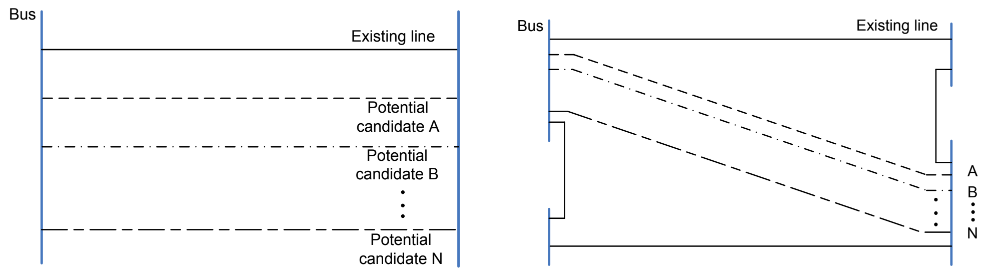


(a) Possible expansion locations and various types: parallel to an existing line

(b) Possible expansion locations and various types: connection at new locations

Figure 6.2.1: Possible locations and types of expansion candidates

   - New transmission corridors: candidates are placed between buses which are not previously connected, shown in Fig. 31.1b

- *Type*: At each location, different types of expansion technologies or lines can be applied, shown in both figures of 31.1a and 31.1b

### 6.2.2 Mathematical Formulation

The method uses the DC formulation for the fundamental stage of analysis in the transmission expansion planning problem. The DC formulation offers fast computation and reliable results on the transmission level analysis where the line resistance $R$ is much smaller than the reactance $X$. The mathematical formulation of the problem can be briefly described as follows. The objective function and constraints are modified with respect to the conventional DC-OPF formulation.

#### Objective function

The objective function consists of the minimization of the system fuel cost per year and the annualized unit cost of additional lines for expansion purposes [XW07].

$$minimize \quad C_{Total} = C_{op} + C_{in} \tag{6.2.1}$$

where $C_{Total}$ represents the total cost, $C_{op}$ and $C_{in}$ represent the annual operation cost and the investment cost, given by

$$C_{op} = \sum_{m=1}^{N_g} C_m(P_{g,m}) \cdot 8760 \tag{6.2.2}$$

$$C_{in} = \sum_{o=1}^{N_o} \sum_{k=1}^{N_l} (n^a)_{k,ij,o} (I^a)_{k,ij,o} \tag{6.2.3}$$

where

| | |
|---|---|
| $N_g$ | is the number of generating units |
| $C_m$ | is the quadratic cost function of generating unit $m$ in [k$/h] |
| $P_{g,m}$ | is the power output of generating unit $m$ |
| $N_l$ | is the number of lines before expansion |
| $N_o$ | is the number of candidate options |
| $(I^a)_{k,ij,o}$ | is the investment cost of candidate line $o$ in parallel to $k$th line from bus $i$ to $j$ in [k$/km] |
| $(n^a)_{k,ij,o}$ | is an integer indicating the number of expansion candidates in parallel to line $k$ to alleviate the congestion |

Theoretically from the modelling point of view, for a network consisting of $N_b$ buses the total possible expansion locations are $N_b(N_b - 1)/2$. In practice, not every pair of buses can be connected. Several corridors can be carefully excluded when taking into account framework conditions such as geographical long distance, which reduces the redundancy in computational complexity. In this contribution, it is assumed that new lines are placed in parallel to existing lines. The right-of-way costs and other miscellaneous costs associated with building and placing a new line are aggregated into the cost term $(I^a)_{k,ij,o}$. The index $k$ represents the $k$th line of the system, and indices $i, j$ represent the location of line $k$ starting from bus $i$ and ending at bus $j$. $C_{in}$ then represents the total investment cost for building a copper-plate network that has power transaction without congestions.

Some papers [dS06, GR09] include the possibility of loss of load with a given penalty cost in the objective function. The inclusion of loss of load means that it is acceptable to perform load-shedding in the system expansion study as long as the the penalty cost is cheaper than building a new line in the system or other relatively inexpensive measures. However, [Wikd] claims that although load shedding commonly happens in developing countries, it is considered an unacceptable failure of planning and cause significant political damage to responsible government in developed countries. The assumption of allowing load shedding is not in accordance with [EE10] where the system usually shows very low risks of load shedding as long as the operation conditions qualify as regular. Thus, during the planning phase of the network expansion, the proposed methodology rejects the load shedding action by excluding the loss of load terms in the objective function. The underlying message remains that in the planning phase of the network expansion, no load-shedding should be performed during the normal operation i.e. under all foreseen circumstances. Instead, the normal operation should provide sufficient transfer capacity to serve the load without jeopardizing the system security.

### Constraints

***Active power balance constraints***
The net active power injection at each node is the difference between the active power generation and the active power demand for that node.

$$P_i = P_{g,i} - P_{d,i} \tag{6.2.4}$$

$$P_i = \sum_{j=1}^{N_b} (B_b^a)_{ij} \delta_j \tag{6.2.5}$$

$$(B_b^a)_{ij} = \begin{cases} (B_b^{old})_{ij} + \sum_{o=1}^{N_o} (n^a)_{k,ij,o} B_{ij,o} & i \neq j \\ (B_b^{old})_{ij} + \sum_{j=1}^{N_b} \sum_{o=1}^{N_o} (n^a)_{k,ij,o} B_{ij,o} & i = j \end{cases} \tag{6.2.6}$$

where

| | |
|---|---|
| $N_b$ | is the number of buses |
| $P_i$ | is the net active power injection at bus $i$ |
| $P_{d,i}$ | is the active load at node $i$ |
| $(B_b^a)_{ij}$ | is the $ij$th element of the imaginary part of bus admittance matrix after expansion. |
| $(B_b^{old})_{ij}$ | is the $ij$th element of the imaginary part of bus admittance matrix before expansion |
| $B_{ij,o}$ | is the imaginary part of bus admittance of expansion candidate $o$ |

***Power flow constraints***
Inequality constraints define the upper bound on the power flowing through every branch in the system as follows

$$|P_{k,ij}| \leq (1 + \sigma W_{k,ij}) \overline{P_{k,ij}} \tag{6.2.7}$$

$$|P_{k,ij,o}| \leq (n^a)_{k,ij,o} \overline{P_{k,ij,o}} \tag{6.2.8}$$

$$\sum_{k=1}^{N_l} W_{k,ij} \leq d \tag{6.2.9}$$

$$W_{k,ij} (n^a)_{k,ij,o} = 0 \tag{6.2.10}$$

$$P_{k,ij} = \sum_{i=1}^{N_b} (B_f^{old})_{ij} (\delta_i - \delta_j) \tag{6.2.11}$$

$$P_{k,ij,o} = \sum_{i=1}^{N_b} (B_f^a)_{ij} (\delta_i - \delta_j) \tag{6.2.12}$$

$$B_f^{old} = \begin{pmatrix} (B_f^{old})_{11} & \cdots & (B_f^{old})_{1N_b} \\ \vdots & \ddots & \vdots \\ (B_f^{old})_{N_l 1} & \cdots & (B_f^{old})_{N_l N_b} \end{pmatrix} \tag{6.2.13}$$

$$(B_f^a)_o = \begin{pmatrix} (B_f^a)_{11,o} & \cdots & (B_f^a)_{1N_b,o} \\ \vdots & \ddots & \vdots \\ (B_f^a)_{N_l 1,o} & \cdots & (B_f^a)_{N_l N_b,o} \end{pmatrix} \tag{6.2.14}$$

$$(B_f^a) = \begin{pmatrix} (B_f^a)_1 \\ \vdots \\ (B_f^a)_{N_o} \end{pmatrix} \cdot \begin{pmatrix} (n^a)_{1,o} \\ \vdots \\ (n^a)_{N_l,o} \end{pmatrix} \tag{6.2.15}$$

where

| | |
|---|---|
| $P_{k,ij}$ | is the active power flow on line $k$ from bus $i$ to $j$ |
| $\overline{P_{k,ij}}$ | is the transfer capacity on line $k$ |
| $P_{k,ij,o}$ | is the active power flow on expansion candidate line $o$ in parallel to line $k$ |
| $\overline{P_{k,ij,o}}$ | is the transfer capacity on candidate line type $o$ |
| $\sigma$ | is the maximum allowable percentage of temporary overloading |
| $W_{k,ij}$ | is a logical vector indicating allowable overloading, 1 is overloading and 0 otherwise |
| $d$ | is the maximum number of allowable congestion occurring concurrently |
| $B_f^{old}$ | is the imaginary part of the line admittance matrix before expansion |
| $(B_f^a)_o$ | is the imaginary part of the line admittance matrix of expansion candidates $o$ |
| $B_f^a$ | is the imaginary part of the admittance matrix of all expansion candidates |

To minimize $W$, a small penalty factor of 100 is added to the objective function, $C_{Total} = C_{in} + C_{op} + C_{Wp}$, where $C_{Wp}$ is $\sum_{k=1}^{N_l} W_{k,ij} \cdot 100$. This properly selected penalty factor does not jeopardize the result optimization but to control $W$ only. In other words, $W$ can only be 1 if it is necessary due to this penalty factor, otherwise $W$ is always zero.

In the power balance and flow constraints, $(B_f^a)_o$ has the same matrix structure as $(B_f^{old})$, because the expansion candidates will be placed in parallel to the existing grid. Different expansion options $o$ in $(B_f^a)_o$ form the complete possible expansion option set $B_f^a$. The power flow pattern before the expansion will be different from the pattern after the expansion, because the admittance matrix and power transfer distribution factor (PTDF) of the system change with the addition of new lines.

From the network topology point of view, the $B_b$ and $B_f$ matrices are formulated such that power flow differences before and after the expansion is considered. Before the expansion, the candidates are 'potentially' placed in parallel with the existing grid. The $(n^a)_{k,ij,o}$'s are zeros for the initial expansion state. When an optimal expansion plan is found in the optimization, one or more $(n^a)_{k,ij,o}$'s become positive integers. The lines added to the system together with the existing grid form the new system topology. The $B$ matrix in the power balance constraint include both original and candidate options, are applied to the new system topology, and thus take into account power flow differences between the original and new network structures.

**Remark on over-investment**

Some reports [oE06, oE09] argue that although congestion is a reflection of legitimate reliability or economic concerns, not all transmission congestion can or should be reduced or 'solved', mainly because the building transmission facilities are costly and may not be cost-effective, in additional to the common public objection of building extra lines and towers. It is intuitive to say that a small percentage (e.g. 1%) of overloading on one line is not worth the investment of building a new transmission corridor. To address the concerns of such over-investment, the proposed model differentiates the 'unnecessary' congestion cases where the overloading levels are not severe. Both acceptable overloading levels and the number of such incidents happening concurrently are controlled so that the over-investment as well as the acceptable congestions occurring in the system are well balanced.

In order to filter out these unnecessary expansion circumstances, a limited number of non-heavily overloaded lines Eq. (31.7) are allowed to appear in the calculation by introducing parameters $\sigma$ and $W_{k,ij}$. $\sigma$ represents the maximum allowable percentage of temporary overload, and the binary $W_{k,ij}$ controls which line is allowed to have this allowable overload. Since the method allows these overloadings, the expansion options will not be triggered by these 'small' congestions.

Theoretically, all lines in the system are allowed an minor overload of $\sigma$ percentage of $\overline{P_{k,ij}}$, resulting in a new maximum transfer capacity of $(1 + \sigma W_{k,ij})\overline{P_{k,ij}}$. As an additional control layer, Eq. (31.9) controls the total number of allowable overload occurring at the same time in the system (i.e. smaller than $d$). Assuming that only one random line in the system is allowed (i.e. $d$=1) to have a maximum of 10% overload (i.e. $\sigma = 10\%$), the congestion alleviation algorithm thus will not treat any single line loading between 100% and 110% as a congestion case, because at this moment the new transfer capacity of this line is 110% of the original capacity. That is, when the power flow is between the normal transfer capacity and maximum allowable capacity, the algorithm considers this case as a normal operation condition and no expansion is necessary.

In this way the algorithm focuses on those severe congestions, and in turn prevents over-investment on negligible congestions. $W_{k,ij,o}$ is mutually exclusive to $(n^a)_{k,ij,o}$ in Eq. (31.10). This means that if an allowable overloading is presented in the system, then the expansion should not be activated at the same time on this particular line, i.e. $W_{k,ij}$ is one, $(n^a)_{k,ij,o}$

is zero. After the expansion by adding parallel lines to the heavily congested line, the congestion should be removed and the system should be in a normal operation condition, i.e. $(n^a)_{k,ij,o}$ is non-zero, $W_{k,ij,o}$ is zero. In other words, after the expansion, no congestion should occur on either the 'originally allowable congested lines', nor on the newly built line.

**Remark on the incentive of the network expansion**

The expansion methodology proposed does not utilize monetary terms, i.e. the values of LMPs and operational cost, directly as the incentive to build new transmission infrastructure. Instead, they are used as economic indicators to show how much, in terms of monetary values, the cost will be when a copper-plate network structure is proposed. To be more specific, the hardcore expansion incentive in the mathematical formulation is the expansion boundary of power flows of $(1 + \sigma W_{k,ij})\overline{P_{k,ij}}$ as the absolute maximum (taking into account the over-investment issue already) and the expansion criteria are $\mu$'s $= 0$ in Eq. (31.17) in the next section.

***Generator constraint***
The generator constraints define the power generators working range.

$$\underline{P_{g,m}} \leq P_{g,m} \leq \overline{P_{g,m}} \tag{6.2.16}$$

where $\underline{P_{g,m}}$ and $\overline{P_{g,m}}$ are the minimum and maximum active power output of generating unit $m$.

***Congestion alleviation constraint***
To enforce the copper plate network condition, we set the following constraints, reflecting the fact that in optimal electricity market condition where no congestion occurs, the LMPs of all buses in the system are equal.

$$\mu_k = 0 \tag{6.2.17}$$

where $\mu_k$ is the LM of line $k$. According to the Karush-Kuhn-Tucker (KKT) condition, if the power flow constraint along the line $k$ is an unbinding constraint, then the multiplier associated with the constraint is zero.

The congestion alleviation constraint ensures that the optimization process looks for the optimal solution using the expansion term $C_{in}$, when there is congestion in the system. Any occurrence of congestions in the system will violate this constraint, and the $C_{in}$ term, related to additional expansion lines, relaxes the congestion violation. Recall that the conventional OPF calculation provides two types of solutions regarding congestion appearing in the system, either infeasible or feasible with congestion. The salient feature of Eq. (31.17) provides the optimal solution to a copper-plate topology from either infeasible or congested grid topology.

Note that the congestion alleviation constraint directly uses LM related to the power flow, which by default in conventional OPF formulation cannot be readily used. Additional derivation of such LMs is essential so that such LMs are able to be incorporated within the optimization framework. The derivation is presented in the next section.

### 6.2.3 Congestion Alleviation Derivation

Taking the quadratic optimization problem that only considers power balance, power flow and generating constraints, the Lagrangian function is obtained as follows.

$$\begin{aligned} L \quad = \quad & \sum_{m=1}^{N_g} C_m(P_{g,m}) + C_{in} + \sum_{i=1}^{N_b} \lambda_i (P_i - P_{g,i} + P_{d,i}) \\ & + \sum_{k=1}^{N_l} \mu_{p,k}(P_{k,ij} - (1+\sigma W_{k,ij})\overline{P_{k,ij}}) \\ & + \sum_{k=1}^{N_l} \mu_{n,k}(-P_{k,ij} - (1+\sigma W_{k,ij})\overline{P_{k,ij}}) \\ & + \sum_{m=1}^{N_g} \overline{\eta_m}(P_{g,m} - \overline{P_{g,m}}) \\ & + \sum_{m=1}^{N_g} \underline{\eta_m}(-P_{g,m} + \underline{P_{g,m}}) \\ & + \sum_{k=1}^{N_l} \mu_{p,k,o}(P_{k,ij,o} - (n^a)_{k,ij,o}\overline{P_{k,ij,o}} \\ & + \sum_{k=1}^{N_l} \mu_{n,k,o}(-P_{k,ij,o} - (n^a)_{k,ij,o}\overline{P_{k,ij,o}} \\ & + \text{other terms that do not contain } P_g \text{ or } \delta \end{aligned} \qquad (6.2.18)$$

Indices $m, i$ are for generating units and buses respectively, and $m \in i$. $\mu_{p,k}$ and $\mu_{n,k}$ represent the multipliers with respect to the positive and negative power flow directions of the existing lines. $\mu_{p,k,o}$ and $\mu_{n,k,o}$ correspond to the positive and negative power flow directions of the expansion candidate lines. In DC-OPF calculations where losses are neglected, by taking the gradient of the Lagrangian function with respect to the variables $P_g$ and $\delta$, and by setting the gradients to zero (KKT conditions), we obtain the equations

$$\frac{\partial L}{\partial P_{g,m}} = 0$$

$$2a_m P_{g,m} + b_m + \lambda_m + \overline{\eta_m} - \underline{\eta_m} = 0 \tag{6.2.19}$$

$$\frac{\partial L}{\partial \delta_i} = 0$$

$$(B_b^a) \cdot \lambda + (B_f^{old})^{\mathbf{T}} \mu_p - (B_f^{old})^{\mathbf{T}} \mu_n + (B_f^a)^{\mathbf{T}} \mu_{p,o} - (B_f^a)^{\mathbf{T}} \mu_{n,o} = 0 \tag{6.2.20}$$

where

$$B_b^a = \begin{pmatrix} (B_b^a)_{11} & \cdots & (B_b^a)_{1N_b} \\ \vdots & \ddots & \vdots \\ (B_b^a)_{N_b,1} & \cdots & (B_b^a)_{N_b,N_b} \end{pmatrix} \tag{6.2.21}$$

$$\lambda = \begin{pmatrix} \lambda_1 \\ \vdots \\ \lambda_{N_b} \end{pmatrix} \tag{6.2.22}$$

$$\mu_p = \begin{pmatrix} \mu_{p,1} \\ \vdots \\ \mu_{p,N_l} \end{pmatrix} \quad \mu_n = \begin{pmatrix} \mu_{n,1} \\ \vdots \\ \mu_{n,N_l} \end{pmatrix} \tag{6.2.23}$$

$$\mu_{p,o} = \begin{pmatrix} \mu_{p,1,o} \\ \vdots \\ \mu_{p,N_l,o} \end{pmatrix} \quad \mu_{n,o} = \begin{pmatrix} \mu_{n,1,o} \\ \vdots \\ \mu_{n,N_l,o} \end{pmatrix} \tag{6.2.24}$$

$$\mu_{pa} = \begin{pmatrix} \mu_{p,1} \\ \vdots \\ \mu_{p,N_o} \end{pmatrix} \quad \mu_{na} = \begin{pmatrix} \mu_{n,1} \\ \vdots \\ \mu_{n,N_o} \end{pmatrix} \tag{6.2.25}$$

In Eq. (31.19), the partial differentiation with respect to generator output $P_g$ is shown. This equation yields all coefficients related to $P_g$. For any user-specified additional constraints related to generators, such as reserve requirement, emission constraints, additional multipliers will show up in this equation. On the contrary, Eq. (31.20) focuses on the derivation related to bus angle $\delta$, i.e. the power flow. Similar to the previous statement related to generators, adding any power flow related constraints will need additional derivation in Eq. (31.20). Eq. (31.20) is presented in matrix form to avoid confusion of the variable indexing, and $\mathbf{T}$ is the transpose of a matrix. All terms that do not contain $P_g$ and $\delta$ are omitted in the partial differentiation.

Eq. (31.21) is the explicit representation of Eq. (31.6). Eq. (31.23) represents $\mu$ of all existing lines, whereas Eq. (31.24) represents the $\mu$ of a certain type of expansion candidate at all locations, ranging from location 1 to location $N_l$ as stated that the potential expansion locations are in parallel with all existing lines. Eq. (31.25) consists of all expansion candidate types ranging from type 1 to type $N_o$.

The KKT conditions of complementarity for inequality constraints are presented below, for every line and generating unit of the system. The conditions are satisfied either when the multipliers are zero for unbinding constraints or that the constraint terms are zero in case of binding constraints.

$$\mu_{p,k}(P_{k,ij} - (1 + \sigma W_{k,ij})\overline{P_{k,ij}}) = 0 \tag{6.2.26}$$
$$\mu_{n,k}(-P_{k,ij} - (1 + \sigma W_{k,ij})\overline{P_{k,ij}}) = 0 \tag{6.2.27}$$
$$\overline{\eta_m}(P_{g,m} - \overline{P_{g,m}}) = 0 \tag{6.2.28}$$
$$\underline{\eta_m}(-P_{g,m} + \underline{P_{g,m}}) = 0 \tag{6.2.29}$$
$$\mu_{p,k,o}(P_{k,ij,o} - (n^a)_{k,ij,o}\overline{P_{k,ij,o}}) = 0 \tag{6.2.30}$$
$$\mu_{n,k,o}(-P_{k,ij,o} - (n^a)_{k,ij,o}\overline{P_{k,ij,o}}) = 0 \tag{6.2.31}$$

Recall that in the DC-OPF, generator active power outputs, phase angles and LMPs $\lambda$ are unknowns. According to the KKT condition of complementarity, without constraint violations (unbinding constraints), all LMs $\mu, \eta$ are zeros, from Eq. (31.27) to (31.31). For binding constraints, their respective $\mu, \eta$ become non-zero unknowns, but the respective 'original unknowns' $P_g, \delta$ will become known values, which are equal to their constraint values. Note that the optimization problem of the transmission expansion is a mixed integer non-linear programming (MINLP) problem.

Based on the equations derived above, we are able to control LMs related to power transfer constraints $\mu$'s as optimization variables, which are incorporated as extra constraints in the primal optimization formulation, shown in Eq. (31.17).

### Additional Constraints

More constraints can be added to the optimization formulation, such as system reserve requirement, system emission limit, etc [SYL02]. Depending on the level of details, these additional constraints are mostly related to the generators and can be directly implemented in the optimization framework. In the next section where the detailed derivation is presented, one may notice that adding such generator related constraints yields additional introduction of LMs to the congestion alleviation formulation, in addition to these constraints themselves. To be more specific, additional multipliers should be placed in those generator-related constraints such as Eq. (31.19) and Eq. (31.26).

## 6.3 Solving Environment and Algorithm

Again, the MINLP expansion planning problem is solved by using the AIMMS [AIM99c,AIM99a,AIM99b] Outer Approximation (AOA) algorithm. The algorithm is based on a decomposition technique in which the MINLP transmission expansion planning problem is decomposed into a relaxed master problem and a primal sub-problem. The master problem is a mixed-integer-programming (MIP) problem considering constraints containing integers $n$ and $W$, whereas the primal sub-problem considers the non-linear constraints related to technical and operational issues. The expansion problem is solved firstly by identifying the candidate transmission line options of the relaxed integer investment variable of the master problem. Then the NLP operation sub-problem is solved. This process iterates until either the algorithm finds the optimal expansion plan or the termination criteria are fulfilled.

## 6.4 Case Study: IEEE 39-bus Test System

To test the method, we apply it to the IEEE 39-bus New England test system, shown in Fig. 33.1. The cost function is taken from [FBA08]. The network parameters, generation and load data are taken from 'case39.m' in [ZST11]. The investment cost of transmission lines is $1083k per kilometer, using the investment cost of a 400 kV overhead line single circuit in Germany as reference [pro08a]. For the sake of simplicity, we assume the investment cost for 345 kV lines to be the same as the costs for 400 kV lines, and further we assume that the length of the branches in the test system are the same, 100 km each line. Two types of expansion options are assumed to be available at all locations in parallel with the existing grid. $X_{k,ij}$ represents the reactance of line $k$ between bus $i$ and $j$.

- Type A: $\overline{P_{k,ij,1}} = 0.75 \cdot \overline{P_{k,ij}}$; $\quad 1/X_{k,ij,1} = 0.75 \cdot (1/X_{k,ij})$; $(I^a)_{k,ij,1} = 0.75 \cdot (I^a)_{k,ij}$
- Type B: $\overline{P_{k,ij,2}} = 1.25 \cdot \overline{P_{k,ij}}$; $\quad 1/X_{k,ij,2} = 1.25 \cdot (1/X_{k,ij})$; $(I^a)_{k,ij,2} = 1.25 \cdot (I^a)_{k,ij}$

***Scenario 1*** Towards the greener power generation mix, $CO_2$ emissions are reduced by shutting down the fossil power plant at bus 33, meanwhile doubling the nuclear generating capacity at bus 31. The system load data have been increased by 6.3%, assuming that the power consumption increases with 1.55% each year for 4 years. The limited allowable overloading is $\sigma$=10% and the maximum allowable number of overloaded lines in the system is one ($\sum W_{k,ij} \leq 1$). In this scenario, no implementation infeasible cases are considered, meaning that the selection of candidates is free in terms of type and possible locations.

### Results

The simulation results are presented in Table 33.1 and Fig. 33.2. Before the expansion, the network experiences congestion as indicated by the difference

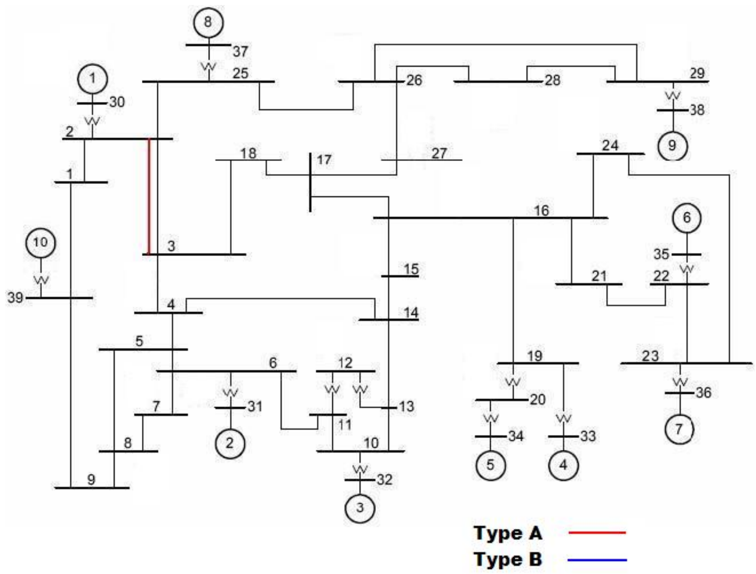


Figure 6.4.1: Schematic layout of IEEE 39-bus New England test system [Pai89] and optimal network expansion plan

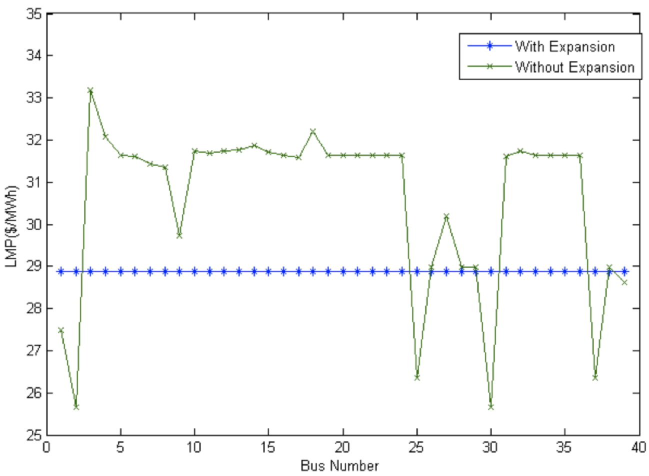


Figure 6.4.2: Locational marginal prices of all buses in scenario 1

Table 6.4.1: Before and after expansion in scenario 1

| | Before Expansion | After Expansion |
|---|---|---|
| Annual operation cost (k$) | 978085.5 | 974116 |
| Multipliers $\mu_{23}$ | 9.414 | 0 |
| LMPs $\lambda$'s ($/MWh) | 25.6 - 32.84 | 28.87 |
| No. of Extra lines | N/A | 1 at line 2-3 of Type A |
| $W$ Overloading variable | N/A | 0 at each bus |

in LMPs $\lambda$'s and the multipliers $\mu$'s. LMPs in this case range from 25.6 to 32.84 in the system and the congested line 2-3 has the non-zero $\mu$ of 9.414. Applying the expansion algorithm with congestion alleviation constraint to the optimization problem, the algorithm searches the optimal solution by adding the necessary lines in parallel to the existing congested line, in this case line 2-3. In Fig. 33.2 we immediately see the flattened LMPs, indicating the copper plate structure is achieved. The expansion strategy chooses Type $A$ as the optimal solution to be expected, because Type $A$ is a cheaper solution (assumed by default in the case study) meanwhile fulfils all operational and technical constraints. By adding a new line of Type $A$ to the system, the LMPs are equalized to the same value, which corresponds to the target market clearing price. Multiplier $\mu$ of the line 2-3 reduces to zero, representing that the congestion across line 2-3 has been alleviated. $W$, the logical variable that corresponds to temporary overloading coefficient, is zero throughout the system, indicating that no overloading occurs in the system after expansion. Moreover, the expansion option reduces the operational cost approximately $3,969k per year against the expenses for a new line of $108,300k. Assuming 40-year lifetime of such overhead lines, the expected total saving reaches $50,460k. Looking at another side of the story, as shown in Section 31.2, if obtaining the copper-plate grid topology is the ultimate goal of the expansion activity, the operational and investment costs are still important but not the driving force for the network expansion. Thus the operational saving of installing a new line (operation cost difference between before and after expansion) is not our primary focus. It is also worth pointing out that savings can vary depending on the severity of congestions of different generation and load scenarios. Note that this scenario reflects the solution Type $A$ stated in the previous section, before the network expansion, the solution to the optimization problem is feasible, but with congestions. The methodology is able to upgrade the network to a copper plate by adding new lines at the lowest expenses of operation and investment.

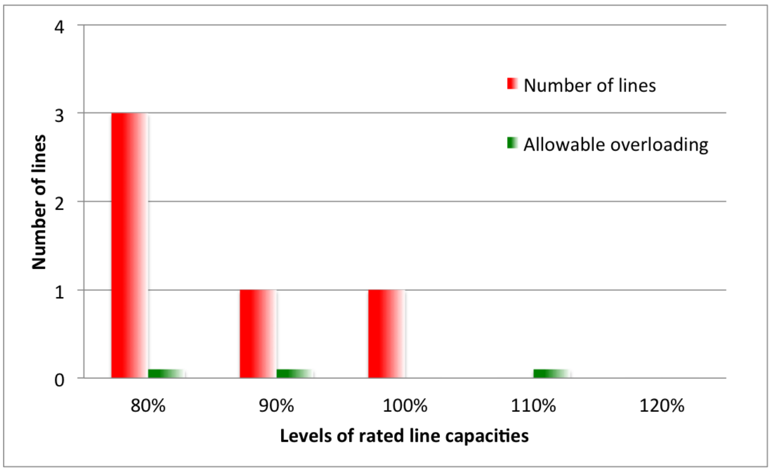


(a) Expansion plans and allowable overloads

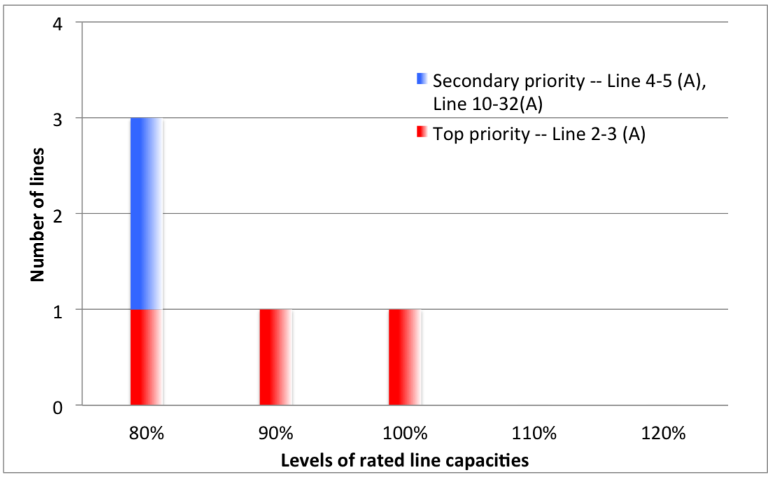


(b) Priority of expansion plans

Figure 6.4.3: Overview of expansion plans under different rated capacities

### 6.4.1 Sensitivity analysis

Another aspect related to the expansion plan is the sensitivity analysis, which determines the sensitivity of the expansion plan subject to different levels of rated transfer capacity of each transmission line in the system. The rated capacity of the network has been set to 80%, 90%, 100%, 110% and 120% of the original rated maximum. Fig. 33.3 shows number of lines that are deemed necessary to be installed subject to various capacity values, as well as the occurrence of allowable overload.

When the transfer capacity is tightened to 80%, three additional lines need to be installed in various locations in the system, with the presence of allowable overload. The tight constraint in the 80% case requires further enhancement of additional two lines compared to the 90% case, where the enhancement of Type $A$ on line 2-3 is only required. In other words, these two lines, which were originally loaded between 80% to 90%, are now considered as potential risks in the system. The difference between the 90% case and the 100% nominal case is that the allowable overload diminishes when the full capacity of 100% is adopted. We observe that line 2-3 appears in all 80%, 90% and 100% and is considered as a major threat of overload in the system. When the capacity is further loosed to 110%, line 2-3 is not considered as a major threat to the system, but a minor allowable overload. In the end, in case of 120% case, line 2-3 does not appear a threat at all which may endanger the system security. To further conclude from the sensitivity analysis, line 2-3 is deemed necessary to be reinforced by Type $A$ to ensure the copper plate grid structure. To further eliminate the potential risks, line 10-32 and line 4-5 should be considered as secondary priority for expansion planning.

Another interesting observation is that the LMPs of all five cases remain identical at 28.87. This shows one of the great advantage of copper plate grid structure, which is no market power is presented in the system and all low-cost generators are producing at their maximum capacity. The market clearing price always reaches the marginal cost of the marginal generator, which is the lowest cost that the generators could offer to the market.

## 6.5 Additional Implementation Constraints

### 6.5.1 Background and Overview

One practical issue regarding the network expansion planning is that raising public objections to the building of overhead high voltage transmission lines forces network planners to consider public opinion in planning new projects [Eur03]. Objections can stem from the environmental concerns about the visual impact, impact during construction and operation, magnetic and electrical fields [otEC03]. Geographic implementation brings another set of constraints. In the context of Europe [EE11], cross-border electricity transport must consider the geographical barriers (e.g. the Pyrenees and the Alps for the connections between Spain Italy and France). Such 'implementation constraints' should be taken into account before and/or during the planning process.

### 6.5.2 Infeasible Implementation Constraint

In the proposed methodology, all possible expansion options have been modelled in the $B$ matrix, giving the full potential to further customize any additional constraints related to the possible expansion options. The $B$ matrix contains line parameters of both existing lines and all possible expansion options, shown in Eq. (39.6). Since the final expanded lines are defined as $B_{ij,o}(n^a)_{k,ij,o}$ in Eq. (39.6) where $n^a$ vector controls the number of expanded lines, one way of controlling different expansion options is to control the integer vector $n^a$. The modelling is explained in the following section.

This way of modelling significantly reduces the modelling effort since any additional constraints related to the expansion optional can be explicitly controlled by the $n^a$ vector without affecting the backbone of the network, the entire $B$ matrix. The optimization process is able to select the optimal solution based on the freedom of $n^a$. In particular, a subset of implementation infeasibilities (belongs to $n_a$) can be defined prior to the optimization in order to formulate additional constraints related to the selection of expansion candidates.

$$(n^a)_{k,ij,o'} = 0 \tag{6.5.1}$$

where $(n^a)_{k,ij,o'}$ is a subset of $(n^a)_{k,ij,o}$, which denotes the number of *infeasible* candidate expansion lines that could have been installed in parallel to the existing lines if no implementation constraints are imposed. To force the subset to zero, implementation constraints ensure that the expansion algorithm minimizes the total cost $T$ and discards the implementation constraints.

The derivation of the Lagrangian function in Eq. (31.18) remains the same, except the 'other terms that do not contain $P_g$ and $\delta$'. The essential terms regarding $P_g$ and $\delta$ are not affected by the new constraint on the implementation feasibility.

***Scenario 2*** For a longer term of planning, the system load increases by 16.6%, representing 10 year lump sum power consumption with 1.55% annual increase. The generation scenario is the same as in scenario 1, removing the fossil fuel plant at bus 33 and increasing the capacity of the nuclear plant at bus 31. However, this time, the public opinion is against technology Type $A$ to be deployed in the upper half of the network, which is separated by the green line in Fig. 34.1.

## Results

The results is presented in Table 34.1. The test case provides two distinctive properties, a) the original grid is infeasible due to insufficient transfer capacity, so that the conventional OPF calculation is not capable of evaluating the transmission bottlenecks without additional modification, and b) there are implementation constraints in certain area where applicability of certain technology choices is limited.

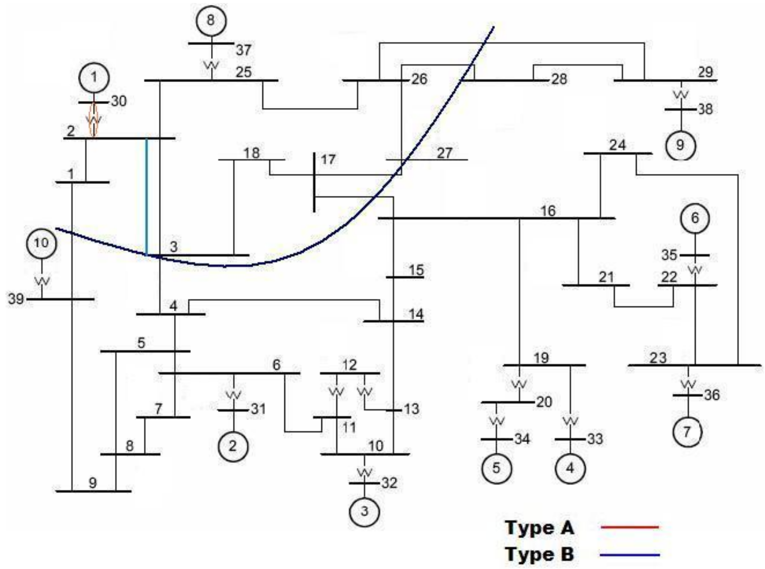


Figure 6.5.1: Optimal network expansion plan under infeasible implementation constraints

Table 6.5.1: Before and after expansion in scenario 2

| | Before Expansion | After Expansion |
|---|---|---|
| Operation Cost (k$) | N/A due to Infeasibility | 1154801 |
| Multipliers $\mu$'s | N/A | 0 |
| LMPs $\lambda$'s (\$/MWh) | N/A | 35.77 |
| No. of Extra lines | N/A | 1 at line 2-3 of Type B |
| $W$ Overloading variable | N/A | 1 at line 2-30, 0 elsewhere |

The methodology applied to this infeasible scenario is able to identify the location of insufficient capacity and add minimum number of new lines to bring the system from the infeasible state to the copper plate state, with minor allowable congestion. Moreover, due to the public objection, one additional line of Type $B$ rather than Type $A$ is selected to be installed in parallel to line 2-3, since the expansion variable $n_{a,o}$ of Type $A$ has been forced to zero due to the implementation infeasibility of public objection. We also observe that the optimization solution becomes feasible only if line 2-30 is slightly overloaded. This is as expected as stated in the remark on over-investment; a minor overloading of $\sigma$=10% on any particular line ($\sum W_{k,ij} \leq 1$) is allowed in the system to avoid an over-investment. The number $\sigma$ should be applied to the analysis with a certain discretion. That is, if the system cannot handle the temporary overloading by 10% before the expansion, $\sigma$ then should be reduced to an appropriate level which adapts the network condition subject to generation and load scenarios, and vice versa. Since it is not our intention to investigate the reasonable $\sigma$, we select 10% based on our judgement and on dialogues with the involved TSO.

It is worth noting that HVDC technology can also be modelled as a feasible network expansion technology and integrated to the expansion framework. Such model of HVDC is trivial as described in [ZS11]. Since HVDC technology can be primarily modelled as generators with a binary investment cost, i.e. zero cost if no installation is required, and large capital investment otherwise, the incorporation of HVDC technology model in this case will not bring much modelling value on the transmission expansion modelling, but to modify generators parameters and their associated investment cost. The additional option of including HVDC lines between two locations will impose economical competition between the AC and DC expansion candidates, which in this case out of the scope of the work. To this extent, the HVDC technology is not included in the general expansion modelling framework.

## 6.6 Summary

This chapter mainly focuses on the snapshot-based transmission network expansion studies. It proposes a methodology that is able to identify the location and type of expansion lines to alleviate network congestions throughout the system at the minimum cost given the generation and load conditions. Actively optimizing LMs in the optimization problem is used as a tool for the network expansion, providing the copper-plate topology from either a congested or an infeasible grid. The proposed method has been applied to the IEEE 39-bus test system. To avoid the potential over-investment issues, an overloading factor $W$ is introduced in the model to avoid the unnecessary expansion under slight overloading situations. Furthermore, the proposed modelling structure contains both the existing network and all possible expansion candidates, we also discuss the advantages of such modelling framework, focusing on the application to incorporating additional constraints related to expansion option selection, namely infeasible implementation constraints.

## 6.7 Conclusion and Comments

Investigating the snapshot based transmission expansion planning methodology, we showed that the method can effectively alleviate the congestion in the system by properly selecting the most economical expansion candidate meanwhile fulfilling all technical and operational constraints, providing the copper-plate network structure that all consumers in the network can take advantage of using the cheapest electricity, in addition to its ability of mitigation of abusive market power.

We further showed that the method is able to achieve the congestion-free network from either 'infeasible' network or a congested network at the minimum cost. This method greatly simplifies the effort in finding the optimal network topology, when the existing grid is initially 'infeasible' from the OPF calculation.

The total cost (fuel cost plus investment cost) can be used as the reference for the regulators to shape the vision of future investment. In the future, merchant investment themes may come into the picture where the private investors are allowed to utilized the congestion revenue as the incentive to help in addressing a perceived problem of under-investment. However, achieving the copper-plate network under the normal operation is still the current practice of the TSOs' planning vision and regulatory framework. The method provides, in general, a benchmark of the capital investment (i.e. the cheapest solution to form the copper plate network), and leaves the policy decision to the regulators to define the investment themes in the liberalized market environment. On the other front, the method focuses on congestion alleviation of any given scenarios, leaving the assessment of the variability of RES integration out of the scope. In other words, there might be other possible scenarios related to the RES integration that fall out of the foreseen scenario development, thus the network infrastructure may or may not be able to deliver the 'copper-plate' promise to all other unforeseen cases, e.g. originated from wind uncertainty and variability. A more comprehensive methodology that further encompasses the RES infeed into the expansion studies is introduced in the next chapter.

Some additional comments on the optimization solver on the modelling formulation. AIMMS offers many solvers that are able to handle the MINLP problem. In fact, we used a built-in AOA algorithm [Hun11] in AIMMS which requires to further specify which solver to use for MIP problem and which one for NLP problem. Amongst others, the combination of GUROBI (for MIP) and SNOPT (for NLP) offers the best performance in terms of computational speed about 90 seconds and feasible solutions. It is not the intention to investigate in detail about different solvers, but it is worth mentioning that different solver combinations may achieve different local optima. Due to the non-linear characteristics of the problem formulation, AIMMS calculates local optimum rather than global optimum. To ensure the feasible local optimum is close enough to the global optimum, pre-solve and multiple-start treatments should be used to improve the accuracy of the solution as the expense of computational speed.

# Chapter 7

# Multi-Stage Expansion

## 7.1 Introduction

In the previous chapter, the snapshot-based network expansion methodology has been presented and discussed, focusing on finding the optimal network structure to facilitate the power transfer for a specific generation pattern and demand. This chapter expands this concept in two dimensions: firstly, it focuses more on the longer planning horizon answering the question of *when* to build the transmission lines in addition to the questions of where, how many lines and which type; secondly, it introduces the system variability caused by wind energy infeed to the planning process. To tackle the longer term planning problem, the complete planning horizon is divided into different chronological stages; the enhanced OPF calculation suggests the optimal plan based on the generation and load scenarios at each stage. The wind variability is tackled by coupling the optimisation model to the modeling of wind infeed, as presented in Chapter 4.

Within each stage of investigation, a modular approach is adopted to answer the question of how to find the most economical solution to the network expansion planning problem aiming at a congestion free (copper-plate) network configuration. To find the solutions to expansion at each stage, the snapshot-based expansion method is adopted, as presented in Chapter 6. Conventional OPF is used to evaluate the network state and the economic benefits of each plan, and the mini-max regret method is used as a decision making and risk assessment technique to evaluate the optimal solutions at each stage.

Section 38 presents the overview of the multi-stage methodology. Section 39 further presents the enhanced single-stage expansion planning (ESSEP) by focusing on a single stage expansion problem, including both theoretical and mathematical formulations. At the end a case study is presented to which the proposed method is applied.

## 7.2 Overview

The basic objective of the multi-stage transmission expansion problem formulation is to determine the number, location, type and construction time frame of new transmission subject to specific design criteria. To reduce the complexity of the dynamic modelling problem, the modelling idea is to decompose the long-horizon transmission expansion problem into a sequence of enhanced single-stage expansion problems. In the multi-stage expansion planning, the entire planning horizon is equally divided into several time spans (stages) and the corresponding optimal expansion plan of each stage is determined, as shown in Fig. 38.1. The information available to the network planner at time $T_0$ is the current network topology, anticipated future generation, load, wind power infeed at each stage, expansion candidates with possible locations and associated costs. The planner needs to expand the current network to the copper-plate status step-by-step by first facilitating the generation/load scenarios at stage 1 ($T_1$) at the minimum cost subject to all technical and operational constraints. Note that at $T_1$ a number of foreseen scenarios are under investigation. The underlying message is that the network expansion should be completed before time $T_1$, which means that the network is fully equipped with new lines in order to support all possible generation/load scenarios at $T_1$ so that the expanded grid (existing grid + expansion decision) will not experience congestion. After the optimal expansion at for $T_1$, the network has been updated from the original network at $T_0$ to $T_1$. The procedure takes $T_1$ as a new starting point and moves forward to facilitate new scenarios at $T_2$ and then $T_3$, until reaching the end of the planning horizon.

The chronological approach ensures the optimal expansion plan at each stage aiming at a congestion-free configuration. Also, at each stage of planning horizon, it is rather evident that various generation/load snapshots are incorporated in the modelling framework, so that the final expansion plan is robust to withstand all investigated scenarios along the planning horizon. Due to the nature of the chronological approach, the optimum for the stage does not guarantee the global optimum for the whole planning horizon, thus sanity check on the optimal solution on each stage and its impact on the next stage should be performed to avoid unnecessary expansion activities.

## 7.3 Enhanced Single-Stage Expansion Planning

In the previous section, the overview of the complete multi-stage expansion planning is presented. This section zooms into each stage of expansion, namely enhanced single-stage expansion planning (ESSEP), according to the flow chart shown in Fig. 39.1.

Before going into details in different models, it is necessary to reflect

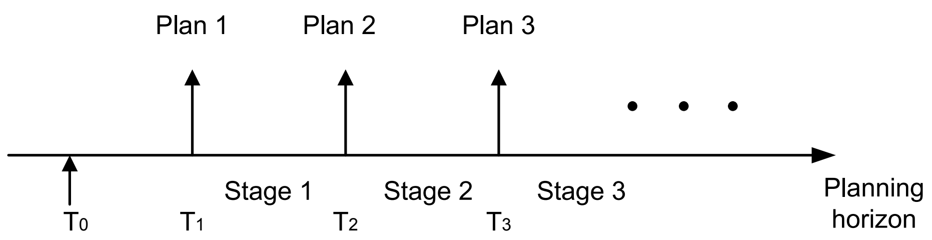


Figure 7.2.1: Multi-stage transmission expansion horizon

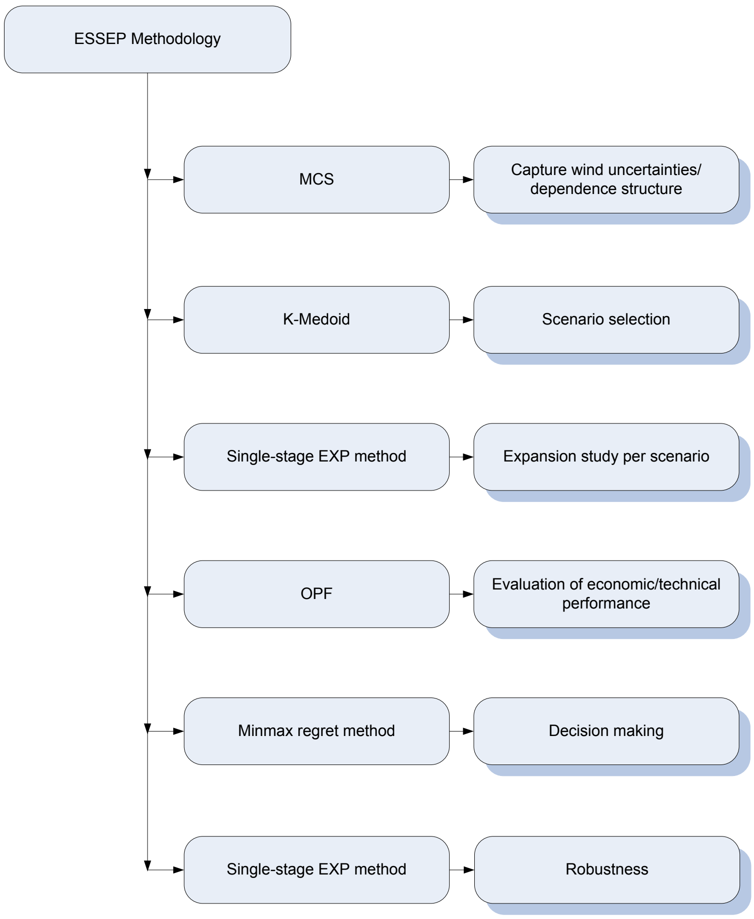


Figure 7.3.1: Modular approach of enhanced single-stage expansion planning methodology

on the modelling philosophy. Modular design [BC02] is an approach that divides the complete task into separate modules, which will be independently created and later joined together to fulfil the complete task functionalities. Modular design is suitable for the large and complex problem modelling. In general, modular design offers the following advantages [BC02] on

- Modularity creates options
  - Modularity makes complexity manageable;
  - Modularity enables parallel work; and
  - Modularity is tolerant of uncertainty.
- Modular designs evolve as the options are pursued and exercised.

Our objective is to provide the optimal grid topology at some certain times of the expansion horizon, taking into account the stochastic renewable infeeds. To achieve this, ESSEP problem is decomposed into six modules: 1) Monte-Carlo simulation of intermittent energy sources for capturing their uncertainty and dependence structure. 2) Scenario selection step to refine the scenario space to be investigated. Scenario selection enables the faster computational speed. 3) Single-stage expansion planning studies in order to evaluate all selected scenarios, providing the possible expansion candidates for the network expansion. 4) OPF calculates the economic indicators for each expansion candidate against all selected scenarios. 5) A decision making technique is adopted to select the best expansion candidate among all possible ones, based on the economic performance evaluated in the previous step. 6) To ensure the robustness of the best expansion plan, one more iteration of single-stage expansion planning simulation is performed, checking the best plan against all selected scenarios. The results are then considered the final optimal expansion plan for this stage of investigation. In the following sections, the ESSEP methodology is presented in detail.

### 7.3.1 MCS and Sample Selection

As presented in the previous chapters, Monte-Carlo simulation (MCS) is used to capture the stochastic dependency structure of wind speed, as well as load. One of the most salient feature of the MCS simulation is its time and scenario independence. That being said, based on the historical wind speed dataset, such 10000 wind speed samples can be used in all stages in the multi-stage expansion studies because MCS captures the characteristics of the wind speed dataset so that we do not need to simulate 10000 samples for every stage of expansion study[1]. The advantage is that redundancy of modeling wind speed distribution for different stages can be eliminated.

[1]Since new wind energy developments in new areas may prevail, the wind to power exercise needs to be updated.

Theoretically all 10000 MCS samples can be fed into the expansion studies as input data of RES infeed. The drawback is rather trivial. Due to the nature of the expansion formulation (non-convexity, non-linear, mixed integer), running 10000 iterations of expansion optimization process is computationally intensive.

To overcome the drawback, a number of typical net load scenarios at this stage should be determined in order to capture the 'complete' spectrum of network operation. Clustering is the process of grouping data into classes or clusters such that data points in clusters are more similar to each other than data points in separate clusters [HK04, Hua11]. The similarities of the data points are mostly assessed by using distance measure. Different clustering algorithms can be used, such as connectivity-based clustering [HT09], Centroid-based clustering [KU12], Distribution-based clustering, Density-based clustering, etc.

K-medoids method is adopted for its robustness against noise and outliers in the dataset. The mathematical formulation and an illustrative example are presented in the Appendix 46. The K-medoids clustering method is used to select $k$ typical exemplars from the complete datasets. The main idea of using K-medoids method is to reduce the repetitive computational effort within the large sample space, especially in computationally intensive calculations. The selected $k$ samples can then be used to represent the original large dataset.

After the scenario analysis is performed, the set of candidate transmission expansion plans is obtained subject to the selected scenarios by solving the deterministic transmission expansion model, as presented in Chapter 5.

### 7.3.2 Expansion Study

Each scenario is evaluated to form a candidate plan, as shown in Fig. 39.2. Plan 1, denoted as $p_1$, is the most economical expansion solution for scenario $s_1$ to achieve a copper-plate network. Similar treatment applies to $p_2 - s_2$ pair, $p_3 - s_3$ pair, towards the last scenario $p_n - s_n$ pair under investigation.

As stated in the previous chapter, single-stage expansion methodology is able to perform the network expansion from an infeasible or congested state to a copper-plate state with the least cost. In general, the single-stage expansion model takes $s_1$ as input, and yields $p_1$ as the optimal solution[2]. The iterative process goes through all $k$ clustered scenarios to formulate $k$ expansion plans. At this stage, no comparison among plans is made. The main focus is to formulate the potential plans ranging from $p_1$ to $p_k$, in which the best plan will be chosen in the following step.

[2]An expansion plan consists of the number, location, type of the expansion candidates. In order to evaluate the performance of the plan, the plan has to be integrated to the original network to form the 'optimal' network.

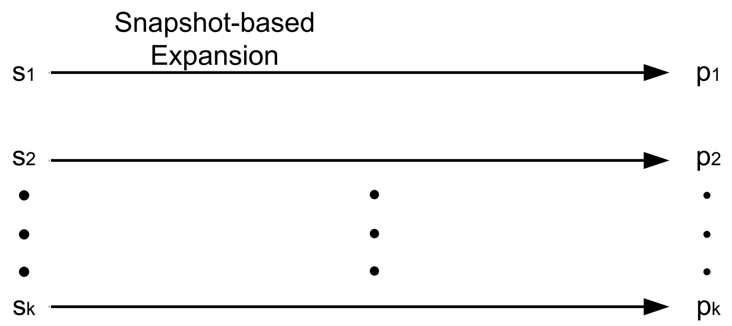


Figure 7.3.2: Candidate investment identification of a single stage expansion plan

### ESSEP formulation

The formulation of ESSEP based on the DC-OPF is similar to the equations introduced in Chapter 6. The formulation originates from the conventional DC-OPF, with particular emphasis on the congestion alleviation constraint by introducing the Lagrangian multipliers as optimization variables in the modelling framework. Within a single-stage model, $k$ typical scenarios of wind power infeed are under investigation with certain generation mix. The ESSEP expansion model iterates $k$ times to propose the $k$ number of expansion candidate plans. For a given planning time horizon $T$, the ESSEP formulation is given as follows[3],

**Objective function**

$$minimize \quad C_{Total} = C_{op} + C_{in} \tag{7.3.1}$$

where $C_{Total}$ represents the total cost, $C_{op}$ and $C_{in}$ represent the annual operation cost and the investment cost, given by

$$C_{op} = \sum_{m=1}^{N_g} C_m(P_{g,m}) \cdot 8760 \tag{7.3.2}$$

$$C_{in} = \sum_{o=1}^{N_o} \sum_{k=1}^{N_l} (n^a)_{k,ij,o}(I^a)_{k,ij,o} \tag{7.3.3}$$

**Constraints**

$$P_i = P_{g,i} - P_{d,i} \tag{7.3.4}$$

[3]Some of the equations in this section are the same as shown in the single stage expansion studies in Chapter 6 on which Chapter 7 is based. To avoid reference confusion, the equations are listed independently in Chapter 7 to provide the complete view of the multi-stage methodology

$$P_i = \sum_{j=1}^{N_b} (B_b^a)_{ij}\delta_j \tag{7.3.5}$$

$$(B_b^a)_{ij} = \begin{cases} (B_b^{old})_{ij} + \sum_{o=1}^{N_o}(n^a)_{k,ij,o}B_{ij,o} & i \neq j \\ (B_b^{old})_{ij} + \sum_{j=1}^{N_b}\sum_{o=1}^{N_o}(n^a)_{k,ij,o}B_{ij,o} & i = j \end{cases} \tag{7.3.6}$$

$$|P_{k,ij}| \leq \overline{P_{k,ij}} \tag{7.3.7}$$

$$|P_{k,ij,o}| \leq (n^a)_{k,ij,o}\overline{P_{k,ij,o}} \tag{7.3.8}$$

$$P_{k,ij} = \sum_{i=1}^{N_b} (B_f^{old})_{ij}(\delta_i - \delta_j) \tag{7.3.9}$$

$$P_{k,ij,o} = \sum_{i=1}^{N_b} (B_f^a)_{ij}(\delta_i - \delta_j) \tag{7.3.10}$$

$$B_f^{old} = \begin{pmatrix} (B_f^{old})_{11} & \cdots & (B_f^{old})_{1N_b} \\ \vdots & \ddots & \vdots \\ (B_f^{old})_{N_l1} & \cdots & (B_f^{old})_{N_lN_b} \end{pmatrix} \tag{7.3.11}$$

$$(B_f^a)_o = \begin{pmatrix} (B_f^a)_{11,o} & \cdots & (B_f^a)_{1N_b,o} \\ \vdots & \ddots & \vdots \\ (B_f^a)_{N_l1,o} & \cdots & (B_f^a)_{N_lN_b,o} \end{pmatrix} \tag{7.3.12}$$

$$(B_f^a) = \begin{pmatrix} (B_f^a)_1 \\ \vdots \\ (B_f^a)_{N_o} \end{pmatrix} \cdot \begin{pmatrix} (n^a)_{1,o} \\ \vdots \\ (n^a)_{N_l,o} \end{pmatrix} \tag{7.3.13}$$

$$\underline{P_{g,m}} \leq P_{g,m} \leq \overline{P_{g,m}} \tag{7.3.14}$$

$$\mu_k = 0 \tag{7.3.15}$$

$$\frac{\partial L}{\partial P_{g,m}} = 0$$

$$2a_mP_{g,m} + b_m + \lambda_m + \overline{\eta_m} - \underline{\eta_m} = 0 \tag{7.3.16}$$

$$\frac{\partial L}{\partial \delta_i} = 0$$

$$(B_b^a)\cdot\lambda + (B_f^{old})^{\mathbf{T}}\mu_p - (B_f^{old})^{\mathbf{T}}\mu_n + (B_f^a)^{\mathbf{T}}\mu_{p,o} - (B_f^a)^{\mathbf{T}}\mu_{n,o} = 0 \tag{7.3.17}$$

where

$$B_b^a = \begin{pmatrix} (B_b^a)_{11} & \cdots & (B_b^a)_{1N_b} \\ \vdots & \ddots & \vdots \\ (B_b^a)_{N_b,1} & \cdots & (B_b^a)_{N_b,N_b} \end{pmatrix} \tag{7.3.18}$$

$$\lambda = \begin{pmatrix} \lambda_1 \\ \vdots \\ \lambda_{N_b} \end{pmatrix} \tag{7.3.19}$$

$$\mu_p = \begin{pmatrix} \mu_{p,1} \\ \vdots \\ \mu_{p,N_l} \end{pmatrix} \quad \mu_n = \begin{pmatrix} \mu_{n,1} \\ \vdots \\ \mu_{n,N_l} \end{pmatrix} \tag{7.3.20}$$

$$\mu_{p,o} = \begin{pmatrix} \mu_{p,1,o} \\ \vdots \\ \mu_{p,N_l,o} \end{pmatrix} \quad \mu_{n,o} = \begin{pmatrix} \mu_{n,1,o} \\ \vdots \\ \mu_{n,N_l,o} \end{pmatrix} \tag{7.3.21}$$

$$\mu_{pa} = \begin{pmatrix} \mu_{p,1} \\ \vdots \\ \mu_{p,N_o} \end{pmatrix} \quad \mu_{na} = \begin{pmatrix} \mu_{n,1} \\ \vdots \\ \mu_{n,N_o} \end{pmatrix} \tag{7.3.22}$$

$$\mu_{p,k}(P_{k,ij} - \overline{P_{k,ij}}) = 0 \tag{7.3.23}$$

$$\mu_{n,k}(-P_{k,ij} - \overline{P_{k,ij}}) = 0 \tag{7.3.24}$$

$$\overline{\eta_m}(P_{g,m} - \overline{P_{g,m}}) = 0 \tag{7.3.25}$$

$$\underline{\eta_m}(-P_{g,m} + \underline{P_{g,m}}) = 0 \tag{7.3.26}$$

$$\mu_{p,k,o}(P_{k,ij,o} - (n^a)_{k,ij,o}\overline{P_{k,ij,o}}) = 0 \tag{7.3.27}$$

$$\mu_{n,k,o}(-P_{k,ij,o} - (n^a)_{k,ij,o}\overline{P_{k,ij,o}}) = 0 \tag{7.3.28}$$

The expansion model runs sequentially from the first representative to the last one, proposing a set of expansion solutions corresponding to each representative. Next step is to evaluate the most suitable candidate to all representatives. The evaluation method is presented in the following section.

### 7.3.3 Expansion Plan Evaluation

This step evaluates $k$ expansion plans one-by-one in order to select the best plan among them all. After identifying all possible candidate expansion plans in the first step, it is necessary to evaluate each candidate subject to other possible scenarios. In other words, we know that $p_1$ is the optimal solution for $s_1$, what about the performance of $p_1$ in $s_2$, $s_3$ and $s_4$? How can we quantify the economic benefits of applying $p_1$ to $s_3$, or $p_2$ to $s_3$, so

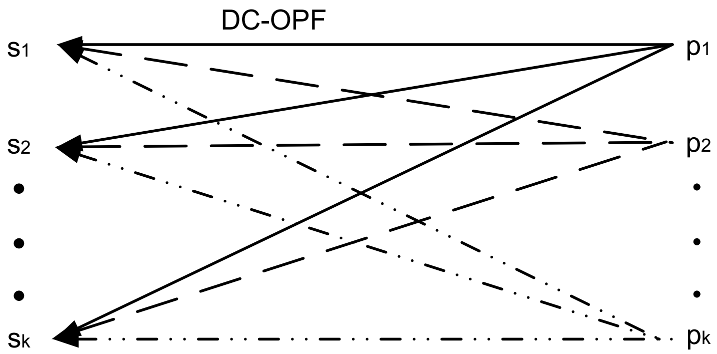


Figure 7.3.3: Operational analysis of a single stage expansion plan

that we can further compare economically which one the preferred solution is between $p_1$ and $p_2$?

The conventional DC-OPF calculation is used to assess associated economic indicators such as congestion surplus[4] of each expansion plan which are later used for the decision analysis in the next step. To achieve this, the proposed plan (namely the location, type, number of candidates) has to be integrated to the existing network topology to form the complete network topology. To be specific, $p_1$, 'originated from $s_1$', is first integrated to the existing network to form the complete network topology $P_1$. Then, $P_1$ is subject to conventional DC-OPF under the generation/load scenario of $s_1$, to evaluate the technical and economic performance, followed by $s_2$, $s_3$ ... $s_k$. Similar approach applies to $p_2$ to $p_k$. This is illutrated in Fig. 39.3.

In total, the number of $k^2$ DC-OPF simulations are performed, yielding a $k - by - k$ table. From the data flow viewpoint, the input data are the $n$ candidate expansion plans and existing system information (generation, the existing and new candidate interconnection and load scenarios). The outputs are the present value of the system operation cost and congestion surplus for the decision making stage.

### Congestion surplus

Congestion surplus is defined as follows [KS04],

$$\begin{aligned} CS &= Payment_{Total} - Revenue_{Total} \\ &= \sum_{i=1}^{N_b} \lambda_i (P_{d,i} - P_{g,i}) \end{aligned} \tag{7.3.29}$$

[4]Merchandising surplus is defined as the difference between payments and revenues. Since the surplus is due to the congestion in the network, it is also called congestion surplus [KS04].

where $CS$ denotes the congestion surplus, which shows the benefits that the operational cost could have saved from the congestion alleviation.

### 7.3.4 Decision Analysis

In the last step the best expansion option out of all $k$ candidate expansion plans is selected by applying the decision making technique, namely Minimax Regret method [Sav51]. The minimax regret method evaluates the congestion surplus associated with all plans for all scenarios by first selecting the maximum regrets and then selecting one minimum out of all maximum regrets. So far, the selected plan is the best plan out of $k$ plans. However, this may not be the robust plan that is able to alleviate all congestions for all $k$ scenarios. That is to say, the current best plan is the 'intermediate' best plan which only guarantees to be the most economical solution, comparing with the rest plans.

To ensure the selected plan is capable to alleviate congestions subject to other scenarios, the selected optimal solution is cross-checked once again whether it satisfies the operating condition of all the considered scenarios for its robustness. The 'intermediate' best solution will be updated once again using single-stage transmission expansion planning model, as described in section 39.2. The updated best plan is considered as the optimal expansion solution at this stage for all scenarios considered. Together with the existing network structure, the final network topology for this stage is proposed by the expansion model.

The final network topology for this stage is adopted as the starting point of the planning for the next stage. Sequentially, the planning procedures iterate towards the next planning phase and stop at the end of the entire planning horizon.

#### Mini-Max regret formulation

To select the best plan among various options, a decision analysis scheme must be adopted to take into account the uncertainty of uncontrollable factors. The main goal of the decision analysis is to determine the best plan which is robust and minimizes the maximum possible economic loss caused by the uncertainty [ALL06]. From the expansion result of each scenario, a set of candidate expansion plans are formed. Then, for every candidate plan in the generation/load scenario, the regret incurred for not having chosen this plan as the best plan for the future condition is calculated. The minimax regret criterion, often named as the criteria of min-max risk or losses tries to avoid the regret that may result from making a non-optimal solution [LDS05]. In this framework for a particular future scenario $s$, the regret in an expansion plan $p$ is defined as the difference between the value of the attribute[5] of the system under selected expansion plan and the value of the minimum attribute that would have been attained if the network planner had a prior knowledge that this scenario would take place. In other words, regret is defined as the opportunity loss to the decision maker if a plan $p$ is selected and scenario $s$ happens [LDS05]. The three main steps of the decision analysis schemes of minimax regret criteria are given as:

First for the set scenarios $S$ and candidate expansion plans $P$, the attribute value of each plan scenario pair is calculated as [AAC10]:

$$f^{s,p} = val(s,p) \quad \forall s \in S, \forall p \in P \tag{7.3.30}$$

Next, the regret $R(s,p)$ of the expansion plan $p$ under future scenario $s$ is given as

$$R(s,p) = val(s,p) - \underline{val(s,p)} \quad \forall s \in S, \forall p \in P \tag{7.3.31}$$

where

$$\underline{val(s,p)} = \min_{p \in P}(val(s,p))$$

Finally, the optimal expansion plan that minimizes the maximum regret over all future scenarios is selected as the final best plan. This means we search for each expansion plan $p$ the maximum regret among all future scenarios, and then among all plans select the plan with the smallest maximum regret as the best plan [MP98]. It is formulated as:

$$\min_p\{\max_s\{R(s,p)\}\} \tag{7.3.32}$$

$$\min_p\{\max_s\{v^s \cdot R(s,p)\}\} \tag{7.3.33}$$

An intuitive example of Mini-Max regret method is presented in Appendix 46.

## 7.4 Case study: IEEE 39-bus Test System

To test the method, we apply it to the IEEE 39-bus New England test system. The cost function is taken from [FBA08]. The network parameters, generation and load data are taken from case39.m in [ZST11]. The investment cost of transmission lines is $1,000k per kilometer, using the investment cost of a 400 kV overhead line single circuit in Germany from [pro08a]. This system is modified by including ten wind parks (denoted by W1-W10) each with installed capacity of 100 MW. The location of these wind parks are shown in Fig. 40.1.

For the sake of simplicity, we assume investment cost for 345 kV lines same as the costs for 400 kV lines; further the length of the branches in the

[5]The attribute here is the congestion surplus.

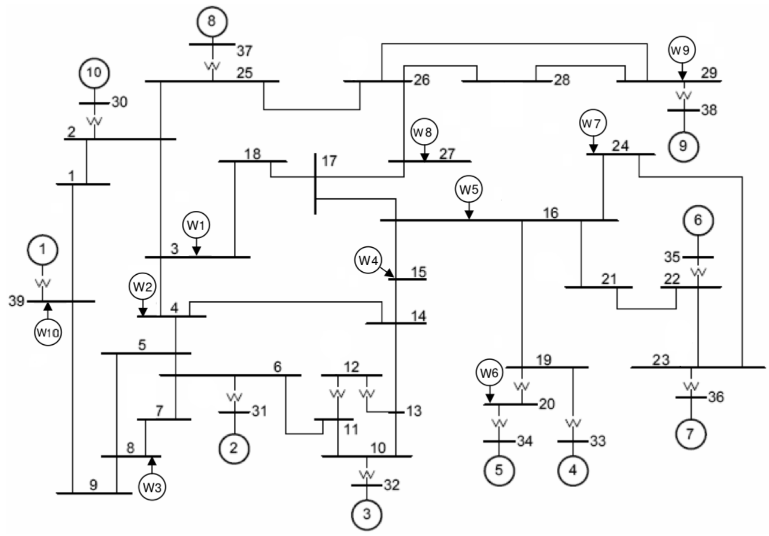


Figure 7.4.1: Modified New England test system with wind power infeed

test system are assumed to be the same, 100 km each line. The maximum power transfer capacities of all transmission line are assumed to be 80% of the actual power transfer capacity given in [ZST11]. Two types of expansion options are assumed to be available, with respect to the existing grid. $X_{k,ij}$ represents the reactance of line $k$ between bus $i$ and $j$

- Type A: $\overline{P_{k,ij,1}} = 0.75 \cdot \overline{P_{k,ij}}$; $\quad 1/X_{k,ij,1} = 0.75 \cdot (1/X_{k,ij})$; $(I^a)_{k,ij,1} = 0.75 \cdot (I^a)_{k,ij}$
- Type B: $\overline{P_{k,ij,2}} = 1.25 \cdot \overline{P_{k,ij}}$; $\quad 1/X_{k,ij,2} = 1.25 \cdot (1/X_{k,ij})$; $(I^a)_{k,ij,2} = 1.25 \cdot (I^a)_{k,ij}$

Each stage spans seven years, an average of a typical transmission project duration between five and ten years. This means that the investment for the expansion is performed in a period of seven years (in year 0, 7 and 14). The annual load growth rate is assumed about 1.2% [Age12a] and the average wind power generation growth rate is assumed to be 12% [WM12]. The interest rate is assumed to 5% per year.

The analysis has been implemented in the optimization software 'AIMMS' version 3.12.

### 7.4.1 Results

The K-medoid method is applied to the 10000 net load samples which are calculated by subtracting the wind power generation from the load profile. The number of clusters is assumed to be six for demonstration purposes,

Table 7.4.1: Candidate expansion plan of the six future load conditions of each stage

| Stages | Location(type) | Plans(no. of lines) | | | | | |
|---|---|---|---|---|---|---|---|
| | | p1 | p2 | p3 | p4 | p5 | p6 |
| Stage 1 | 16-19(A) | | 1 | 1 | | | |
| Stage 2 | 6-11(A) | | 1 | | | | |
| | 16-19(A) | | 1 | | | | 1 |
| | 19-33(A) | 1 | 1 | 1 | | 1 | 1 |
| Stage 3 | 15-16(A) | | | | | 1 | |
| | 26-27(A) | | | | | 1 | |
| | 26-29(A) | | | | 1 | 1 | |
| | 28-29(A) | | | 1 | | | |
| | 29-38(A) | 1 | | 1 | | 1 | |
| | 2-25(A) | | | 1 | | | |

data provided in Appendix 46. The identified medoids are defined as the representative typical scenarios that are able to 'capture' the complete picture of net load patterns. These representative scenarios are used as typical load conditions of the planning year for the multi-stage transmission expansion problem.

Given the above assumption and procedure, the multi-stage transmission expansion planning model is solved for six future typical load scenarios (denoted as $s1, s2, s3, s4, s5$ and $s6$) and six optimum transmission expansion plans (denoted as $p1, p2, p3, p4, p5$ and $p6$, respectively) are obtained. The overview of the expansion plans is presented in Table 40.1, together with he candidate expansion plans of the three stage planning horizon are given in Table 40.1. The number in the bracket indicates the type of the transmission line options. Looking at the stages sequentially, the scenarios considered at stage 1 result in a candidate expansion plan of building one line in branch 16-19 (the optimal expansion plan corresponding to scenario $s2$ and $s3$) and Do-Nothing (the expansion plan corresponding to scenarios $s1, 4, 5$, and 6). At this phase of analysis, no evaluation among $p1$ to $p6$ is made. Later, one of the plans will be chosen as the best expansion plan amongst others.

After identification of the candidate expansion plan of the stage, to select the optimal plan the operational and decision analysis step is performed. For assessing the economic aspect of the plan the congestion surplus is used as selection criteria. The congestion surplus of each plan-scenario combination is computed by running the DC-OPF calculations. Therefore it forms a $p$ = 1,2,...,6 by $s$ = 1,2,...,6 attribute table and the best plan is selected by

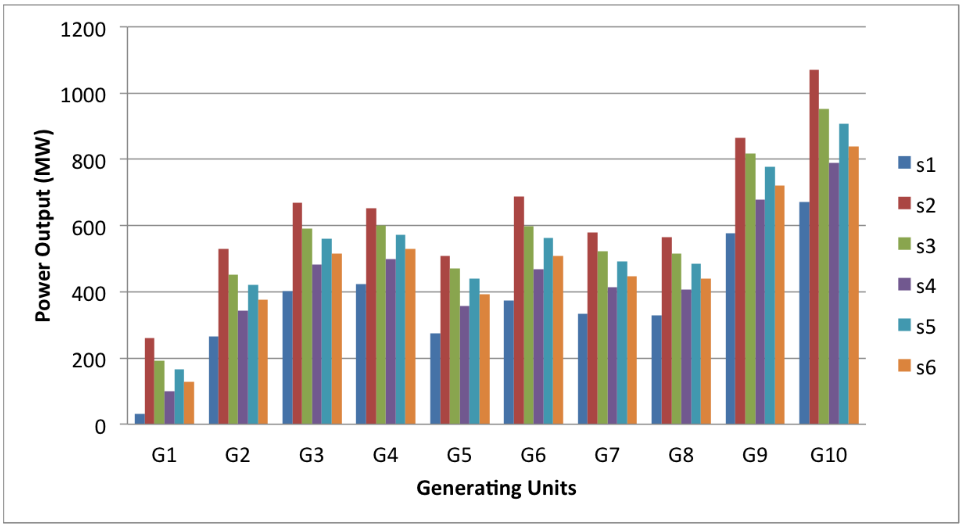


Figure 7.4.2: Generation dispatches of six expansion options at stage 1

Table 7.4.2: Attribute table for scenario-candidate plan combination at stage 1 (k$)

| | s1 | s2 | s3 | s4 | s5 | s6 | Max(s,p) |
|---|---|---|---|---|---|---|---|
| 16-19 (p2, p3) | 0 | 0 | 0 | 0 | 0 | 0 | 0 |
| 'Do Nothing' (p1, p4, p5, p6) | 0 | 2,451 | 1,632 | 0 | 0 | 0 | 2,451 |

applying the minimax regret decision making analysis procedure.

Finally, at stage 1, the best expansion that is able to withstand all scenarios is chosen as the starting point of stage 2.

Similarly, the candidate expansion plans of the other stages can be interpreted. At stage 2 and 3, six expansion plans are forms respectively.

It is of importance to have the insight to each stage and its corresponding procedures. The results coming from zooming into each stage are presented in the following sections.

*Stage 1*: In general, two expansion plans are determined at this stage. One is to build a new line in parallel to branch 16-19, obtained by satisfying the generation/load scenarios of $s2$ and $s3$, and 'Do Nothing', obtained by satisfying $s1, s4, s5$, and $s6$. Generation dispatches of six expansion options are presented in Fig. 40.2.

In Fig. 40.3, in scenarios $s1, 4, 5$ and 6 all branches in the grid are oper-

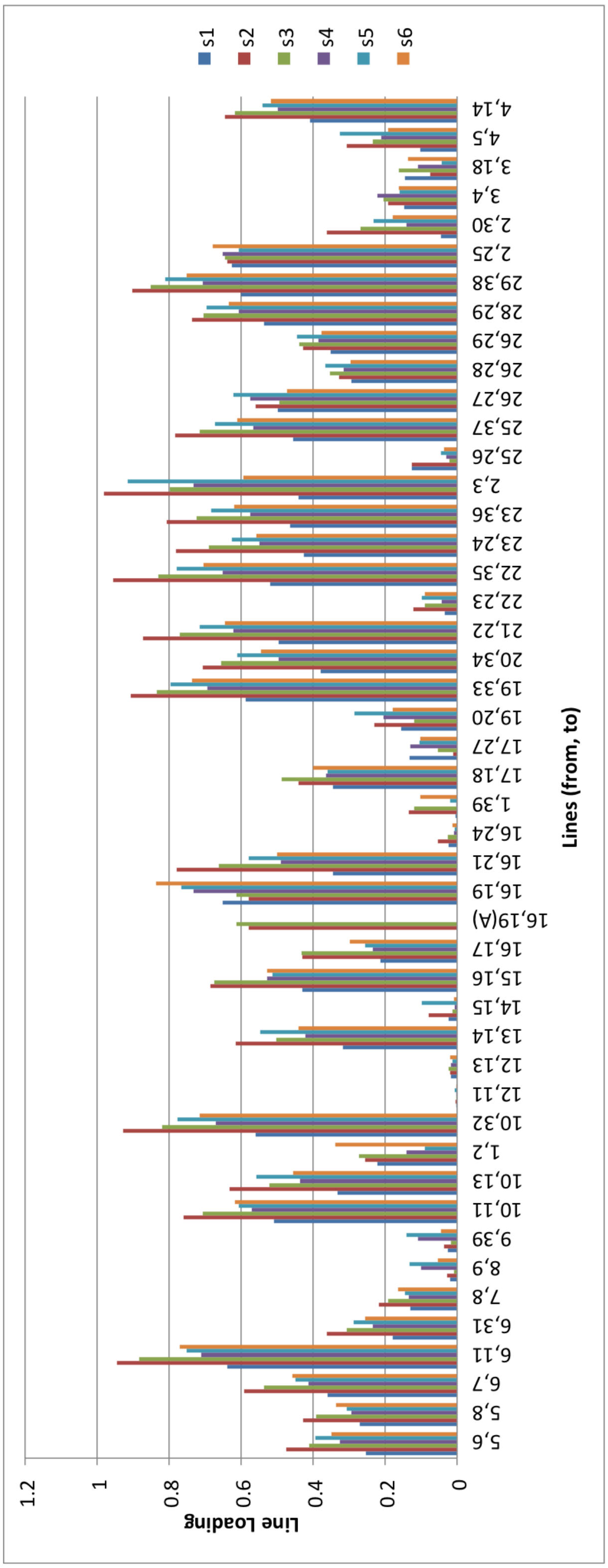


Figure 7.4.3: Branch loadings of six expansion options at stage 1

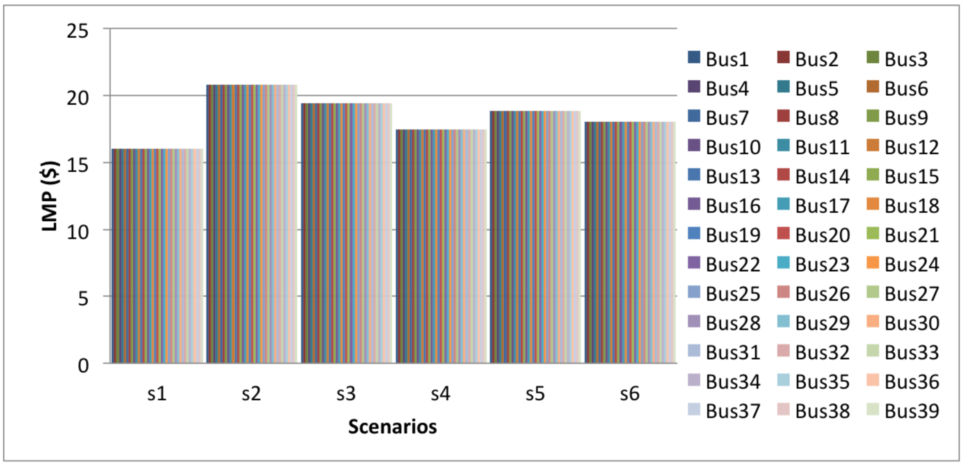


Figure 7.4.4: LMPs of six expansion options at stage 1

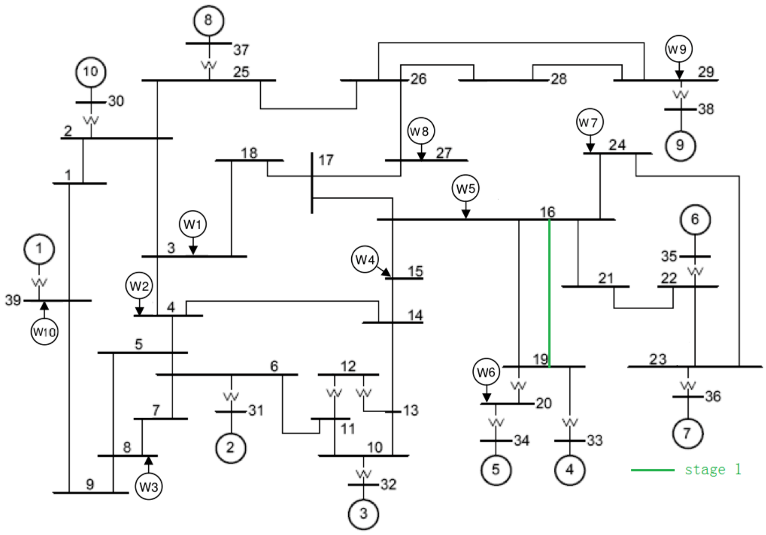


Figure 7.4.5: IEEE 39-bus New England test system after stage 1

ated under the maximum allowable limits without the need of adding any new lines. On the contrary, in $s2$ and $s3$ the branch loadings of the whole grid is under the maximum limit only after adding a new line of type $A$ between bus 16 and 19. We are able to observe that the line loading of the newly deployed line is the same as the existing line between bus 16 and 19. This is because the reactance $X$ and the power flow limit of the new line are proportional to those of the existing line. The actual power flow along both lines are different, but the loadings are the same.

Fig. 40.4 presents the LMPs at 39 buses of all six scenarios. LMPs range from \$14.79 to \$19.75 across various scenarios, but remain the same within each scenarios, providing the uniform Market Clearing Price (MCP) of the copper-plate grid structure.

To evaluate the performance of each plan, the attribute matrix of congestion surplus is given in Table 40.2.

We observe that adding line 16-19 leads to zero congestion surplus in the system. Thus, in order to fulfil all six scenarios, line 16-19 ($p2$ or $p3$) is selected as the final optimal expansion plan for this stage, and will be integrated to the existing network to form the starting network for stage 2. The network experiences congestion if the 'Do Nothing' option is selected, and thus the option is discarded. The optimal expansion plan is presented in Fig. 40.5.

*Stage 2*: At stage 2, it is assumed that the generation mix is changed. A new generator, named $G12$ is connected to bus 33, with the capacity of 500 MW. Given the optimal expansion plan of the stage 1, the new starting network topology is investigated subject to the same aforementioned annual growth rate of load and wind power generation. The four candidate investment plans are shown in Table 40.1.

The generator dispatches of six proposed plans are shown in Fig. 40.6. It is observed that scenario $s2$ requires the largest generating output across all scenarios by applying plan $p2$, whereas $s4$ requires the minimum power output from generators, given the plan $p4$ is applied. The output pattern of eleven generating units generally follows the same dispatching trend, because of the same fuel costs applied to all six scenarios with different system load levels.

Fig. 40.7 shows the condensed view of line loading of six plans from scenarios. We also observe that after the expansion plans are applied to the existing grid, all line loadings are below the branch capacities. For instance, for scenario $s2$, it is essential to build another branch in parallel with 6-11 of Type $A$ to mitigate the overloading on the existing branch 6-11. Other scenarios do not require the expansion action at this particular location. Similar observation can be seen at branch 16-19 and 19-33. We can also verify the results from the LMP plot in Fig. 40.8, where the LMPs of all buses are the same for individual scenario.

The attribution matrix is presented in Table 40.3. The attribution ma-

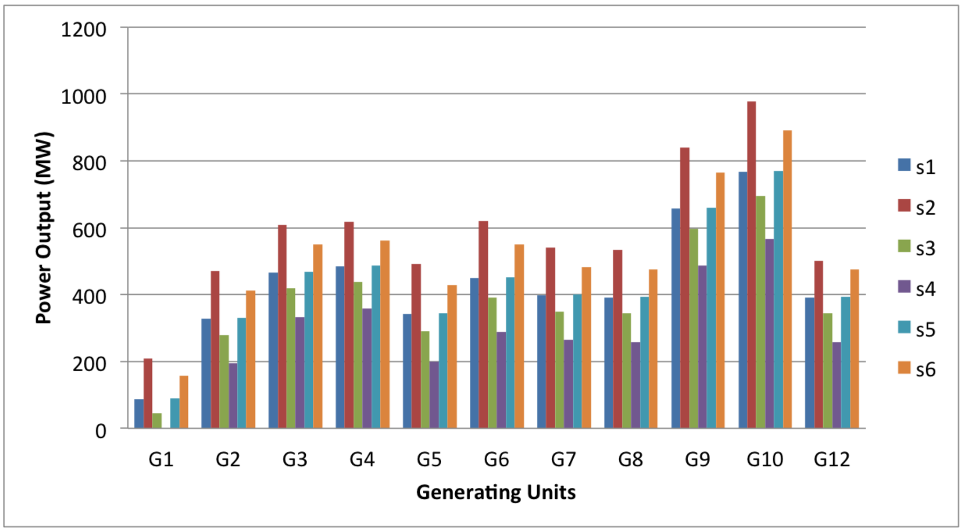


Figure 7.4.6: Generation dispatches of six plans at stage 2

Table 7.4.3: Attribute table for scenario-candidate plan combination at stage 2 (k$)

| | s1 | s2 | s3 | s4 | s5 | s6 | Max(s,p) |
|---|---|---|---|---|---|---|---|
| p1,p3,p5 | 0 | 5,184 | 0 | 0 | 0 | 860 | 860 |
| p2 | 0 | 0 | 0 | 0 | 0 | 0 | 0 |
| p4 | 10,851 | 31,004 | 4,310 | 0 | 11,134 | 22,138 | 31,004 |
| p6 | 0 | 641 | 0 | 0 | 0 | 0 | 641 |

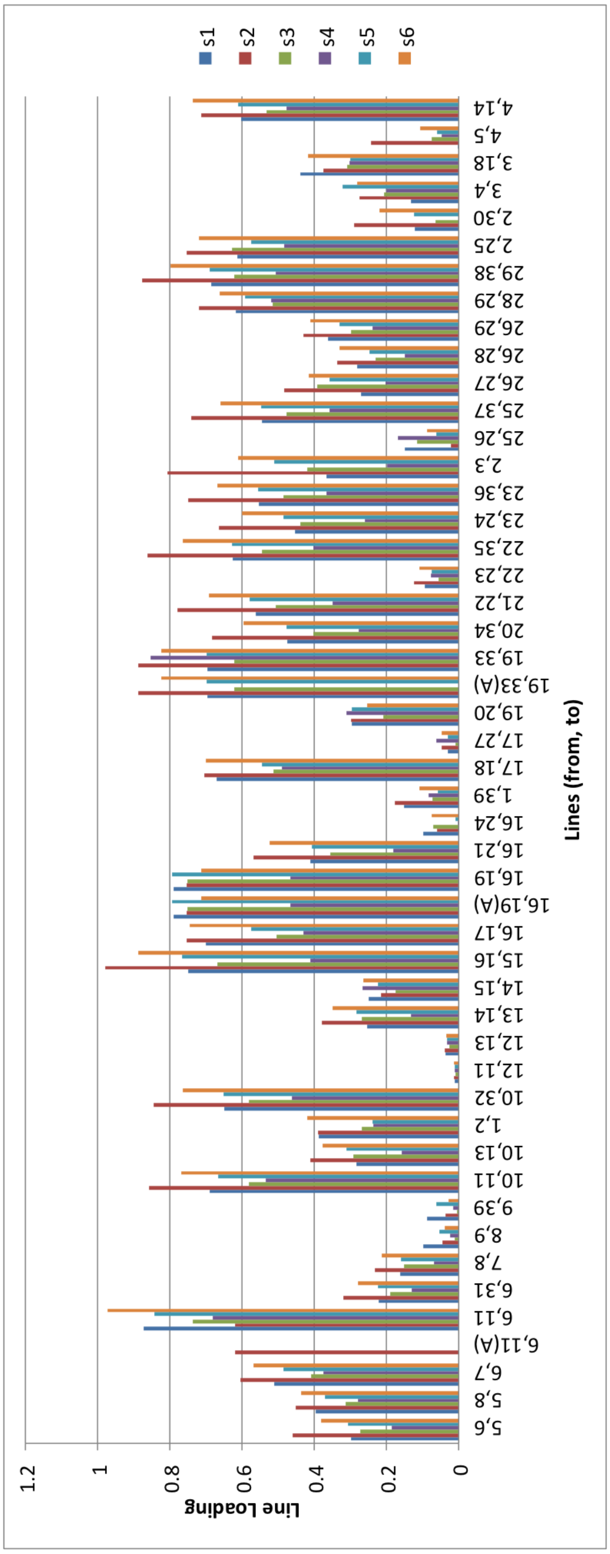


Figure 7.4.7: Branch loadings of six expansion options at stage 2

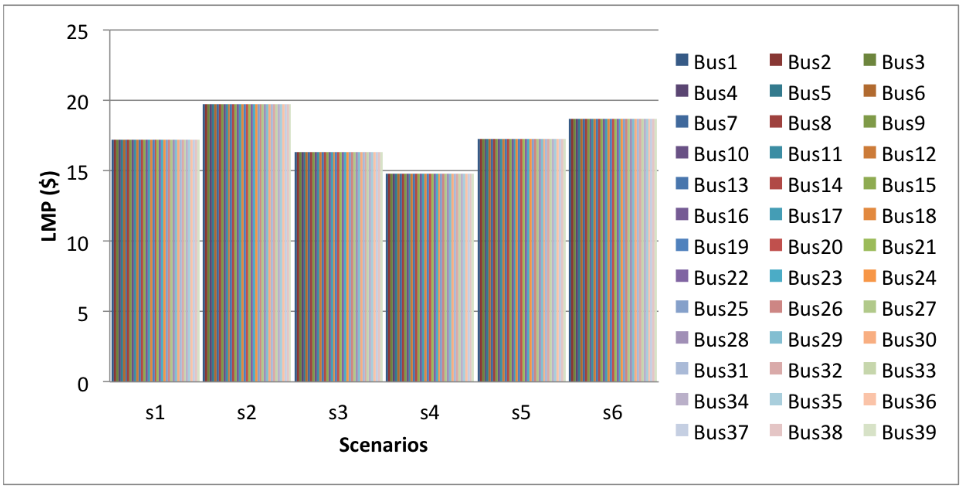


Figure 7.4.8: LMPs of six expansion options at stage 2

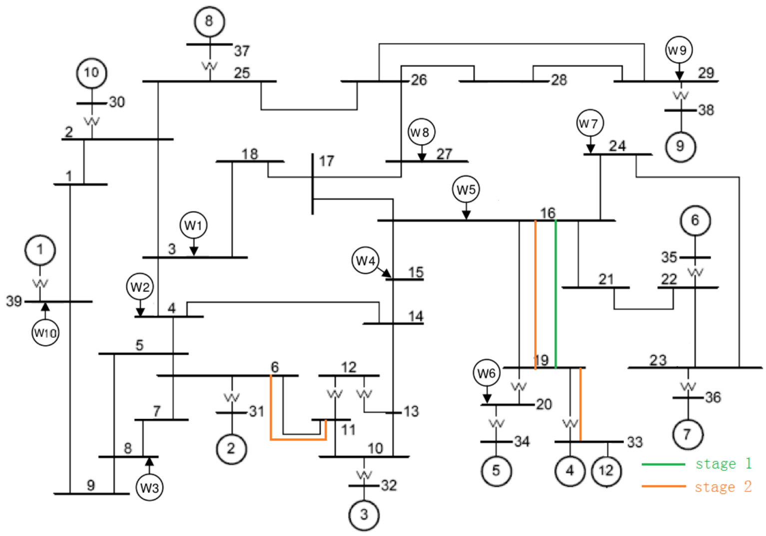


Figure 7.4.9: IEEE 39-bus New England test system after stage 2

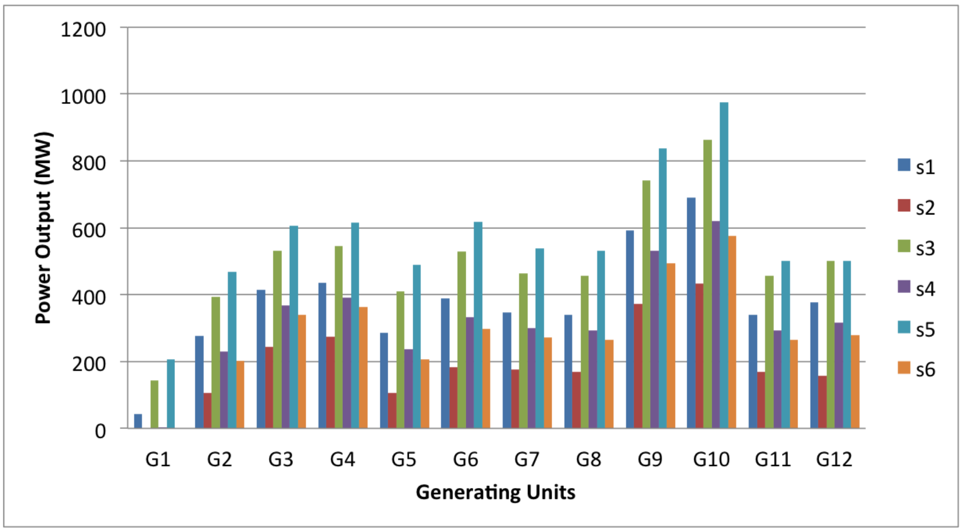


Figure 7.4.10: Generation dispatches of six plans at stage 3

trix determines which expansion plan will be selected as the best plan for stage 2. It is evident that $p2$ gives the least congestion surplus comparing with other plans, and thus it is taken as the best plan at this stage. Note that since $p2$ has already provided the copper-plate structure of all scenarios, it is not necessary to perform robust analysis to upgrade $p2$ in order to make $p2$ a copper-plate solution for all scenarios. This is the same observation as seen in stage 1. At the end of this stage the cumulated expansion plan of stage 1 and 2 is presented in Fig. 40.9

*Stage 3*: At stage 3, it is further assumed that a new generator is added, named $G11$ of 500 MW at bus 38.

Similar observation is seen at stage 3, regarding the generation dispatch in Fig. 40.10 with the highest capacity requirements comes from scenario $s5$, with the support of new unit $G12$. The attribute matrix is presented in Table 40.4. The last column in Table 40.4 gives the maximum regret of each plan over all scenarios. According to the minimax regret criteria, the plan that minimizes the maximum regret of all plans is selected as an optimal plan. Therefore, plan 5 $p5$ which corresponds to building four transmission lines in branches 15-16, 26-27, 26-29 and 29-38 is selected as the current best solution. However, the optimal expansion plan of the minimax regret criteria is the optimal solution only for scenarios $s1, s2, s4, s5, s6$. This shows that the expansion plan 5 $p5$, resulted from the highest total demand level of all considered scenarios, is not able to remove all the congestion of all scenarios. This emphasizes that the transmission expansion should be able to support the multiple load and power generation configuration. Therefore, the current optimal solution $p5$ must be upgraded so that it fulfils the normal operating condition of $s3$, i.e. removing the congestion of $s3$. The upgrade

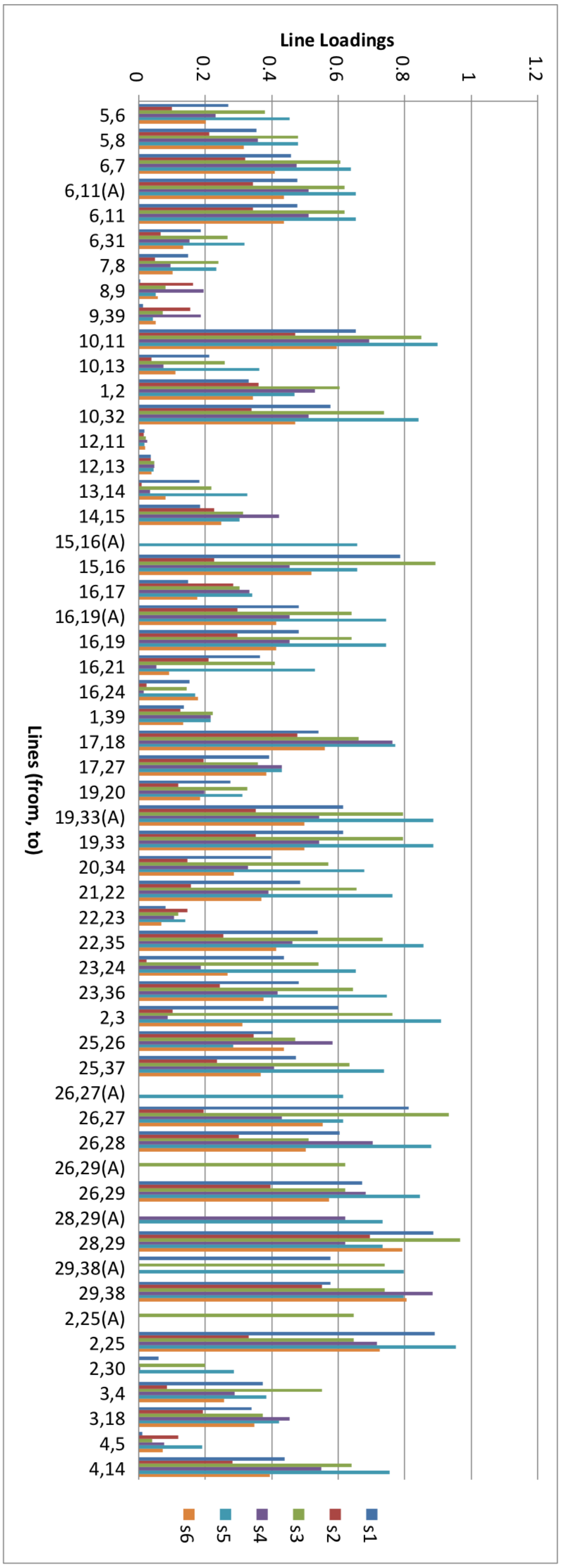


Figure 7.4.11: Branch loadings of six expansion options at stage 3

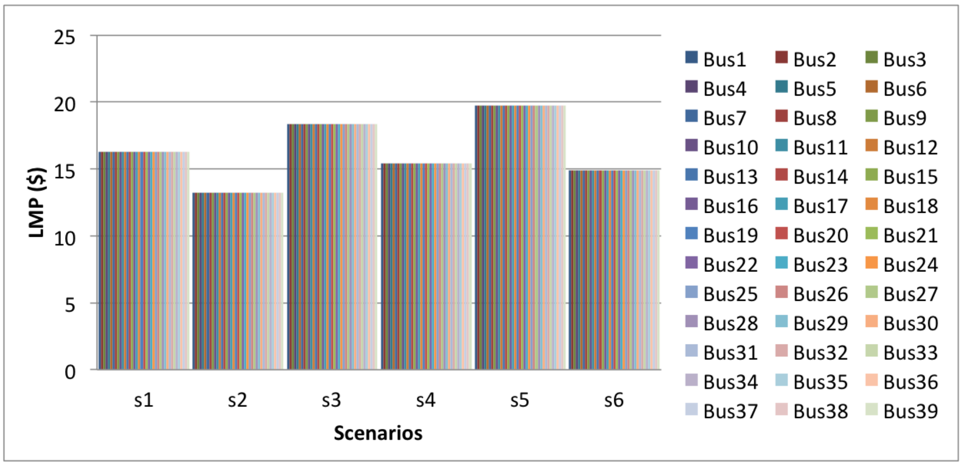


Figure 7.4.12: LMPs of six expansion options at stage 3

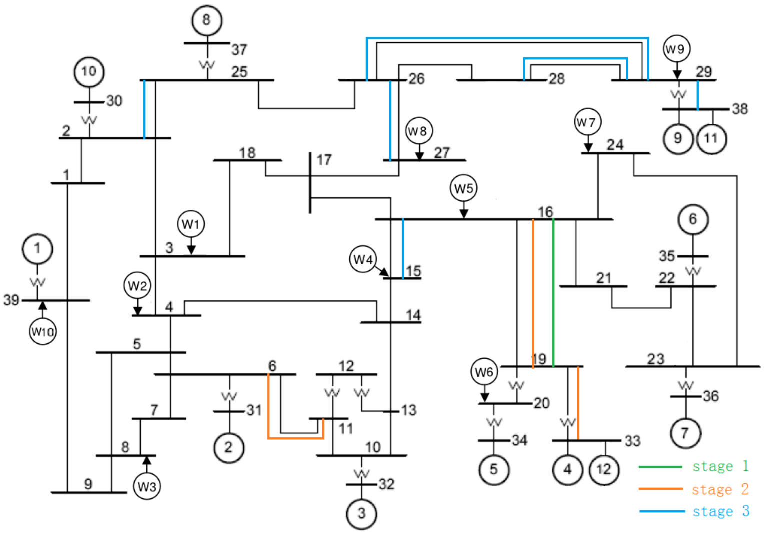


Figure 7.4.13: IEEE 39-bus New England test system after stage 3

Table 7.4.4: Attribute table for scenario-candidate plan combination at stage 3 (k$)

| | s1 | s2 | s3 | s4 | s5 | s6 | $\max\{R(s,p)\}$ |
|---|---|---|---|---|---|---|---|
| p1 | 0 | 0 | 8,499 | 1,277 | 26,542 | 0 | 26,542 |
| p2,p6 | 685 | 0 | 22,225 | 1,277 | 37,862 | 0 | 37,862 |
| p3 | 0 | 0 | 0 | 0 | 7,280 | 0 | 7,280 |
| p4 | 685 | 0 | 22,225 | 0 | 37,862 | 0 | 37,862 |
| p5 | 0 | 0 | 81 | 0 | 0 | 0 | 81 |

results in building one additional line at branch 2-25. The branch loadings in Fig 40.11 and LMPs in Fig. 40.12 further verifies the importance of the upgrade at branch 2-25. The final optimal expansion plan of the multi-stage expansion plan and the stage at which the installation will be performed is given in Fig. 40.13 and Table 40.5. The last column shows the net present value of the expansion plans. The investment cost of stage 1 is \$81,300k, when the planner is sitting at time 0 ($T_0$), whereas the investment cost at stage 2 requires \$243,900k when the planner calculates the cost at $T_1$. Converting to the present value at $T_0$, the investment cost is \$173,335k for three additional lines. Similarly at stage 3, the net present value converts to \$346,670k. The total investment cost can thus be added to \$520,005k.

### 7.4.2 Computer Configuration and Speed

The methodology requires many iterations of MINLP optimization problems. The computational speed is an essential parameter for the assessment of expandability and applicability of the methodology. The basic configuration of the computer hardware used is: CPU is Intel Core 2 6320 at 1.86 GHz with 2 GB of RAM running Windows XP SP3. The computational speed of MCS and selection technique is negligible, whereas the heavy computational effort on the MINLP optimization applied to IEEE 39-bus test system is roughly 1 hour.

## 7.5 Summary

In this chapter, a multi-stage expansion planning methodology is presented, which proposes the optimal network topology at different time horizon chronically, taking into account the uncertainties of the wind power generation. The entire planning horizon is divided into multiple stages, utilizing the methodology of enhanced single-stage expansion modelling. Within each

Table 7.4.5: Final investment plan of the multi-stage expansion model

| Results | Location(type) | No. of Exp. | Inv. cost(k$) | NPV |
|---|---|---|---|---|
| Stage 1 | 16-19(A) | 1 | 81,300 | 81,300 |
| Stage 2 | 6-11(A)<br>16-19(A)<br>19-33(A) | 1<br>1<br>1 | 243,900 | 173,335 |
| Stage 3 | 15-16(A)<br>26-27(A)<br>26-29(A)<br>28-29(A)<br>29-38(A)<br>2-25(A) | 1<br>1<br>1<br>1<br>1<br>1 | 487,800 | 346,670 |
| Total investment (k$) | | | | 520,005 |

planning stage, the ESSEP method is designed using modular approach, consisting of MCS sampling for wind power infeed, selection of typical scenarios using clustering technique, single-stage expansion methodology aiming at copper plate grid structure, DC-OPF for performance assessment of proposed expansion plans, decision making phase of using minmax regret method, and the final phase of using expansion method again applied to the best plan to make it 'bullet-proof' to all selected typical scenarios. After each stage of planning, the proposed network is able to withstand all generation/load scenarios, result in a copper-plate network structure for the given foreseen scenarios. The ultimate expansion plan fulfils the operating condition of all the representative scenarios. Finally, the methodology is applied to the New England 39 bus test system for two generation/load scenarios to verify its validity and effectiveness.

## 7.6 Conclusion and Comments

The methodology proposed is able to achieve the modelling objective, namely proposing the congestion-free grid topology at the minimum cost at different time horizon of interest, taking into account uncertainties from wind power infeed.

The modular approach of functionally partitioning the multi-stage planning methodology offers many advantages including reducing computational effort, easy to modify the existing modules or adapt other modules for other grid investigations, amongst others. Computational speed takes roughly

1 hour for the proposed test system. It is anticipated that using the latest CPU of i7 (quad-core) at 3.9 GHz with more RAM, the computational speed could be drastically improved. The speed improvement implies that the methodology is applicable to larger grid and/or more typical scenarios for the offline expansion studies. Speaking of easy to modify/adjust modules, the proposed modelling framework first provides modules that functionally partition the modelling objective, and proposes how to model each module such that all modules works together to achieve the objective. Since each module is 'broadly' independent, the methods of implement modules can differ. That is to say, MCS and Copula method is one of the good approaches that are able to model the wind infeed, but other wind power prediction method using such as fuzzy logic [DATD04], neural networks [LWOG01] and time series [BKM84] can also do the job well with different strength and weakness. However, they, as independent modules of wind power infeed modelling, can be rather easily substitute the proposed MCS Copula approach into the multi-stage planning framework.

Based on the interest and final objective of the planner the applied decision making criteria may vary. The selection of the investment plan can be seen from different angles. This is particular important for the attribution selection. In this chapter, congestion surplus is used, mainly for minimizing the additional payment incurred to the end-users of the electricity due to the insufficient transfer capacity. This may not be the universal appreciated by all stakeholders in the electricity market, especially the private investors who advocate Merchant Transmission Investment (MTI) scheme. If the market mechanism incentivizes MTI, building a copper plate grid may not be the objective of investors because under the current market mechanism, manipulating power flow to create congestions would be financially in favour of MTI line investors.

Additional comment on the expansion modelling in AIMMS. Due to the complexity of the model, it seems that solver selection and their associated setting are crucial to obtain the satisfactory results. To be specific, the single-stage expansion module is a non-convex MINLP problem, and thus it is essential to use non-linear presolve to obtain the feasible solution. The solvers for solving MINLP are SNOPT (for NLP) and GORUBI (for MIP). The subsequent module is the DC-OPF model that assesses the plan performance. The DC-OPF is a convex NLP [WVSO96] that MOSEK solver suits better under the same presolve condition. Both modules are implemented in AIMMS under one program, since most of the variables are the same for the expansion module and the DC-OPF module. Bottom line is that the entire framework contains different modules with different types of optimization problems. Appropriate solvers should be used for each module.

# Chapter 8

# Conclusion

This thesis proposes models and solutions to two problems, a) Weak network points identification and b) network expansion studies. Both models share similarities and certainly differences.

## 8.1 Weak Network Points Identification

In the weak network points identification analysis, we have shown that the proposed method is able to identify the weak network points, regarded as highly frequent overloaded lines in the system. Applying the methodology to the test system, the distribution of the investigated variable incorporates all possible system behaviour subject to MCS samples. The method is named 'S-OPF', which is found to be suitable for the steady-state assessment of the power system when the variability of system input parameters is taken into account.

Because of using Monte-Carlo method, such network assessment method enables incorporation of policy uncertainties, which leads to the uncertain generation mixes in the future. Since MCS samples are independent from the future generation mix, the S-OPF greatly improves the computational speed by repeatedly using the same MCS samples for all different possible future generation scenarios. In essense, the method computes the complete spectrum of the optimal power flows subject to various possible generation mix and wind scenarios, without imposing additional computational burden to the simulation.

## 8.2 Network Expansion - Single Stage

Investigating the single-stage transmission expansion planning methodology, we found that the proposed method can effectively alleviate the congestion in the system by selecting the most economical expansion candidate, providing the copper-plate network structure that all consumers in the network can take advantage of using the cheapest electricity, in addition to its ability of mitigation of abusive market power.

We further found that the method is able to achieve the congestion-free network from either 'infeasible' network or a congested network at the minimum cost. This method greatly simplifies the effort in finding the optimal network topology, when the existing grid is initially 'infeasible' from the OPF calculation.

Due to the nature of the modelling, the method focuses on congestion alleviation of one or certain given scenarios, leaving the assessment of the variability of RES integration out of the scope. In other words, there might be other possible cases related to the RES integration that fall out of the foreseen scenario development, thus the network infrastructure may or may not be able to deliver the 'copper-plate' promise to these the unforeseen cases. Thus, although the method strives to provide the copper-plate network structure on one snapshot case, the network may not be copper-plate taking into account other possible future scenarios.

## 8.3 Network Expansion - Multiple Stages

To overcome the shortcoming that mentioned in the single-stage method, the multi-stage network expansion methodology is proposed and validated that is able to achieve the modelling objective, namely proposing the congestion-free grid topology at the minimum cost at different time horizon of interest, taking into account uncertainties from wind power infeed.

The proposed modelling framework first provides modules that functionally partition the modelling objective, and proposes how to model each module such that all modules works together to achieve the objective. Since each module is 'broadly' independent, the methods of implement modules can differ.

The entire planning horizon is divided into multiple stages, utilizing the methodology of enhanced single-stage expansion modelling. After each stage of planning, the proposed network is able to withstand all generation/load scenarios, result in a copper-plate network structure for the given foreseen scenarios. The ultimate expansion plan fulfils the operating condition of all the representative scenarios.

## 8.4 Comments and Future work

### WNPs Identification

Additional comments on the MCS simulation applicability: Previously Monte-Carlo method has been viewed as computational-intensive method. It has been widely recognized as an effective method for offline assessment, particularly according to the feedback from TSOs on the operational level. However, besides the computer technology grows rapidly in the past ten twenty years, the algorithm of power flow calculation also improves dramatically. A new method of using Newton-Krylov solver to solve very large scale network of million buses power flow achieved very promising results of more than 100 times faster than a direct solver. We may further anticipate that MCS in the near future will be applicable to the online assessment of power system when the solvers and computing power is significantly enhanced.

Another interesting research direction is to include HVDC technology into the analysis. Point-to-point HVDC connection can be single-handedly modelled as the negative load, and thus does not bring any additional challenges in terms of power flow formulations. Multi-terminal HVDC is another story. The numerical iterative analysis used in the AC formulation may not be directly used in a multi-terminal HVDC power flow analysis. It would be of interest if multi-terminal HVDC technology is incorporated in the mixed AC-DC power flow analysis for the weak network points identification.

Additional effort can be made to incorporate contingency analysis to the expansion studies. This thesis assumes 80% of the rated capacity as the maximum allowable capacity to simulate $N-1$ criteria. After enhancing the methodology by including the contingency criteria, the expansion planning problem can then be evaluated subject to $N - 1 or more$. The associated computational time may also increase due to introducing more optimization variables and iterations in the problem formulation, thus properly reduction/simplification should also be wisely implemented, especially more snapshots are under investigation.

### Network Expansion Studies

The total cost (fuel cost plus investment cost) can be used as the reference for the regulators to shape the vision of future investment. In the future, merchant investment themes may come into the picture where the private investors are allowed to utilized the congestion revenue as the incentive to help in addressing a perceived problem of under-investment. However, achieving the copper-plate network under the normal operation is still the current practice of the TSOs' planning vision. The method provides, in general, the upper bound of the capital investment, and leaves the policy decision to the regulators to define the investment themes in the liberalized market environment.

Based on the interest and final objective of the planner the applied decision making criteria may vary. The selection of the investment plan can be seen from different angles. This is particular important for the attribution selection. In this chapter, congestion cost is used, mainly for minimizing the additional payment incurred to the end-users of the electricity due to the insufficient transfer capacity. This may not be the universal appreciated by all stakeholders in the electricity market, especially the private investors who advocate Merchant Transmission Investment (MTI) scheme. If the market mechanism incentivizes MTI, building a copper plate grid may not be the objective of investors because under the current market mechanism, manipulating power flow to create congestions would be financially in favour of MTI line investors.

Some additional comments on the optimization solver on the TEP problems. AIMMS offers many solvers that are able to handle the MINLP problem. In fact, we used AIMMS' AOA algorithm which requires to further specify which solver to use for MIP problem and which one for NLP problem. Amongst others, the combination of GUROBI (for MIP) and SNOPT (for NLP) offers the best performance in terms of computational speed and feasible solutions. It is not the intention to investigate in detail about different solvers, but it worth mentioning that different solver combinations may achieve different local optimum. Due to the non-convex characteristics of the TEP formulation, AIMMS calculates local optimum rather than global optimum. To ensure the feasible local optimum is close enough to the global optimum, pre-solve and multiple start treatments also come in handy. In general,

Additional comment on the expansion modelling in AIMMS. Due to the complexity of the model, it seems that solver selection and their associated setting are crucial to obtain the satisfactory results. To be specific, the single-stage expansion module is a non-convex MINLP problem, and thus it is essential to use non-linear presolve to obtain the feasible solution. The solvers for solving MINLP are SNOPT (for NLP) and GORUBI (for MIP). The subsequent module is the DC-OPF model that assesses the plan performance. The DC-OPF is a convex NLP that MOSEK solver suits better under the same presolve condition. Both modules are implemented in AIMMS under one program, since most of the variables are the same for the expansion module and the DC-OPF module. Bottom line is that the entire framework contains different modules with different types of optimization problems. Appropriate solvers should be used for each module.

Taking into account aforementioned issues, improvements can be made in various directions including the solver development, application to the large-scale network, incorporation of MTI investment scheme and multi-terminal HVDC technology.

# Appendix A

# K-Medoid Method

The K-medoids algorithm is a clustering algorithm related to the k-means algorithm and the medoid shift algorithm. Both the k-means and k-medoids algorithms are partitional (breaking the dataset up into groups) and both attempt to minimize the distance between points labelled to be in a cluster and a point designated as the center of that cluster.

It is more robust to noise and outliers as compared to K-means because it minimizes a sum of pairwise dissimilarities instead of a sum of squared Euclidean distances.

A medoid can be defined as the object of a cluster, whose average dissimilarity to all the objects in the cluster is minimal i.e. it is a most centrally located point in the cluster.

The most common realisation of K-medoid clustering is the Partitioning Around Medoids (PAM) algorithm and is as follows:

- Initialize: randomly select $K$ of the $n$ data points as the medoids
- Associate each data point to the closest medoid. ("closest" here is defined using any valid distance metric, most commonly Euclidean distance, Manhattan distance or Minkowski distance)
- For each medoid $m$
  - For each non-medoid data point $o$,
    - Swap m and o and compute the total cost of the configuration
- Select the configuration with the lowest cost.

More information about data clustering and K-medoids can be found in [KMe13, HK01].

# Appendix B

# Min-Max Regret Method

Regret (also called opportunity loss) is defined as the difference between the actual payoff and the payoff that would have been obtained if a different course of action had been chosen. This is also called difference regret. Furthermore, the ratio regret is the ratio between the actual payoff and the best one.

The minimax regret method is to minimize the worst-case regret by assessing the difference or ratio of the payoffs. of what-if among different choices. The aim of this is to perform as closely as possible to the optimal course. The minimax criterion applied here is to the regret (difference or ratio of the payoffs) rather than to the payoff itself.

One benefit of minimax is that it is independent of the probabilities of the various outcomes: thus if regret can be accurately computed, one can reliably use minimax regret.

More knowledge of decision theory and min-max regret method can be found in [Wik12].

An example of mini-max regret theory [Hos05]:

You are sometimes given a table with stocks and there possible payoffs (i.e. 0.6 payoff will indicate a 0.6 cents profit on every dollar invested) at consecutive times.

| Stock | Year 1 | Year 2 | Year 3 | Year 4 |
|---|---|---|---|---|
| Intel | -0.3 | 0.9 | 0.4 | 0.5 |
| Microsoft | 0 | 0.5 | 0.1 | 0.4 |
| Disney | 0.6 | 0.4 | 0 | 0.6 |
| Shell | 0.3 | -0.1 | -0.7 | 0.7 |
| Barclay | -0.2 | -0.6 | 0.4 | 0 |

In the minimax regret problem, you are required to minimize your highest regret when you choose one stock over the other.

Step 1: We look at the first payoff time in this case Year 1, and find the stock with the highest payoff. In this case it is the Disney stock which has a payoff of 0.6 (font in bold).

| Stock | Year 1 | Year 2 | Year 3 | Year 4 |
|---|---|---|---|---|
| Intel | -0.3 | **0.9** | **0.4** | 0.5 |
| Microsoft | 0 | 0.5 | 0.1 | 0.4 |
| Disney | **0.6** | 0.4 | 0 | 0.6 |
| Shell | 0.3 | -0.1 | -0.7 | **0.7** |
| Barclay | -0.2 | -0.6 | **0.4** | 0 |

Now we ask ourselves, suppose we bought Intel Stock instead of Disney Stock, how much I would have lost (or regretted) making this decision.

Since Disney Stock is 0.6 and Intel Stock is -0.3, then the amount we regret will be: 0.6 - (-0.3) = 0.9. We have thus potentially lost a 0.9 payoff.

Similarly, we would ask how much I would regret buying Microsoft Stock with 0 payoff versus Disney Stock with a 0.6 payoff in the first year, 0.6 - 0 = 0.6. My regret will thus be 0.6 if I bought Microsoft stock.

We continue similarly for the rest of the stocks in that year. You will note there is no regret in buying Disney stock, i.e. Regret for Disney Stock in Year 1, 0.6 - 0.6 = 0

We now construct a table call a Regret Table to put these values in:

| Stock | Year1 | Year 2 | Year 3 | Year 4 |
|---|---|---|---|---|
| Intel | 0.9 | | | |
| Microsoft | 0.6 | | | |
| Disney | 0 | | | |
| Shell | 0.3 | | | |
| Barclay | 0.8 | | | |

Step 2. Similarly to Step 1, we look under the second column, in this case Year 2, and look for the stock with the highest payoff. In this case, it is Intel stock with a 0.9 payoff.

We now, ask ourselves, how much we will regret investing in Microsoft instead of Intel which has a payoff of 0.5. The regret will then be 0.9 - 0.5 = 0.4

We continue similarly for Disney, Shell and Barclay Stock. Obviously, there will be no regret in investing in Intel Stock. We can thus fill in the regrets for Year 2 (in bold).

| Stock | Year1 | Year 2 | Year 3 | Year 4 |
|---|---|---|---|---|
| Intel | 0.9 | **0** | | |
| Microsoft | 0.6 | **0.4** | | |
| Disney | 0 | **0.5** | | |
| Shell | 0.3 | **1** | | |
| Barclay | 0.8 | **1.5** | | |

Step 3. We now look at the Year 3 column. You will notice that Intel and Barclay has the same payoff of 0.4. Therefore, we will have no regret in investing Barclay vs Intel or vice versa. We can choose between Intel and Barclay arbitrarily to be our highest payoff stock, in this case I will choose Barclay. The regret of Intel vs Barclay is: 0.4 (Intel) - 0.4 (Barclay) = 0

We can now fill in our regret for Year 3 in a similar fashion (in bold).

| Stock | Year1 | Year 2 | Year 3 | Year 4 |
|---|---|---|---|---|
| Intel | 0.9 | 0 | **0** | |
| Microsoft | 0.6 | 0.4 | **0.3** | |
| Disney | 0 | 0.5 | **0.4** | |
| Shell | 0.3 | 1 | **1.1** | |
| Barclay | 0.8 | 1.5 | **0** | |

Step 4. We now look at our last column Year 4, the highest payoff in this column is for the Shell Stock with a 0.7 payoff. We therefore calculate the regret of buying Intel, Microsoft, Disney and Barclay versus that of Shell. These values are filled in the Year 4 column (in bold)

| Stock | Year1 | Year 2 | Year 3 | Year 4 |
|---|---|---|---|---|
| Intel | 0.9 | 0 | 0 | **0.2** |
| Microsoft | 0.6 | 0.4 | 0.3 | **0.3** |
| Disney | 0 | 0.5 | 0.4 | **0.1** |
| Shell | 0.3 | 1 | 1.1 | **0** |
| Barclay | 0.8 | 1.5 | 0 | **0.7** |

Step 5. We now insert a new column in our table and call it the Maximum Regret column. Let us take the Intel Stock firstly, and look at the regret of not investing in this stock over the Year 1 to Year 4 (in italic). We see that we will most regret not investing in Intel in Year 1 since it gives a potential payoff of 0.9 as compared to the other stocks. Thus, our maximum regret for Intel is 0.9, we will insert this number in our Maximum Regret column (in bold and italic).

| Stock | Year1 | Year 2 | Year 3 | Year 4 | Max Regret |
|---|---|---|---|---|---|
| Intel | *0.9* | *0* | *0* | *0.2* | ***0.9*** |
| Microsoft | 0.6 | 0.4 | 0.3 | 0.3 | |
| Disney | 0 | 0.5 | 0.4 | 0.1 | |
| Shell | 0.3 | 1 | 1.1 | 0 | |
| Barclay | 0.8 | 1.5 | 0 | 0.7 | |

Looking at the Microsoft Stock (in italic) row for the four years, our maximum regret is 0.6 in Year 1. We thus enter this value in the Maximum Regret column (in bold and italic).

| Stock | Year1 | Year 2 | Year 3 | Year 4 | Max Regret |
|---|---|---|---|---|---|
| Intel | 0.9 | 0 | 0 | 0.2 | 0.9 |
| Microsoft | *0.6* | *0.4* | *0.3* | *0.3* | ***0.9*** |
| Disney | 0 | 0.5 | 0.4 | 0.1 | |
| Shell | 0.3 | 1 | 1.1 | 0 | |
| Barclay | 0.8 | 1.5 | 0 | 0.7 | |

We continue in this same manner for the Disney, Shell and Barclay Stock, to fill in the Maximum Regret Column (in bold and italic).

| Stock | Year1 | Year 2 | Year 3 | Year 4 | Max Regret |
|---|---|---|---|---|---|
| Intel | 0.9 | 0 | 0 | 0.2 | ***0.9*** |
| Microsoft | 0.6 | 0.4 | 0.3 | 0.3 | ***0.6*** |
| Disney | 0 | 0.5 | 0.4 | 0.1 | ***0.5*** |
| Shell | 0.3 | 1 | 1.1 | 0 | ***1.1*** |
| Barclay | 0.8 | 1.5 | 0 | 0.7 | ***1.5*** |

Step 6. We now want to choose the stock that will minimize regret i.e. the stock that we invest in when compared to the others won't make us feel too bad about its payoff being lower than the others in Year 1 to Year 4. We now look for under the Maximum Regret column, for the stock with the lowest Maximum Regret, in this case it is the Disney Stock (in bold and italic), with a Maximum Regret of 0.5.

| Stock | Year1 | Year 2 | Year 3 | Year 4 | Max Regret |
|---|---|---|---|---|---|
| Intel | 0.9 | 0 | 0 | 0.2 | 0.9 |
| Microsoft | 0.6 | 0.4 | 0.3 | 0.3 | 0.6 |
| Disney | 0 | 0.5 | 0.4 | 0.1 | ***0.5*** |
| Shell | 0.3 | 1 | 1.1 | 0 | 1.1 |
| Barclay | 0.8 | 1.5 | 0 | 0.7 | 1.5 |

Thus, we will invest in the Disney Stock based on the Minimax Regret

Method. If you go back to our payoff table, you will observe that the Disney Stock offered a somewhat consistent and decent payoff.

# Appendix C

# Gaussian Copula

A copula is a kind of distribution function that are used to describe the dependence between random variables. There are many parametric copula families available, which usually have parameters that control the strength of dependence. Gaussian copula is one of the copula families that are used in the finance and statistics.

A example of Gaussian copula joining bivariate distribution functions $u$ and $v$ (i.e joining two random variables) is presented as follows, with $\Phi_\rho$ being the standard bivariate normal CDF with correlation $rho$, the Gaussian copula function is

$$C_\rho(u, v) = \Phi_\rho(\Phi^{-1}(u), \Phi^{-1}(v)) \tag{C.0.1}$$

where $u, v \in [0, 1]$ and $\Phi^{-1}$ is the inverse CDF of a standard normal CDF $\Phi$. $\Phi_\rho$ denotes the joint CDF of a multivariate normal distribution, i.e. $u, v$ in this case, with mean vector zero and covariance matrix equal to the correlation matrix $\rho$.

More information on stochastic dependence modelling using copula is explained in [Pap07].

# Appendix D

# Scenarios for Multistage Analysis

Six net load and generation capacity scenarios at stage 1, 2 and 3 are presented as follows,

Table D.0.1: Six load scenarios at stage 1 (MW)

| | Scenario 1 | Scenario 2 | Scenario 3 | Scenario 4 | Scenario 5 | Scenario 6 |
|---|---|---|---|---|---|---|
| Bus 1 | 102.0467 | 16.31628 | 35.9892 | 67.76254 | 58.64014 | 80.8112 |
| Bus 3 | 175.2575 | 345.3751 | 302.7444 | 247.6638 | 319.1655 | 227.1703 |
| Bus 4 | 271.2823 | 482.3551 | 440.5847 | 388.4821 | 435.818 | 364.2342 |
| Bus 7 | 165.9631 | 270.5182 | 247.8324 | 201.3703 | 219.6562 | 211.5157 |
| Bus 8 | 302.8167 | 484.0049 | 426.6013 | 380.3556 | 420.1677 | 320.9093 |
| Bus 9 | 4.065627 | 6.698874 | 6.557523 | 5.273728 | 6.466019 | 5.919495 |
| Bus 12 | 5.706136 | 9.93354 | 9.8771 | 7.251334 | 8.236583 | 7.801386 |
| Bus 15 | 195.1794 | 366.7419 | 318.0753 | 256.1157 | 293.0896 | 257.3003 |
| Bus 16 | 158.0498 | 351.0194 | 314.3531 | 224.887 | 272.2934 | 240.3828 |
| Bus 18 | 107.7973 | 180.7996 | 168.8555 | 131.6877 | 155.8654 | 137.6254 |
| Bus 20 | 384.5909 | 673.7353 | 556.9922 | 505.1104 | 644.4501 | 520.1416 |
| Bus 21 | 190.8558 | 254.6009 | 236.5853 | 212.7934 | 237.4406 | 223.9668 |
| Bus 23 | 146.7687 | 263.1845 | 234.1859 | 171.8171 | 237.0639 | 221.9214 |
| Bus 24 | 215.3472 | 349.3467 | 317.6305 | 258.746 | 303.9266 | 273.5477 |
| Bus 25 | 137.4928 | 248.2255 | 246.8958 | 161.8417 | 220.2423 | 184.9961 |
| Bus 26 | 10.23342 | 154.6535 | 152.9752 | 46.07222 | 112.8148 | 79.93308 |
| Bus 27 | 175.8301 | 263.4558 | 210.611 | 213.5327 | 248.1796 | 177.3298 |
| Bus 28 | 116.472 | 195.6905 | 168.1248 | 140.0732 | 158.2297 | 161.6832 |
| Bus 29 | 150.2453 | 306.6513 | 269.1948 | 202.1412 | 230.104 | 235.1839 |
| Bus 31 | 5.721849 | 10.25237 | 10.16504 | 6.805474 | 8.69151 | 8.245515 |
| Bus 39 | 656.1213 | 1148.971 | 1032.944 | 712.5134 | 789.5292 | 953.7764 |

Table D.0.2: Six load scenarios at stage 2 (MW)

| | Scenario 1 | Scenario 2 | Scenario 3 | Scenario 4 | Scenario 5 | Scenario 6 |
|---|---|---|---|---|---|---|
| Bus 1 | 65.24023 | 45.60385 | 71.12973 | 46.93911 | 67.73273 | 115.4624 |
| Bus 3 | 268.7391 | 362.0564 | 208.5129 | 120.8596 | 196.0953 | 298.7429 |
| Bus 4 | 295.3864 | 511.4887 | 332.1916 | 248.1127 | 401.3031 | 458.0783 |
| Bus 7 | 251.1176 | 267.5901 | 184.9998 | 219.7985 | 235.6211 | 255.9918 |
| Bus 8 | 331.3853 | 458.9138 | 326.2686 | 233.6207 | 419.4486 | 440.9711 |
| Bus 9 | 7.287418 | 6.259622 | 4.799719 | 6.023629 | 5.827938 | 6.970493 |
| Bus 12 | 9.64476 | 10.01716 | 6.793801 | 8.26356 | 8.604237 | 8.882047 |
| Bus 15 | 240.187 | 366.3258 | 236.3858 | 70.06708 | 259.6811 | 298.7086 |
| Bus 16 | 211.8151 | 317.2294 | 204.3113 | 73.0238 | 215.1338 | 286.3143 |
| Bus 18 | 146.378 | 188.2987 | 122.7831 | 113.9458 | 140.6201 | 168.8713 |
| Bus 20 | 554.1487 | 705.2841 | 440.7383 | 423.3877 | 556.9061 | 611.7134 |
| Bus 21 | 207.177 | 287.5912 | 194.9016 | 164.8328 | 220.9772 | 246.6435 |
| Bus 23 | 225.4965 | 280.5299 | 166.8945 | 176.9234 | 203.0574 | 245.1782 |
| Bus 24 | 170.1311 | 347.2965 | 244.2268 | 125.6951 | 236.6357 | 323.5762 |
| Bus 25 | 218.1257 | 242.1746 | 147.3791 | 145.2577 | 192.7213 | 228.3869 |
| Bus 26 | 106.6667 | 126.5777 | 10.18662 | 8.24281 | 76.07099 | 113.7636 |
| Bus 27 | 144.2921 | 254.3782 | 183.9149 | 67.70951 | 185.8947 | 221.7517 |
| Bus 28 | 161.0559 | 183.5216 | 137.0151 | 178.0036 | 165.8793 | 159.1113 |
| Bus 29 | 188.6203 | 289.0114 | 206.1425 | 122.1548 | 218.2248 | 250.9258 |
| Bus 31 | 9.312736 | 10.6245 | 6.820629 | 7.596894 | 9.109401 | 9.218007 |
| Bus 39 | 950.1104 | 1147.031 | 755.4707 | 643.232 | 771.4681 | 997.5014 |

Table D.0.3: Six load scenarios at stage 3 (MW)

| | Scenario 1 | Scenario 2 | Scenario 3 | Scenario 4 | Scenario 5 | Scenario 6 |
|---|---|---|---|---|---|---|
| Bus 1 | 51.38993 | 72.4335 | 111.3927 | 81.39821 | 51.85004 | 57.97519 |
| Bus 3 | 226.3358 | 2.870512 | 234.3502 | 100.9291 | 379.1579 | 161.4576 |
| Bus 4 | 329.7388 | 89.94654 | 495.6783 | 297.643 | 546.5707 | 225.3121 |
| Bus 7 | 223.6109 | 265.6211 | 262.9612 | 273.6145 | 291.302 | 220.7824 |
| Bus 8 | 364.5903 | 0 | 459.1222 | 187.5402 | 475.0922 | 259.8877 |
| Bus 9 | 5.189816 | 5.96746 | 7.055778 | 5.368439 | 6.780374 | 4.917771 |
| Bus 12 | 7.836312 | 8.983136 | 10.39544 | 8.520563 | 10.98052 | 7.285488 |
| Bus 15 | 288.5967 | 0 | 277.2665 | 14.80717 | 407.2967 | 129.6523 |
| Bus 16 | 228.5057 | 0 | 320.71 | 133.2092 | 348.5244 | 120.4968 |
| Bus 18 | 124.3484 | 152.3108 | 168.4662 | 185.3862 | 201.1302 | 129.9293 |
| Bus 20 | 485.9101 | 191.6062 | 645.3067 | 378.7653 | 713.2377 | 338.4539 |
| Bus 21 | 175.2766 | 213.4471 | 274.7074 | 306.3797 | 296.1416 | 221.5261 |
| Bus 23 | 176.0188 | 257.939 | 260.6341 | 262.045 | 291.4081 | 174.7857 |
| Bus 24 | 282.994 | 0 | 328.8491 | 96.83323 | 395.0034 | 213.2893 |
| Bus 25 | 177.2969 | 202.7922 | 230.6965 | 287.6565 | 286.2452 | 183.1949 |
| Bus 26 | 30.01605 | 74.89671 | 92.87966 | 178.0306 | 175.6605 | 41.89052 |
| Bus 27 | 201.3079 | 0 | 275.9329 | 0 | 309.219 | 80.87582 |
| Bus 28 | 135.6513 | 189.9108 | 218.8518 | 183.5518 | 194.3395 | 139.1058 |
| Bus 29 | 221.2636 | 5.497479 | 256.1994 | 0 | 315.1438 | 118.0942 |
| Bus 31 | 7.941918 | 10.1565 | 9.889525 | 9.341862 | 11.08617 | 7.439894 |
| Bus 39 | 788.6711 | 645.4284 | 1094.44 | 927.1275 | 1179.52 | 719.197 |

Table D.0.4: Generation capacity scenarios (MW)

| | Stage 1 | Stage 2 | Stage 3 |
|---|---|---|---|
| Gen 1 | 1040 | 1040 | 1040 |
| Gen 2 | 646 | 646 | 646 |
| Gen 3 | 725 | 725 | 725 |
| Gen 4 | 652 | 652 | 652 |
| Gen 5 | 508 | 508 | 508 |
| Gen 6 | 687 | 687 | 687 |
| Gen 7 | 580 | 580 | 580 |
| Gen 8 | 564 | 564 | 564 |
| Gen 9 | 865 | 865 | 865 |
| Gen 10 | 1100 | 1100 | 1100 |
| Gen 11 | 0 | 0 | 500 |
| Gen 12 | 0 | 500 | 500 |

# Appendix E

# Symbols and Abbreviations

## Capital letters

| Symbol | Units | Description |
|---|---|---|
| $B_{ij}$ | | imaginary part of $Y$ admittance matrix |
| $B, G$ | $S$, $S$ | susceptance, conductance |
| $C_i$ | $e$, \$ | hourly quadratic cost function of generating unit $i$ |
| $C_{TOTAL}$ | $e$, \$ | total cost (hourly) |
| $C_{in}, C_{op}$ | $e$, \$ | investment cost, operational cost (hourly) |
| $C_{Wp}$ | $e$, \$ | dummy penalty cost (Chapter 6) |
| $G_{ij}$ | | real part of $Y$ admittance matrix |
| $I^a$ | $e, \$/km$ | investment cost of a candidate expansion option |
| $I_i$ | A | current injection at bus $i$ |
| $L$ | | Lagrangian function |
| $N_g, N_b, N_l, N_o$ | | number of generators, number of buses, number of lines, number of candidate options |
| $P^*, Q^*$ | | the agreed price and quantity between generation and load in the market (Chapter 3) |
| $P$ | MW | active power |
| $Q$ | MVar | reactive power |
| $R, X, Z$ | $\Omega$,$\Omega$,$\Omega$ | resistance, reactance, impedance |
| $R(s, p)$ | | regret of scenario $s$ and plan $p$ |
| $S$ | MVA | Apparent power |
| $S, P$ | | scenarios, corresponding plans |
| $TOP^T$ | | network topology at time $T$ |
| $V_i$ | V | voltage at bus $i$ |

| | | |
|---|---|---|
| $W$ | | allowable overloading binary, 1 is overloading and 0 otherwise |
| $Y_{ij}$ | | admittance matrix |

## Others

| | | |
|---|---|---|
| $\delta_i$ | deg, rad | phase angles at bus $i$ |
| $\zeta_{ij}$ | | loading factor of line $ij$ |
| $\eta$ | | Lagrangian multiplier related to generator constraints |
| $\theta_{ij}$ | deg, rad | phase angle of $Y$ matrix element between position $i, j$ |
| $\lambda$ | $e, \$/MWh$ | Lagrangian multiplier related to power balance constraint, also known as, locational marginal cost |
| $\mu$ | | Lagrangian multiplier related to power flow constraints |
| $\sigma$ | | maximum allowable percentage of temporary overloading |
| $d$ | | maximum number of allowable congestion occurring concurrently |
| $n^a$ | | number of expansion candidates, integer |
| $val(s, p)$ | | attribute value of scenario $s$ and plan $p$ |

## Abbreviations

| | |
|---|---|
| AC-OPF | Alternating Current OPF |
| AOA | Outer Approximation Algorithm |
| CCGT | Combined-Cycle Gas Turbine |
| APG | Austrian Power Grid |
| CCS | Carbon Capture and Storage |
| CDF | Cumulative Density Function |
| CS | Congestion Surplus |
| CSP | Concentrating Solar Power |
| DC-OPF | Linearised OPF |
| DNI | Direct Normal Irradiation |
| DSM | Demand Side Management |
| EC | European Commission |
| ESII | European Solar Industry Initiative |
| ESSEP | Enhanced Single-Stage Expansion Planning |
| EU | European Union |

| | |
|---|---|
| FACTS | Flexible AC Transmission System |
| ICT | Information and Communications Technology |
| IGCC | Integrated Gasification Combined Cycle |
| IRENE-40 | Infrastructure Roadmap for Energy Networks in Europe |
| KKT | Karush Kuhn Tucker condition |
| LM | Lagrangian Multiplier |
| LMP | Locational Marginal Price |
| LP | Linear Programming |
| MCP | market clearing price |
| MCS | Monte-Carlo Simulation |
| MINLP | Mixed Integer Non-Linear Programming |
| MTI | Merchant Transmission Investment |
| NLP | Non-Linear Programming |
| OCGT | Open-Cycle Gas Turbine |
| OPF | Optimal Power Flow |
| PF | Power Flow |
| PHP | Pumped-storage Hydro Plant |
| PJM | Regional transmission organization (RTO) including all or parts of 13 states and the District of Columbia |
| PTDF | Power Transfer Distribution Factor |
| PV | Photovoltaic |
| RES | Renewable Energy Sources |
| RWE | Rheinisch-Westflisches Elektrizittswerk AG |
| S-OPF | Stochastic-OPF |
| TSO | Transmission System Operators |
| TTB | TenneT B.V. the Netherlands |
| UC | Unit Commitment |
| UCTE | Union for the Coordination of the Transmission of Electricity |
| WP | Work Package |

# Bibliography

[AAC10] J. M. Arroyo, N. Alguacil, and M. Carrion. A risk-based approach for transmission network expansion planning under deliberate outages. *Power Systems, IEEE Transactions on,*, 25:1759–1766, 2010.

[Ack05] T. Ackermann. *Wind Power in Power Systems.* John Wiley and Sons, Jan 2005.

[Age08] European Environment Agency. Air pollution from electricity-generating large combustion plants, 2008.

[Age09a] United States Environmental Protection Agency. `http://www.epa.gov/cleanrgy/energy-and-you/affect/coal.html`, 2009.

[Age09b] United States Environmental Protection Agency. `http://www.epa.gov/cleanrgy/energy-and-you/affect/natural-gas.html`, 2009.

[Age12a] European Environmental Agency. Final electricity consumption by sector (ener 018) - assessment published apr 2012, 2012.

[Age12b] International Renewable Energy Agency. Renewable energy technologies: Cost analysis series: Hydropower. Technical report, 2012.

[AIM99a] AIMMS. *The Language Reference.* Paragon Decision Technology, 1999.

[AIM99b] AIMMS. *Optimization Modeling.* Paragon Decision Technology, 1999.

[AIM99c] AIMMS. *The User's Guide.* Paragon Decision Technology, 1999.

[ALL06] H. Agabus, M. Landsberg, and O. Liik. *Optimal investment strategies for energy sector under uncertainty.* PhD thesis, Tallinn University of Technology, Department of Electrical Power Engineering, 2006.

[BC02] C.Y. Baldwin and K.B. Clark. The option value of modularity in design, an example from design rules, volume 1: The power of modularity. Technical report, Harvard Business School, May 2002.

[BEF10] C. Bruynooghe, A. Eriksson, and G. Fulli. Load-following operating mode at nuclear power plants (npps) and incidence on operation and maintenance costs. compatibility with wind power variability. Technical report, 2010.

[BfU09a] Naturschutz und Reaktorsicherheit Bundesministerium fur Umwelt. Atomkraft - kein weg fur die zukunft (tranlated), 2009.

[BfU09b] Naturschutz und Reaktorsicherheit Bundesministerium fur Umwelt. Hindernis atomkraft: Die auswirkungen einer laufzeitverlangerung der atomkraftwerke auf erneuerbare energien (tranlated), 2009.

[BG09] D. Bindel and J. Goodman. Principles of scientific computing, 2009.

[BHM77] S.P. Bradley, A.C. Hax, and T.L. Magnanti. *Applied Mathematical Programming.* Addison Wesley, 1977.

[BKM84] B.G. Brown, R.W. Katz, and A.H. Murphy. Time series models to simulate and forecast wind speed and wind power. *J. Climate Appl. Meteor.*, 23:1184–1195, 1984.

[BMD11] A. Brown, S. Mueller, and Z. Dobrotkova. Renewable energy markets and perspects by technology. Technical report, 2011.

[Bro08] R.E. Brown. Impact of smart grid on distribution system design. *IEEE/PES Conversion and Delievery of Electrical Energy in 21st Century*, Jan 2008.

[BV04] S. Boyd and L. Vandenberghe. *Convex Optimization.* Cambridge University Press, 1st edition, 2004.

[Cou12] Global Wind Energy Council. Global wind report, annual market update 2011, 2012.

[DATD04] I.G. Damousis, M.C. Alexiadis, J.B. Theocharis, and P.S. Dokopoulos. A fuzzy model for wind speed prediction and power generation in wind parks using spatial correlation. *Energy Convers, IEEE Transactions on,*, 19:3352–3361, 2004.

[dS06] A.M.L. da Silva. Evolution strategies to transmission expansion planning considering unreliability costs. IEEE PMAPS, Jun 2006.

[ea02] M. Kanamitsu et al. Ncep-deo amip-ii reanalysis (r-2), Nov 2002.

[ea12a] Z. Liu et al. Challenges, experiences and possible solutions in transmission system operation with large wind integration. Nov 2012.

[ea12b] Z. Liu et al. Innovative operational security tools for the development of a stable pan european grid. In *Cigre Canada*, Montreal, Sept 2012.

[EBD09] J. Egerer, L. Bckers, and G. Drondorf. Sustainable energy networks for europe-the integration of large-scale renewable energy sources until 2050 wp-em-35. Technical report, 2009.

[EE] Data portal ENTSO-E, Resources. https://www.entsoe.eu/resources/data-portal/.

[EE09] ENTSO-E. *The 50 Year Success Story - Evolution of a European Interconnected Grid*. Secretariat of UCTE, Brussels, 2009.

[EE10] ENTSO-E. Ten-year network development plan 2010-2020. Technical report, 2010.

[EE11] ENTSO-E. Research and development plan: European grid: Towards 2020 challenges and beyond. Technical report, 2011.

[EE12] ENTSO-E. Ten-year network development plan 2012. Technical report, 2012.

[Eur03] Eurelectric. Public acceptance for new transmission overhead lines and substations. Technical report, 2003.

[FBA08] C.M. Ferreira, F.P.M. Barbosa, and C.I.F. Agreira. Transient stability preventive control of an electric power system using a hybrid method. In *Proc. of the 12th International Middle East Power System Conference*, Mar 2008.

[Fou10] Desertec Foundation. `http://www.desertec.org`, 2010.

[FT11] M. Fuchs and W. Timpf. The load change ability of nuclear power plants  experience and outlook, 2011.

[GH91] F.D. Galiana and M. Hunneault. A survey of the optimal power flow literature. (6):762–770, 1991.

[GJ94] J.J. Grainger and W.D. Stevenson Jr. *Power System Analysis*. McGraw Hill, Singapore, 1994.

[Gor] G. Gordan. Linear programming, lagrange multipliers, and duality.

[GR09] L. Garces and R. Romero. Specialized genetic algorithm for transmission network expansion planning considering reliability. Intelligent System Applications to Power Systems, ISAP,, Nov 2009.

[GW86] G.R.Shorack and J.A. Wellner. *Empirical processes with applications to statistics*. Wiley, New York, 1986.

[HA06] I.A. Hiskens and J. Alseddiqui. Sensitivity, approximation, and uncertainty in power system dynamic simulation. 21:1808–1820, Nov 2006.

[HK01] J. Han and M. Kamber. *Data Mining: Concepts and Techniques*. Academic Press, 1st edition, 2001.

[HK04] J. Han and M. Kamber. *Data Mining: Concepts and Techniques*. Morgan Kaufmann, 2nd edition, 2004.

[HMO+07] H. Holttinen, P. Meibom, A. Orths, F. van Hulle, B. Lange, M. O'Malley, J. Pierik, B. Ummels, J.O. Tande, A. Estanqueiro, M. Matos, E. Gomez, L. Soder, G. Strbac, A. Shakoor, J. Ricardo, J. Charles Smith, M. Milligan, and E. Ela. Design and operation of power systems with large amounts of wind power. Technical report, 2007.

[HOO11] K.W. Hedman, S.S. Oren, and R.P. O'Neil. A review of transmission switching and network topology optimization. *IEEE PES Tutorials*, 2011.

[Hos05] A. Hosein. `http://prejudice.tripod.com/ME30B/minimax_regret.htm`, 2005.

[HT09] T. Hastie and R. Tibshirani. *The Elements of Statistical Learning*. Springer, 2nd edition, 2009.

[Hua11] D. Huang. Msc. thesis: Implementation of ptdf in the market model, 2011.

[Hun11] M. Hunting. The aimms outer approximation algorithm for minlp, an aimms white paper. Technical report, Nov 2011.

[IEE01] IEEE/PES WM-2001. *ANN-Based short-term load forecasting in electricity markets*, Columbus, Ohio, Jan 2001.

[ILVvdS12] R. Idema, D. J. P. Lahaye, C. Vuik, and L. van der Sluis. Scalable newton-krylov solver for very large power flow problems. *IEEE Trans. on Power Syst.*, 27, Feb 2012.

[Ins11] Global CCS Institute. The global status of ccs: 2011. Technical report, 2011.

[IRE12] IRENE-40. Infrastructure roadmap for energy network in europe. `http://www.irene-40.eu/`, 2012.

[KMe13] Wikipedia, k-medoids. `http://en.wikipedia.org/wiki/K-medoids`, 2013.

[KS04] D.S. Kirschen and G. Strbac. *Fundamentals of Power System Economics*. John Wiley & Sons, 1st edition, 2004.

[KU12] H. Kile and K. Uhlen. Data reduction via clustering and averaging for contingency and reliability analysis. *Electrical Power and Energy Systems*, 43:1435–1442, Aug 2012.

[Lai01] L.L. Lai. *Power System Restructuring and Deregulation: Trading, Performance and Information Technology.* John Wiley, Chichester, 2001.

[LDS05] M. Lu, Z.Y. Dong, and T.K. Saha. Stransient stability preventive control of an electric power system using a hybrid method. In *IEEE/PES Transmission and Distribution Conference*, 2005.

[Lit09] E. Litvinov. Design and operation of the locational marginal prices based electricity markets. *IET Gener. Transm. Distrib.*, 4:315–323, 2009.

[Liu01] J.S. Liu. *Monte Carlo Strategies in Scientific Computing.* Springer, 2001.

[LLZ08] X. Li, Y. Li, and S. Zhang. Analysis of probabilistic optimal power flow taking account of the variation of load power. 23:992–999, Aug 2008.

[LWH08] F. Leuthold, H. Weigt, and C. Von Hirschhausen. Elmod - a model of the european electricity market. Technical report, 2008.

[LWOG01] S. Li, D.C. Wunsch, E.A. O'Hair, and M.G. Giesselmann. Using neural networks to estimate wind turbine power generation. *Energy Convers, IEEE Transactions on,*, 16:276–282, 2001.

[MAT10] MATLAB. *version 7.10.0 (R2010a).* The MathWorks Inc., Natick, Massachusetts, 2010.

[MCC90] A.P.S. Meliopoulos, G.J. Cokkinides, and X.Y. Chao. A new probabilistic power flow analysis method. 5:182–190, Feb 1990.

[McK10] McKinsey. Mckinsey on smart grid. Technical report, 2010.

[MH99] J.A. Momoh and M.E. El Hawary. A review of selected optimal power flow literature to 1993, part i and ii: Nonlinear and quadratic programming approaches. 1999.

[Mom08] James A Momoh. *Eletric Power System Application of Optimization.* CRC Press, New York, 2nd edition, 2008.

[MP98] V. Miranda and L. M. Proenca. Probabilistic choice vs. risk analysis-conflicts and synthesis in power system planning. *Power Systems, IEEE Transactions on,*, 13:1038–1043, 1998.

[MR07] J.M. Morales and J. Perez Ruiz. Point estimate schemes to solve the probabilistic power flow. 22, Nov 2007.

[Nel06] R.B. Nelson. *An Introduction to Copulas.* Springer, 2nd edition, 2006.

[oE06] U.S. Department of Energy. National electric transmisison congestion study. Technical report, Aug 2006.

[oE09] U.S. Department of Energy. National electric transmisison congestion study. Technical report, Dec 2009.

[otEC03] Commission of the European Communities. Background paper: Undergrouding of electricity lines in europe. Technical report, 2003.

[Pai89] M.A. Pai. *Energy Function Analysis of Power System Stability.* Springer, 1989.

[Pap07] G. Papaefthymiou. *Integration of Stochastic Generation in Power Systems.* PhD thesis, Delft University of Technology, 2007.

[Pen02] J. Pengelly. Monte carlo methods, 2002.

[PK09] G. Papaefthymiou and D. Kurowicka. Using copulas for modeling stochastic dependence in power system uncertainty analysis. pages 40–49, Feb 2009.

[PLvdS11] G. Papaefthymiou, Z. Liu, and L. van der Sluis. A stochastic opf approach for identification of the weak network points in systems with high wind power penetration. In *Cigre*, Bologna, 2011.

[Pou03] P. Pourbeik. Modeling of combined-cycle power plants for power system studies. 2003.

[Pow11] RWE Power. Power:perspectives 2011: Lignite - a domestic energy source, 2011.

[pro07] Tradewind project. Wp3.2 grid modelling and power system data. Technical report, Dec 2007.

[pro08a] Realisegrid project. Deliverable 3.1.1 review of existing methods for transmission planning and for grid connection of wind power plants. Technical report, Realisegrid, Jun 2008.

[pro08b] Tradewind project. Wp2.6 equivalent wind power curves. Technical report, Jul 2008.

[pro10] IRENE-40 project. D2.1 methodology for the placement of new network elements. Technical report, Jul 2010.

[pro11] IRENE-40 project. D2.3 methodology for determining impact and value of dsp on system infrastructure development. Technical report, Feb 2011.

[PS98] C.H. Papdimitriou and K. Steiglitz. *Combinatorial Optimization*. Dover Publication INC., New York, 1998.

[PSR05] K. Purchala, M. Shinkai, and F. Regaira. Practices related to internal and cross-border congestion management. In *CIGRE/IEEE PES International Symposium*, 2005.

[rep11] IRENE-40 Internal report. Task 2.3: Scenario synthesis. Technical report, 2011.

[Rez06] M. Reza. *Stability analysis of transmission systems with high penetration of distributed generation*. PhD thesis, Delft University of Technology, 2006.

[RM99] J.C. Rolim and L.J.B. Machado. A study of the use of corrective switching in transmission systems. *IEEE Trans. on Power Syst.*, 14:336–341, Feb 1999.

[Rub81] R.Y. Rubinstein. *Simulation and the Monte Carlo Method*. Wiley-Interscience, 1st edition, 1981.

[Sav51] L. Savage. The theory of statistical decision. *Journal of the American Statistical Association*, 46:55–67, 1951.

[SB95] A. Sankarakrishnan and R. Billington. Sequential monte carlo simulation for composite power system reliability analysis with time varying loads. 10:1540–1545, Aug 1995.

[SDM07] Supply-demand market equilibrium curve. http://lug.wsu.edu/files/final_paper_html_m33ae3f3f.png, 2007.

[SF04] G.B. Shrestha and P.A.J. Fonseka. Congestion driven transmission expansion in competitive power markets. *IEEE Trans. on Power Syst.*, 3:1658–1665, Aug 2004.

[Skl] A. Sklar. *Fonctions de repartition a n dimensions et leurs marges.* Publications de l'Institut de Statistique de L'Universite de Paris.

[SLK06] C. Singh, X. Luo, and H. Kim. Power system adequacy and security calculations using monte carlo simulation incorporating intelligent system methodology. In *International Conf. Probabilistic Methods Applied to Power Systems*, Stockholm, 2006.

[SV05] W. Shao and V. Vittal. Corrective switching algorithm for reliving overloads and voltage violations. *IEEE Trans. on Power Syst.*, 20:1877–1885, Nov 2005.

[SvdS08] P. Schavemaker and L. van der Sluis. *Electrical Power System Essentials.* John Wiley, Chichester, 1st edition, 2008.

[SW03] Y. Song and X. Wang. *Operation of Market-Oriented Power Systems.* Springer, 1st edition, 2003.

[SYL02] M. Shahidehpour, H. Yamin, and Z. Li. *Market Operations in Electric Power Systems, Forecasting, Scheduling, and Risk Management.* John Wiley Sons, New York, 2002.

[Sys12] European Commission: Strategic Energy Technologies Information System. Hydropower, 2012.

[UCT08] Former UCTE. Ucte study model 2008, 2008.

[vHG09] F. van Hulle and P. Gardner. Wind energy - the facts. Technical report, 09.

[Wika] Wikipedia. Availability factor. http://en.wikipedia.org/wiki/Capacity_factor.

[Wikb] Wikipedia. Capacity factor. http://en.wikipedia.org/wiki/Capacity_factor.

[Wikc] Wikipedia. Multivariate random variable. http://en.wikipedia.org/wiki/Multivariate_random_variable.

[Wikd] Wikipedia. Roling blackout.

[Wik12] Wikipedia. `http://en.wikipedia.org/wiki/Regret_(decision_theory)`, 2012.

[WM12] J. Wilkes and J. Moccia. Wind in power, annual statistics 2012. Technical report, 2012.

[WVSO96] F. Wu, P. Varaiya, P. Spiller, and S. Oren. Folk theorems on transmission access: Proofs and counterexamples. *Journal of Regulatory Economics*, 10:5–23, 1996.

[XW07] M. Xie and F.F. Wu. Multiyear transmission expansion planning using ordinal optimization. *IEEE Trans. on Power Syst.*, 22:1420–1428, Nov 2007.

[ZL04] P. Zhang and S.T. Lee. Load flow computation using the method of combined cumulants and gram-charlier expansion. 19:676 – 682, Feb 2004.

[ZS11] R. D. Zimmerman and C. E. Murillo Sanchez. Matpower 4.1 user's manual, 2011.

[ZST11] R.D. Zimmerman, C.E. Murillo Sanchez, and R.J. Thomas. Matpower: Steady-state operations, planning and analysis tools for power systems research and education. *IEEE Trans. on Power Syst.*, 26:12–19, Feb 2011.

# Appendix F

# Publications

## Journal

- Z. Liu, G. Papaefthymiou, L. van der Sluis, "Transmission Network Expansion Planning Considering Implementation Constraints–A Copperplate Approach" under review for the *IEEE Transaction on Power Systems*.

- D. Pudjianto, M. Castro, G. Strbac, Z. Liu, L. van der Sluis, G. Papaefthymiou, "Asymmetric Impacts of European Transmission Network Development towards 2050: Stakeholder Assessment based on IRENE-40 Scenarios" under review for the *Energy Economics Special Issue*, 2013

## Conference

- Z. Liu, L. van der Sluis, L. Tao, E. Gaxiola, C. Schwaegerl, C. K. Konstantinidis, "Impact of different balancing zones on the capacity market design in Europe towards 2050", 10th International Conference on the European Energy, Stockholm, May 2013

- D. Pudjianto, M. Castro, G. Strbac, Z. Liu, L. van der Sluis, G. Papaefthymiou, "Asymmetric Impacts of European Transmission Network Development towards 2050 on Its Stakeholders based on IRENE-40 Scenarios", 51st Meeting of the Euro Working Group on Commodities and Financial Modelling, London, May 2013

- Z. Liu et. al, "Innovative operational security tools for the development of a stable pan-European grid", 2012 CIGRE Canada conference: Technology and innovation for the evolving power grid, Montreal, September 2012

- Z. Liu et. al, "Challenges Experiences and Possible Solutions in Transmission System Operation with Large Wind Integration", 11th International Workshop on Large-Scale Integration of Wind Power into Power Systems, Lisbon, November 2012
- G. Papaefthymiou, Z. Liu, L. van der Sluis, "Stochastic OPF for the identification of weak network points under scenarios of wind locational uncertainty", 12th international conference on probabilistic methods applied to power systems, Istanbul, June 2012
- Z. Liu, G. Papaefthymiou, L. van der Sluis, "Collaborative transmission network expansion planning for congestion alleviation using Lagrangian multipliers", Asia-Pacific power and energy engineering conference, Shanghai, March 2012
- Z. Liu, B. Tessema, G. Papaefthymiou, L. van der Sluis, "Transmission expansion planning for congestion alleviation using constrained locational marginal price", IET Conference on Reliability of Transmission and Distribution Networks, London, November 2011
- G. Papaefthymiou, Z. Liu, L. van der Sluis, "A Stochastic OPF approach for identification of the weak network points in systems with high wind power penetration", Cigre 2011 Bologna Symposium The Electric Power System of the Future, Bologne, September 2011
- N. Farkhondeh Jahromi, Z. Liu, L. van der Sluis,"The influence of wind speed on the oscillatory stability of power systems", Proceedings of the 45th international universities' power engineering conference, Cardiff, August 2010

## Contribution to public deliverables in IRENE-40

- Z. Liu et. al, Deliverable 4.0: Roadmap towards a future electricity network
- Z. Liu et. al, Deliverable 3.1: Application guide for the improvement of ecological sustainability, security and competitiveness by infrastructure changes
- Z. Liu et. al, Deliverable 2.3: Methodology for determining impact and value of DSP on system infrastructure development
- Z. Liu et. al, Deliverable 2.1: Methodology for the placement of new network elements
- Z. Liu et. al, Deliverable 1.2: Application guide for the determination of weak network points within the electrical transmission system

# Appendix G

# Curriculum Vitae

Zongyu Liu was born on July 4, 1981, in Harbin, China. He received his secondary school diploma at the Great Lakes College of Toronto in Toronto, Canada in 2001.

From 2001 to 2005, Zong studied Electrical and Computer Engineering at McMaster University in Hamilton, Canada. In 2006, Zong started his master's programme in Electric Power Engineering at Chalmers University of Technology in Gothenburg, Sweden. He conducted his internship and master's thesis under the co-supervision of Dr. Gabriel Olguin and Dr. Tuan Le Anh about the reliability assessment of breaker arrangements at ABB Corporate Research in Västerås, Sweden.

From 2008 to 2012, Zong worked as a PhD student in the Electrical Power Systems group of Prof. Lou van der Sluis at Delft University of Technology. His research was conducted under the EU FP-7 research framework on the roadmap development for Pan-European electricity network toward 2050 (Project acronym: IRENE-40). During his PhD period, Zong was co-supervised by Prof. Lou van der Sluis and Dr. George Papaefthymiou. Between 2012 and 2013, he was responsible for dissemination activities of another EU FP-7 project titled 'Umbrella', and co-supervised research activities under the framework of 'Umbrella' at TU Delft.

In September 2013, Zong joined E-Bridge Consulting B.V. in Oosterbeek as a consultant.